Physico-chemical characterization of urban aerosols from specific combustion sources in West Africa at Abidjan in Côte d'Ivoire and Cotonou in Benin in the frame of the DACCIWA program

Aka Jacques Adon[1], Catherine Liousse[1], Elhadji Thierno Doumbia[2], Armelle Baeza-Squiban[3], Hélène Cachier[1], Jean-Francois Léon[1], Veronique Yoboué[4], Aristique Barthel Akpo[5], Corinne Galy-Lacaux[1], Benjamin Guinot[1], Cyril Zouiten[6], Hongmei Xu[1, 7], Eric Gardrat[1], Sekou. Keita[8].

[1] Laboratoire d'Aérologie, Université de Toulouse, CNRS, UPS, Toulouse, France

[2] Centre National de Recherche Météorologique (CNRM)/Groupe d'étude de l'Atmosphère Météorologique, CNRS-Météo-France, Toulouse, France

[3] Université Paris Diderot, Unité de Biologie Fonctionnelle et Adaptative-RMCX, CNRS, UMR 8251, Paris, France

[4] Laboratoire de Physique de l'Atmosphère, Université Félix Houphouët-Boigny, Abidjan BPV 34, Côte d'Ivoire

[5] Laboratoire de Physique du Rayonnement, Université d'Abomey-Calavi, Abomey-Calavi, Bénin

[6] Géosciences Environnement Toulouse, Université de Toulouse, CNRS, UPS, Toulouse, France

[7] Department of Environmental Science and Engineering, Xi'an Jiaotong University, Xi'an, China

[8] Université de Khorogo, Khorogo, Côte d'Ivoire.

Correspondence to: adonjacks@gmail.com (J. Adon) and lioc@aero.obs-mip.fr (C. Liousse)

Abstract

Urban air pollution in West Africa has yet to be well characterized. In the frame of DACCIWA (Dynamics-Aerosol-Chemistry-Cloud Interactions in West Africa) program, intensive measurement campaigns were performed in Abidjan (Côte d'Ivoire) and Cotonou (Benin), in dry (January 2016 and 2017) and wet (July 2015 and 2016) seasons, at different sites chosen to be representative of African urban combustion sources (i.e. domestic fires (ADF), traffic (AT) and waste burning (AWB) sources in Abidjan and traffic source in Cotonou (CT)). Both the size distribution of particulate matter (PM) and their chemical composition including elemental carbon (EC), organic carbon (OC), water-soluble organic carbon (WSOC), water-soluble inorganic ions (WSI) and trace metals were examined. Results show very high PM concentrations at all sites and a well-marked seasonality as well as a strong spatial variation. The average $PM_{2.5}$ mass concentrations during the wet season are 517.3, 104.1, 90.3 and 69.1 $\mu g.m^{-3}$ at the ADF, CT, AT and AWB sites, respectively. In the dry season, $PM_{2.5}$ concentrations decrease to 375.7 $\mu g.m^{-3}$ at the ADF site, while they increase to 269.7, 141.3 and 175.3 $\mu g.m^{-3}$ at the CT, AT and AWB sites, respectively. The annual $PM_{2.5}$ levels at almost all sites are significantly higher than the WHO guideline level of 10 $\mu g.m^{-3}$. As for PM mass, (EC) and (OC) concentrations are also maximum at ADF site, accounting up to 69% of the total PM mass. Such high content is mainly linked to wood burning for domestic cooking and commercial food smoking activities. Dust contributions are dominant at CT (57-80%), AT (20-70%) and AWB (30-69%) sites and specially in the coarse and fine particle modes at CT and in the coarse fraction at AT site, which may be explained by the impact of long-range desert-dust transport and re-suspended particles from the roads, in addition to anthropogenic sources. The contributions of WSI to the total PM mass, mainly driven by chloride, nitrate and calcium in the fine and/or large particles are highly variable according to the sites but remain less than 30%. Values are generally 1-3 times higher in the wet season than the dry season. This is due to anthropogenic emissions but also to nitrate formation by reaction processes and natural emissions. The concentrations of trace element well reflect the trends of dust at the traffic and AWB sites, with a predominance of Al, Na, Ca, Fe and K, keys markers of crustal dust. This study constitutes an original database that characterizes specific African combustion sources.

Keywords: atmospheric pollution, chemical composition, physicochemical characterization, Particulate matter, traffic, waste burning, domestic fires.

1. Introduction

The impact of anthropogenic pollution on environment and health has been demonstrated by numerous studies in Europe and North America, which have contributed to the implementation of emission reduction policies. By contrast, air pollution in Africa is far from being well characterized, although it is suspected to be responsible for negative health outcomes (*WHO, 2014*). This is a major problem since Africa is an intense emitter of pollution from anthropogenic sources that includes domestic fires, vehicular traffic, waste burning as well as growing oil and mining industries. It has also one of the fastest growing urban populations in the world, especially in West and East Africa (UN, 2019). As a consequence, it has been shown that massive urbanization and rapid economic growth could be responsible for tripling anthropogenic emissions in Africa between 2000 and 2030 (*Liousse et al., 2014*). Moreover, it is important to recall the impact of biomass burning and dust sources in the African atmospheric composition, especially occurring during the dry season. All of this results in a major degradation of urban air quality and an impact on the health of exposed populations. Only a few studies on this subject have been conducted in West Africa (*Val et al., 2013*; *Dieme et al., 2012*; *Kouassi et al., 2009*) despite the high atmospheric pollutant concentrations already measured to be of the same order as in Asian megacities and well above WHO international standards (*WHO, 2014*).

West Africa is then an "unique laboratory" to study urban pollution. Previous studies conducted under the framework of the AMMA (Analyses Multidisciplinaires de la Mousson Africaine) and POLCA (POLlution des Capitales Africaines) programs, have revealed very high average particulate mass concentrations in Cotonou (Benin), Bamako (Mali), Dakar (Senegal) and Yaoundé (Cameroun) during the dry season (*Doumbia et al., 2012; Val et al., 2013*), suggesting that the population may be affected by negative health outcomes. For example, during the dray season in Bamako (Mali) and Dakar (Senegal), *Val et al. (2013)* showed that the inflammatory impact of combustion aerosol depends on the type of emission sources and determined the predominant role of particulate organic matter. This is consistent with global findings showing that fine and ultrafine aerosol fractions, as well as their content in trace metals and organic compounds, induce biological effects due to their ability to reach the distal lung (*Cassee et al., 2013*). Such reasons highlight the need to better understand the size-speciation of aerosol chemical composition for the main West African anthropogenic sources during the different seasons. Within this context, the DACCIWA (Dynamics-Aerosol-Chemistry-Cloud Interactions in West Africa) program, dedicated a specific work package to "Air Pollution and

96 Health" dealing with pollutant characterization related to health issues through toxicological
97 studies and epidemiological studies.

98 Campaigns have been organized from December 2014 to March 2017 in Abidjan and Cotonou.
99 The strategy was to measure aerosol chemical composition in different sites, representative of
100 the main prevailing urban sources in West Africa following *Liousse et al. (2014)* and *Keita et*
101 *al. (2018)*. Two typical traffic-sampling sites were chosen, one in Abidjan (Côte d'Ivoire) and
102 another one in Cotonou (Benin), to take into account differences in terms of fleets, type of fuel
103 used and quality of roads. Indeed, in Cotonou, the majority of population uses two-wheel
104 vehicles susing gasoline fuel or gasoline and oil fuel, whereas in Abidjan, the vehicle fleet is
105 dominated by four-wheel engines using diesel fuel. Measurements were also performed at
106 domestic fire and waste burning sites, both located in Abidjan.

107 For a period of two years, PM$_{2.5}$ mass and carbonaceous aerosol were weekly measured and
108 results are discussed in *Djossou et al. (2018)*. In this paper, we focus on the results from the
109 intensive campaigns. We present measurements obtained at each site during the wet and dry
110 seasons of the studied periods: (i) PM size distribution and mass concentrations and (ii) PM
111 chemical composition including carbonaceous aerosol, water-soluble organic carbon, water-
112 soluble inorganic ions, dust and trace elements in different size fractions. Experimental method
113 including description of sites, types of measurements and analyses, meteorological conditions,
114 will be presented in the section 2, whereas results and discussion are discussed in the sections
115 3 and 4 of the paper, respectively.

2. Experimental method

2.1. Description of sites

119   Measurement campaigns have been performed in wet season (July 20-26, 2015 and July
120 4-13, 2016) and dry seasons (January 7-15, 2016 and January 5-14, 2017) at three sites in
121 Abidjan (Côte d'Ivoire), representative of different sources, i.e. ADF for Abidjan Domestic
122 Fires, AWB for Abidjan Waste Burning and AT for Abidjan Traffic (Figure 1), as well as one
123 traffic site in Cotonou (Benin) (Figure 2).

124 As shown in Figure 3 which presents pictures of the different sampling sites, the ADF site (5˚
125 19' 44 "N, 4˚ 06' 21" W) is situated on a platform, 5 m above ground level, in Yopougon

126 Bracody district near a market (Figure 1). This geographical area is highly populated with
127 various small commercial activities such as a fish and meat-smoking by women. There are also
128 many formal and informal settlements, which mainly use wood and charcoal as a source of fuel
129 for private and professional combustion activities. Other sources of concern contributing to the
130 mix of pollutant emissions in the area include transportation-related emissions, biomass
131 burning, garbage bins or small landfills and various other fugitive sources. The AT site (5° 21'
132 14" N, 4° 01' 04" W) is located in Adjamé, on the roof of « 220 pharmacie logement building »,
133 about 7 m above ground level and roughly 10 m away from the main road. This site, close to
134 the Adjamé market and to a bus station, is highly affected by traffic (Gbaka, bus, taxi, woro-
135 woro, private cars…). The AWB site (5° 21' 12" N, 3° 56' 16" W) is located at Akouédo in the
136 district of Cocody, on the roof of « Talafiguié », a building 15 m above ground level. This site
137 close to the big municipal landfill of Abidjan operational since 1965 and now covering an area
138 of 153 ha, is submitted to frequent waste burning pollution. The Cotonou Traffic (CT) (6° 22'
139 19" N, 2° 26' 5" E) site is located in Cotonou, on the «Sogema» building roof, about 7 m above
140 ground level. This site is close to the Dantokpa market and also to the biggest crossroad of
141 Cotonou (intersection of 4 main roads). This site is highly influenced by intense traffic
142 activities. As previously mentioned, such a site is interesting because the vehicle fleet and fuels
143 are different in Cotonou compared to Abidjan: (1) there are many two-wheel vehicles in
144 Cotonou whereas a few only in Abidjan; (2) in Cotonou, gasoline is of poor quality due to the
145 illegal fuel transport from Nigeria and (3) the roads are in worse conditions in Cotonou than in
146 Abidjan.

147 **2.2. Measurements**

148 During each intensive campaign and on each site, two 3-hour samples collected with
149 cascade impactors operating in parallel are obtained for three consecutive days (i.e. six size-
150 resolved samples per site during each campaign), to allow size-speciated characterization of the
151 aerosol chemical composition. Note that the choice of the 3-hour periods is linked to the period
152 of maximum pollution for each site as shown by preliminary studies (e.g. morning at ADF site
153 (7-10am), afternoon at AT site (4-7pm, morning at CT site (7-10am)). There is no specific
154 period at AWB site since the activities are roughly the same during the day. The first impactor
155 with 4 stages ($PM_{>2.5}$; $PM_{2.5-1}$; $PM_{1-0.2}$; $PM_{<0.2}$) includes 4 quartz fiber filters (QMA, Whatman)
156 for mass and carbonaceous aerosol (EC, OC and WSOC analysis). The second impactor with 3
157 stages ($PM_{>2.5}$; $PM_{2.5-1}$; $PM_{1-0.1}$) is equipped with three Teflon filters (Zefluor, Pall
158 Corporation®), dedicated for water-soluble ions species and trace elements. Due to operational

159 problems in july 2016, this second 3-stage cascade impactor is replaced by another 3-stage

160 cascade impactor with different size cuts ($PM_{>10}$, $PM_{10-2.5}$, $PM_{2.5-1}$). For consistency, results will

161 be presented as an ultrafine (UF), fine (F) and coarse (C) classification. The two first stages

162 ($PM_{>2.5}$ and $PM_{2.5-1}$) being considered as the coarse particulate fraction, the $PM_{1-0.1}$ or $PM_{1-0.2}$

163 stage, the fine particulate fraction and the $PM_{<0.2}$ stage, the ultrafine fraction.

164 All the filters are prepared and analyzed at the Laboratoire d'Aerologie in Toulouse under

165 different protocols described in the following paragraphs. Note that the quartz filters are

166 prefired before sampling.

2.3. Analyses

2.3.1. Gravimetric analyses

169 Aerosol mass concentrations are obtained using a high-precision balance (SARTORIUS

170 MC21S), placed under a controlled temperature and humidity atmosphere (Person and Tymen,

171 2005). Before weighing, the filters are kept 24 hours in the weighing room at an ambient relative

172 humidity of 30 ±15%. The filters are weighed before and after sampling. Result of a gravimetric

173 measurement consists of the average of 2 to 4 weighing whose differences do not exceed 5µg.

174 The standard error on a gravimetric measurement is therefore less than 10 µg, typically

175 representing less than 5% of the particles mass.

2.3.2. Carbonaceous aerosols

177 Carbonaceous aerosol is determined with thermal analysis with a two-step method

178 adapted from Cachier et al. (1989). Two aliquots of the same filter are separately analyzed.

179 One portion is directly analyzed for its total carbon content (TC). The other portion is

180 first submitted to a pre-combustion step (2 h at 340°C under pure oxygen) in order to eliminate

181 Organic Carbon (OC), and then analyzed for its Elemental Carbon (EC) content. Organic

182 carbon (OC) concentrations are calculated as the differences between TC and EC. Note that the

183 aerosol carbon content is quantified by a non-dispersive infrared (NDIR) detector with G4

184 ICARUS instrument with a detection limit of the order of 2 $µgC.cm^{-2}$. Uncertainty is in the

185 order of 5% for TC, while being in the range of 5-20%, for EC and OC.

2.3.3 Water Soluble Organic Carbon analysis

187 WSOC measurements are performed using a total organic carbon analyzer (Sievers M9).

188 A detailed description of this technique is reported in Favez et al. (2008). Briefly, the full

189   oxidation of total organic carbon into CO_2 is obtained by coupling chemical oxidation (with

190   ammonium persulphate) and UV light. CO_2 is then quantified by conductivity. Analyses are

191   conducted on 20 ml of solution extracts. For UF samples, solutions to be analyzed are obtained

192   using a total filter surface of 3cm² (6x0.5 cm² punches symmetrically taken out of each QMA

193   filter), whereas, for C and F sizes, due to the geometry of the spots at the surface of the filters,

194   samples are divided into equivalent parts (1/2 or 1/4 of 47 mm filters, rest of the filters being

195   used for carbonaceous analysis). The extraction protocol consists of 16h soaking under soft

196   shaking in an Erlen-Meyer containing 20mL of ultra-pure water. Prior to WSOC analysis, water

197   extracts are filtered through Teflon (PTFE) filters (0.2μm pore size diameter) in order to remove

198   any suspended particle. Measurement uncertainty, given by the manufacturer, is of the order of

199   7%. The overall calculated blank value is of the order of $2.27 \pm 0.33\,\mu gC.cm^{-2}$, which represents

200   16.4± 8.5% of the mean WSOC content. For each sample, duplicate analyses show a good

201   reproducibility.

202   ### 2.3.4. Water-soluble ionic species

203   Water-soluble ionic species (Na^+, NH_4^+, K^+, Mg^{2+}, Ca^{2+}, SO_4^{2-}, NO_3^- and Cl^-) are

204   analyzed using ion chromatograph (IC), following the analytical protocol described in Adon et

205   al. (2010). Briefly, the aerosol water-soluble fraction is first extracted from half-sampled Teflon

206   filter (the other part being used for trace element analysis), with a 10-min sonication in plastic

207   vials including 6 ml or 10 ml of purified water with a controlled resistivity of 18.2MΩ. Then

208   these vials are subjected to ionic chromatograph analysis or stored at +4°C if not analyzed

209   immediately. Cations are analyzed with Dionex DX-100 and anions with Dionex DX-500 with

210   a detection limit of 1 to 6 ppb depending on ionic species. Uncertainties in the range of 1-50%

211   is found depending on ionic species.

212   ### 2.3.5. Trace elements

213   The protocol to measure trace element concentrations is developed and performed at the

214   Laboratory of Environmental Geosciences of Toulouse. Half-sampled Teflon filters (the other

215   part being used for water-soluble ionic species, see below) are mineralized by acid digestion

216   with a 10 ml concentrated HNO_3 and 0.5 ml HF solution (Lamaison, 2006) using a closed vessel

217   microwave accelerated reaction system (MARS 5, CEM Corporation) at high pressure (700 psi)

218   (Celo et al. 2010). The digestion is realized in 3 steps: a rise in temperature at 130°C in 3min

219   and holding for 1 min, then, a second rise at 160°C in 1 min and holding for 30 seconds and

220   finally a third rise to 180°C in 1 min and holding for 3min. After a 12 h cooling period, the

221   solutions are evaporated at 80°C, and concentrated in 7 ml of 2% concentrated HNO_3 solution,

222   before analysis by ICP-MS which are performed with a 7500 ce Agilent Technologies

223   instrument equipped with a collision cell, and using In and Re as internal standards. The

224   detection limit is less than 10 ppt. For all the samples, the final blank values and detection limit

225   on filters are taken into account for final concentrations calculations. 13 trace metals are

226   considered in this work: Al, Ti, Cr, Mn, Fe, Ni, Cu, Zn, Ba, La, Th, Pb and Cd.

227   **2.3.6. Dust calculation**

228   Many methods can be used to quantify dust concentrations. We have selected three

229   methods (Sciare et al. 2005, Guinot et al. 2007, Terzi et al. 2010) to underline the uncertainties

230   linked to dust estimates.

231   (1) Sciare et al. (2005) method consists of using soluble calcium data obtained with Ionic

232   Chromatography (IC), to estimate the dust concentrations following the relationship:

233   dust = $10.96*nss-Ca^{2+}$, where $nss-Ca^{2+}$ ($=1.02*Ca^{2+}-0.038*Na^+$) refers to non-sea-salt

234   calcium concentration.

235   (2) Guinot et al. (2007) method is based on a chemical closure where fine and coarse

236   particle aerosols are separated in 4 components (EC, POM, WSI and dust). EC, WSI,

237   and total aerosol mass are directly experimentally determined (see below paragraphs).

238   POM concentrations are obtained from OC concentrations experimentally determined

239   and k, the OC/POM conversion factor. Dust concentrations are obtained from measured

240   Ca^{2+} concentrations and f, the abundance of calcium in dust. The k and f values are

241   obtained from a linear regression (L) between the reconstructed and the weighed aerosol

242   mass concentrations. Briefly, first step consists of focusing on the aerosol coarse

243   fraction. k is fixed to 1.8 and as a result of (L) just mentioned, f is obtained to be in the

244   range of 0.012 to 0.15 depending on our sites. Second step deals with the aerosol fine

245   fraction. The f values just obtained for the aerosol coarse fraction are applied to the fine

246   fraction and k ratios are estimated using (L) to be in the range of 1.2 to 2.1. Note that at

247   all of our sites, the correlation between Ca^{2+} and the missing mass between the weighed

248   and the reconstructed aerosol mass is sufficiently good ($r^2=0.9$) to support the

249   consistency of this simple approach for the evaluation of dust. Also, f and k values are

250   included in the range of values provided in the literature (He et al. 2001; Sun et al. 2004;

251   Guinot et al. 2007). However, it is important to mention that the range of f and k

252   coefficients are large which is due to the source mixing observed in this study.

253   (3) In Terzi et al. (2010) method, dust is obtained with the following relationship: dust =

254        $1.89[Al] + 1.21[K] + 1.95[Ca] + 1.66[Mg] + 1.7[Ti] + 2.14[Si] + 1.42[Fe]$. In our study,

255   all these elements are determined except Silica (Si). Consequently, we used mean Si

256   values obtained from different relationships available in the literature ($SiO_2 = 3*Al_2O_3$

257   for Alastuey et al., 2005, $Si = 4.0*Al$ for Zhang et al., 2003 and $Si = 2.03*Al$ for

258   Chiapello et al., 1997).

259   The results of dust concentrations estimated from the three methodologies above described are

260   summarized in the Table 1 for wet season (WS) 2016 and dry season (DS) 2017. Indeed, Ca,

261   Al, and Fe concentrations measured by ICP-MS are only available in WS2016 and DS2017 due

262   to experimental problems, whereas Ca^{2+} concentrations measured by IC are available for all

263   campaigns. As shown in table 1, the dust obtained from Ca^{2+} measured by IC (Sciare et al.,

264   2005) and by the Guinot et al. (2007) method is lower than that obtained from trace elements

265   (Terzi et al., 2010) for DS2017 whereas in the same order of magnitude in WS2016. Such

266   results are in agreement with methodological aspects. Indeed, Al, Fe, Ca … obtained by ICP-

267   MS include both soluble and insoluble particles whereas Ca^{2+} measured by IC only include

268   soluble particles. During the dry season, comparison of Ca measured by ICP-MS (not shown

269   here) is higher than that of the IC, by a factor of 1.7, 1.8, 2.2 and 1.1, at the ADF, AWB, AT,

270   and CT sites respectively. By contrast, this factor is low and constant (1.3) in the wet season

271   for all the sites. In our study, due to the lack of trace element data for WS2015 and DS2016,

272   dust estimations are performed from Guinot et al. (2007) method. This choice globally implies

273   an underestimate of dust concentrations by a factor of 1.5 to 3.5 in DS2017 as shown in Table

274   1.

275

276   **2.3.7. Aerosol chemical closure methodology**

277   As previously mentioned and detailed, aerosol chemical closure is performed following

278   the Guinot et al. (2007) methodology.

279

280   **2.4. Meteorological conditions**

281   In Figure 4, meteorological data (surface temperature, wind directions and speed) issued

282   from the NOAA Integrated Surface database (ISD; see https:// www.ncdc.noaa.gov/isd) and the

283   ASECNA (Agence pour la Sécurité de la Navigation Aérienne en Afrique et à Madagascar) are

284   presented for the South-West Africa region including Abidjan and Cotonou. As expected, this

area is under the influence of the Convergence Zone of two air masses of a different nature, i.e. Harmattan (hot and dry continental trade winds) from the north and Monsoon (humid maritime trade winds) from the south (Figure 4). Ground contact between these two air masses constitutes the intertropical front (ITF) of which the fluctuations during the year determine the seasons in the Gulf of Guinea (Tapsoba, 1997). During the dry season (from November to March), temperatures are relatively high with maximum around 30°C on the coast. The humidity is low, since the prevailing Harmattan wind blows from the desert, usually bringing dust (Figure 4, lower line). The period from June to September, especially in July is the wet season period when daytime temperatures are slightly lower, with maximum around 26/28°C on the coast (Figure 4, upper line). At this season, the humidity level is high across the region. On the coast, rains may occur from March to November.

During our campaigns (not shown here), temperatures are roughly the same at Abidjan and Cotonou, reaching 28°C and 26°C in the dry and wet seasons, respectively. Gentle to moderate wind speeds are observed during the measurement campaigns at the two cities, with average values of 15-20 and 15-22 km.h^{-1} at Abidjan and Cotonou, respectively. There is no precipitation at CT site during the studied periods. In Abidjan on the contrary, low rains occur both in wet and dry periods with cumulative precipitation higher in DS2017 (7mm), than in WS2016 (4.7mm) and WS2015 (2mm). There is no rain in DS2016 (https://www.historique-meteo.net/afrique/).

2.5. Backward trajectories

The Hybrid Single-Particle Lagrangian Integrated Trajectory (HYSPLIT) modelling system (Air resources laboratory, Draxler and Rolph, 2012) is used for the trajectory analysis. HYSPLIT model is run to compute 120 h back trajectories ending at Abidjan and Cotonou at 50 m a.g.l. (Figure 5). Global Data Assimilation System reanalysis database is used as meteorological input, with a 0.25×0.25 degrees horizontal resolution. Results presented in Figure 5, confirm that air masses mainly come from the north with a few from the south-west in dry season (January), whereas from the south-west and the south in wet season (July). Therefore, in January, Abidjan and Cotonou are mainly impacted by polluted air masses from surrounding areas and northern countries with possible dust and west African biomass burning influences, whereas in July, the impact of oceanic sources possibly polluted by long-range south African biomass burning aerosols may be observed.

3. Results

318   **3.1. Aerosol size distribution and mass concentration**

319   In Figure 6, the relative mass distribution of PM for Coarse (C), Fine (F) and Ultra-Fine

320   (UF) particle sizes in percentages are presented with bulk mass concentration averages

321   indicated in the black boxes for each site and for each campaign. As it may be seen, bulk

322   concentrations vary widely from site to site and from campaign to campaign. During the wet

323   season, the average total concentrations range from 82 to 676 µg.m^{-3} in 2015 and 56 to 358

324   µg.m^{-3} in 2016, with the maximum at the Abidjan Domestic Fire (ADF) site. While during the

325   dry season, values range from 168 to 269 µg.m^{-3} in 2016 and from 114 to 559 µg.m^{-3} in 2017,

326   with maximum concentration obtained at the Cotonou Traffic (CT) and ADF sites. In terms of

327   size distribution, concentration peaks may be observed for all aerosol size-fractions which are

328   found to exhibit different seasonal patterns. UF particles (<0.2 µm) represent the highest

329   contributor to the bulk mass at the ADF site, by up to 60 % (335.3 µg.m^{-3}) in DS2017. F particles

330   (1-0.2 µm) are the second most important contributor and both combined particle sizes account

331   for more than 85 % of the total mass at the ADF site. In this site, ultra-fine and fine fractions

332   are also found to be maximum during WS2015 and WS2016 by up to 90 and 83%, respectively.

333   Let us note that C particle contribution in bulk is relatively higher in the traffic and waste

334   burning sites than in ADF site (40%) whereas F and UF particle contributions are on the order

335   of 60%.

336   In terms of PM2.5, the results of this work are presented in Figure 7. The mass

337   concentration of PM2.5 averaged over DS2016 and DS2017 are 154 ± 74, 144 ± 42, 134 ± 7

338   and 211 ± 51 µg.m^{-3} at the ADF, AWB, AT and CT sites, respectively and 338 ± 24, 45 ± 3, 52

339   ± 4 and 70 ± 1 µg.m^3 over the wet seasons (2015-2016). The increase in PM2.5 is of the order

340   of 54% at ADF from dry to wet season, whereas a sharp reduction (more than 60%) is obtained

341   at AWB, AT, and CT sites.

342   **3.2. Carbonaceous aerosol**

343   **3.2.1. EC and OC concentrations**

344   In Figure 8, EC relative mass contributions are presented for each size, site and

345   campaign: wet season 2015 (WS2015), wet season 2016 (WS2016), dry season 2016 (DS2016)

346   and dry season 2017 (DS2017). Mean EC bulk mass concentrations are added in the black boxes

347   for each size and for each campaign. The most striking feature is that the ADF site

348   concentrations are higher than at the other sites in WS2016 and in DS2017, whereas of the same

349   order of CT site concentrations in the other seasons. Mean concentration at the CT site (16µg.m^{-}

350   ^{3}) is slightly higher than at the AT site (10µg.m^{-3}), whereas the lowest concentrations are found

351   at the AWB site. Results of the EC size distribution are very consistent among the different

352   sites (Figure 8). Whatever the site and the season, higher EC concentrations are found in C

353   (42%) and UF (43%) particles compared to F particles.

354   Same data are presented for OC concentrations in Figure 9. It may be underlined that

355   ADF OC values are always higher than in the other sites by a factor ranging from 6 to 30, for

356   all seasons and particle sizes, with highest and lowest values respectively in DS2017 and DS

357   2016. In terms of size distribution, maximum OC concentrations at the ADF site may be found

358   in UF (53%), then F (29%) and finally C (18%) particles. The same distribution is observed for

359   the traffic sites in DS2016, however, for the other campaigns, OC size distribution looks like

360   the EC ones with higher concentrations in UF and C particles than in F particles.

361   As shown in Figure 10, the highest OC/EC ratios are always obtained at the ADF site

362   with a value as high as 25 for F particles in WS2016 whereas the lowest values are found in

363   DS2017. This is the same feature for the other sites with ratios lower than 2 in DS2017. OC/EC

364   ratios in AWB site are higher than in the traffic sites. Note that values at AT site are higher than

365   CT values in the wet season whereas lower in the dry season. Finally, it is interesting to

366   underline that linear correlations between EC and OC are obtained in the ultrafine and fine

367   modes in all campaigns, particularly in DS2017 (r^2 = 0.8, 0.8, 0.9 and 0.9) at the ADF, AWB,

368   AT and CT sites, respectively. This suggests that different studied sources can be assessed as

369   significant sources of both EC and OC.

370

371   **3.2.2. Water-Soluble Organic Carbon**

372   Concentrations of WSOC and WSOC/OC ratios are presented in Table 2 for each size

373   (UF, F, C and PM2.5) and campaign. As seen, WSOC are always higher at the ADF site than

374   in other sites, at least by a factor of 12. Maximum values are obtained in WS2016 with an

375   average of 16.47, 17.08 and 79.68 µgC.m^{-3} for coarse, fine and ultra-fine fractions, respectively,

376   followed by WS2015 and DS2017. WSOC concentrations are the lowest in DS2016, with an

377   average of 4.14, 6.95 and 21.89 µg.m^{-3} for coarse, fine and ultrafine fractions, respectively. In

378   terms of seasonality, there is not a clear trend in WSOC values at the AWB and AT sites,

379   whereas at the CT and ADF sites, WSOC values are found to be respectively higher and lower

380   in dry seasons compared to wet seasons. It is also interesting to note that WSOC are maximum

381   in UF sizes in the AT, ADF and AWB sites. At the CT site, the highest values are found in the

382   coarse particulate fractions, except in DS2016.

383   As expected, WSOC is strongly correlated with OC (r=0.7 at ADF, 0.8 at AT, 0.5 at

384   AWB and 0.7 at CT), whereas correlations with EC are weaker, especially at the AWB and CT

385   sites with values ranging from 0.1 to 0.4, respectively. Finally, when looking at WSOC/OC

386   ratios (Table 2), maximum values are obtained at the ADF site with PM2.5 ratios as high as

387   43%, followed by the AT and AWB sites with 32%. The lowest value (23%) is found at the CT

388   site. Also, Table 2 shows that there is no clear seasonality in WSOC/OC values, excepted at

389   ADF where maximum values occur during the wet season. Note as for WSOC, that ratios are

390   maximum in UF and F fractions for all sites except at the CT site where the ratio for coarse

391   fraction is the highest.

3.3. Water-soluble ionic species

393   Figure 11 shows the relative contribution of the major ions to the total concentration

394   (also given) of the ions in the different particle modes (C and F) at the ADF, AWB, AT and CT

395   sites for the different measurement campaigns. Let us recall here that only C and F fractions

396   may be documented due to the our experimental protocol. Total concentrations present

397   maximum values in ADF and CT sites. Values in AWB and AT sites are of the same order of

398   magnitude and lower by a factor of 2 than in ADF and CT sites. The contribution of different

399   ions show significant variations from site to site. The dominant ionic species at the ADF site

400   over all campaigns is chloride (Cl^-), with a 26% contribution, followed by nitrate (NO_3^-) (16%),

401   calcium (Ca^{2+}) (13%) and potassium (K^{2+}) (12%). Sulfate (SO_4^{2-}), ammonium (NH_4^+), sodium

402   (Na^+) and to a lesser extent magnesium (Mg^{2+}) contributions are lower, ranging from 4 to 7%

403   of the total ion species. The lowest contribution is for organic acids with their total value lower

404   than 5%. NO_3^- is the major ionic component at the AWB and AT sites, representing 24% and

405   29% of the total water soluble inorganic concentration, respectively. The second major

406   contributor in AWB and AT is SO_4^{2-}, accounting for 21% and 17% of the ion mass, respectively

407   followed by Ca^{2+} (12% and 15%) and Cl^- (15% and 13%). In CT, Ca^{2+} is predominant with a

408   relative abundance of 24%, followed by NO_3^- (23%), SO_4^{2-} (19%) and Cl^- (13%). Na^+, NH_4^+

409   and K^+ contributions are lower and in the same order of magnitude in AT, AWB and CT sites,

410   ranging from 4 to 9% of the total ion species. Note that organic ion contributions at AT, CT and

411   AWB is of the same order than in ADF, with lower values at CT. It is interesting to underline

412   in the Figure 11, that NO_3^- contribution is always higher in the coarse than in the fine size.

413   Conversely, K^+ is always higher in the fine than in the coarse size. In CT, Ca^{2+} in the fine

414   fraction is as high as in the coarse fraction whereas in AT, AWB and ADF, Ca^{2+} coarse fraction

415   is predominant. Fine particle contribution may be noticed for Cl^- in ADF whereas in the other

416   sites, Cl^- is most likely dominated by coarse particles. Finally, SO_4^{2-} is mainly found in the fine

417   mode at the AT, AWB and CT sites, but in the coarse mode in ADF site.

418   In terms of seasonal variations, it may be shown in Figure 11 that higher Cl^- values are found

419   in wet seasons than in the dry seasons everywhere, except in ADF site where there is no marked

420   difference between seasons. For example, the mean relative total percentages of Cl^- at the CT

421   site are 38 and 24% in the WS2015 and WS2016, respectively, while these percentages decrease

422   significantly to 18 and 13% in the DS2016 and DS2017, respectively. The Cl^-/Na^+ ratios are

423   about 1.5 everywhere in both seasons, in agreement with the typical sea water ratio (1-1.2)

424   (Hara et al.,2004), except at the ADF site where these ratios increase to 4 and 5 in wet and dry

425   season, respectively and at the AWB site in the dry season (2). K^+ and Ca^{2+} are always higher

426   in dry season than in wet season except for Ca^{2+} in ADF where values are of the same order.

427   Finally, the same trend is observed for NO_3^- and SO_4^{2-} with higher values in dry than in wet

428   seasons at AWB and CT sites whereas values at ADF and AT sites are of the same order of

429   magnitude for the two seasons.

430   **3.4. Trace element concentrations**

431   Table 3 shows the mean values of the major trace elements in bulk aerosol at the

432   different studied sites in WS2016 and DS2017, with their corresponding relative abundances in

433   the total aerosol mass into brackets. Let us recall that data are not available in WS2015 and

434   DS2016. The concentrations of trace elements span a wide range, from 0.2 to 25.2 $\mu g.m^{-3}$.

435   Among the measured elements, Al, K, Na and Ca are the most abundant, followed by Fe and

436   Mg. In DS2017, Al and Na concentrations are higher in AWB than in the other sites. The

437   minimum value for these species is found in ADF site. Values in traffic sites are of the same

438   order of magnitude and higher than in ADF site. Maximum of Ca and K values may be found

439   in CT and ADF site respectively. It is interesting to note that Al, K, Na concentrations are higher

440   in the dry season than in the wet season. Such feature is less clear for Ca, whose seasonal

441   variability is less marked except in AWB and AT sites. In terms of Mg, maximum values are

442   observed in ADF site and of the same order of magnitude whatever the season. Fe abundance

443   is higher in AWB and CT sites than in ADF and AT sites and higher in DS2017 than in WS2016

444   everywhere. The other metals (Ti, P, Zr, Zn, Cr, Mn, Pb and Ni) represent less than 0.5% and

445   2% of the total mass in WS2016 and DS2017, respectively, at all sites, with Cr, Mn, Pb and Ni

446   exhibiting less seasonal variability compared to the rest of the metal elements.

447   To assess the relative contribution of crustal and non-crustal origin of elemental aerosol

448   loadings, source enrichment factor (EF) of a trace element X have been first calculated with the

449   following formula using both literature data of the typical elemental composition of the upper

450   continental crust (Mason and Moore, 1982; Taylor, 1964), measured elemental composition

451   from this study and Al as a reference element :

452

$$EF_X = \frac{\dfrac{[X]_{atm}}{[Al]_{atm}}}{[X]_{soil}\Big/[Al]_{soil}}$$

453   Where $[X]_{atm}$ and $[Al]_{atm}$ are the concentrations of the chemical element X and Al in the

454   atmosphere, respectively, and $[X]_{soil}$ and $[Al]_{soil}$ are the typical concentrations of the element

455   X and Al in the earth's crust, respectively. Al is frequently used as a reference element assuming

456   that its anthropogenic sources in the atmosphere are negligible (Gao et al., 2002; Cao et al.,

457   2005; Xu et al., 2012). In all sampling sites, EF values typically lower than 5 are obtained for

458   several trace elements (Be, Sc, Ti, V, Fe, Ga, Sr, Nb, Rh, Ba, La, Ce, Pr, Nd, Sm, Eu, Gd, Tb,

459   Dy, Ho, Er, Tm, Yb, Lu, Ta, Th and U). This suggests a natural origin of these species (Freitas

460   et al., 2007; Gao et al., 2002). The most enriched elements (EF>100) are Sb, Sn, Zn, Se, Te,

461   Cd, Pb, Bi and Mo at nearly all of the sites, indicating significant anthropogenic origin (Wang

462   et al., 2006). These elements are mainly emitted into the atmosphere through fossil fuel

463   combustion, traffic emission, wear of brake lining materials and industrial processes (Watson

464   and Chow, 2001; Samara and al., 2003). Secondly, source contributions have been estimated

465   from these EF values following the method described by Arditsoglou and Samara (2005). Note

466   that this study refers to ratios for a limited list of sources, perhaps not including the African

467   source specificities. As a result, it may be seen that 30% of trace element concentrations is of

468   anthropogenic origin at ADF site whereas about 17 % at the others sites.

469   **3.5. Dust**

470   Figure 12 shows dust concentrations calculated from Guinot et al. (2007) methodology

471   (see paragraph 2.3.6) for C and F particle sizes at the different sites for each season. Note that

472   as for WSI and trace element and due to our sampling procedure, there are values for fine and

473   coarse particles for all seasons excepted for WS2016 with values for coarse particles only.

474   During the wet season, coarse dust concentrations range from 5 to 25 $\mu g.m^{-3}$ in 2015 and 9 to

475   37 $\mu g.m^{-3}$ in 2016, with higher values at the CT and ADF sites in 2015 and at AT, CT and ADF

476 in 2016. In WS2015, fine dust concentrations range from 12 to 49 with maximum values at

477 ADF and CT sites also. During the dry season, values range from 38 to 156 $\mu g.m^{-3}$ in 2016 and

478 from 41 to 116 $\mu g.m^{-3}$ in 2017, with maximum concentrations obtained at the CT site, followed

479 by AWB site. When considering mean values of the dry seasons, total dust at CT is 2.4 times

480 the values found at AT, 1.6 times at AWB and 3.4 times at ADF. Seasonal comparison shows

481 that total dust concentration is higher in the dry seasons than in WS2015 by a factor of 3 in AT,

482 2.6 in CT and 4 in AWB, but of the same order of magnitude in ADF site.

483   **3.6. Aerosol chemical closure**

484   The aerosol chemical closure obtained using the Guinot et al. (2007) method (see below)

485 at the different sites for each season is presented in Figure 13. Results show clear intra- and

486 inter-annual variations at all of the sites, as well as significant differences among the sites. In

487 total, dust accounts for 39 to 75% of the bulk PM mass at both traffic sites, with no clear

488 seasonal cycle and higher contributions in Cotonou (Figures 13c and 13d). These percentages

489 vary from 32 to 64% at the AWB site, and from 18 to 35% at the ADF site, with percentages

490 1.8 times higher in the dry season than in the wet season in AWB and no clear seasonal

491 difference in ADF (Figures 13a and 13b). Carbonaceous aerosol, the sum of EC and POM,

492 show large contributions at the ADF site (from 49 to 69% of the total PM mass), with relatively

493 similar proportions in each season (Figure 13a). The absence of a clear seasonal pattern is also

494 observed in CT whereas carbonaceous aerosol is slightly higher in WS than in DS in AWB (23

495 and 16% respectively) and AT (37 and 21% respectively) (Figures 13b-d). Carbonaceous

496 aerosol contribution accounts for about 11- 49% of the total mass at both traffic sites with higher

497 values in AT (mean of 30%) than in CT (13%). The ion percentages in PM fractions present

498 the same pattern at AT, CT and AWB sites with higher values in wet than in dry seasons. In

499 these sites, we may notice that mass concentration in coarse particles is larger in the wet season

500 whereas of the same order of magnitude than the one in fine particles in the dry season. In ADF,

501 no marked difference may be found between the seasons and the sizes (Figure 13).

502

503 **4. Discussion**

504 A discussion of the results site by site (Abidjan domestic fire site, traffic sites both together and

505 waste burning site) will be first proposed. We will scrutinize (1) the proximity between the sites

506 and the sources; (2) the source specificity with more or less incomplete combustion (e.g. wood

507 combustion and two-wheel vehicle emission factors are higher than gasoline emission factors

508   (Keita et al., 2018); (3) the relative influence of other local sources or transported sources to

509   the studied sites such as dust and biomass burning; (4) the occurrence of continental air masses;

510   (5) the variation of the boundary layer height (as reported by Colette et al., 2007); and (6) the

511   meteorological parameters (e.g. temperature, relative humidity and wet deposition) to explain

512   the differences of pollutant concentrations and their seasonal and inter-annual variabilities.

513   In a second part, we will present comparison of our values with other DACCIWA values and

514   also with literature values for other intensive campaigns in Africa.

515

516   **4.1. Abidjan Domestic Fires (ADF)**

517   As shown in the above paragraphs, maximum values are obtained at the ADF site, for aerosol

518   mass, EC, OC, WSOC, water-soluble ionic species (e.g. Cl^-, NO_3^-, Ca^{2+} and K^+) and some trace

519   elements such as Mg and K (whereas Al, Na and Fe are lower than in the other sites). Also,

520   aerosol PM2.5 values are well above the annual and daily WHO guidelines of 25 and 10 $\mu g.m^-$

521   ^{3} respectively, whatever the season.

522   Such pattern is due to the proximity of the ADF site to the studied combustion source: in that

523   area, the use of wood combustion is very active due to commercial activities of women drying

524   fish and meat and domestic cooking. This is also confirmed by the high relative importance of

525   total carbon in aerosol mass whatever the size (49 to 69%) and by values of source enrichment

526   factor. Indeed, at least 30% of trace element concentrations are of anthropogenic origin at ADF

527   site. In addition, wood combustion is well known to be highly polluting due to incomplete

528   combustion: this is shown here by the measurements of very high OC/EC ratios at ADF, on the

529   order of the one measured at the source level by Keita et al. (2018). This is also shown by

530   WSOC relative importance which is expected for wood burning following Yu et al. (2018),

531   Tang et al. (2016), Feng (2006) and Saxena and Hildemann (1996) and by the strong correlation

532   of WSOC with biomass burning K^+ tracer.

533   Chloride is most likely associated with sea salt origin (normal chloride concentrations represent

534   at least 55% of marine aerosols following Goldberg (1963)) or secondary aerosol production

535   (Li et al., 2016). Since chloride relative concentration at the ADF site remains lower than the

536   that of sea-sal aerosols, the secondary production source would be the better explanation for

537   high chloride concentrations observed at ADF. The size distributions of Cl^-, K^+, NH_4^+ and SO_4^{2-}

538   support this conclusion : the predominance of these elements in fine particle mode at the ADF

539   site would be associated with anthropogenic emissions, particularly biomass combustion and

540   domestic fires, or with secondary inorganic aerosols origin. This is confirmed by Cl^-/Na^+ ratio

541   values as shown earlier. Contrarily, Ca^{2+} and NO_3^- contributions to the total ions at the ADF

542   site peak mainly in the large particle fraction and may be attributed to quasi natural origin,

543   primarily to dust emissions and nitrate formation by reaction processes, respectively. In

544   addition, Na^+ and Mg^{2+} display similar size distributions at the ADF site, with the major

545   contribution in the coarse particle fraction, suggesting the common sea salt origin of these two

546   elements (Belis et al., 2013).

547   As we have shown above, the lower proportion of metal elements at the ADF site (6.5% of the

548   bulk concentration) can be explained by the less dominant influence of re-suspended dust

549   particles compared to traffic sources. Elements such as Cr, Mn, Pb and Ni have less seasonal

550   variability than other metallic elements. These small proportions of these non-crust elements

551   suggest a low contribution of elements emitted mainly by anthropogenic activities such as

552   industrial processes (Viana et al., 2007 and 2008; Minguillón et al., 2014). Finally, the Zn/Cd

553   ratio has been also examined. A value of 29 close to ratio reported for gasoline vehicle (27, Qin

554   et al., 1997) is obtained for the ADF site, indicating that this site is also impacted by traffic

555   sources.

556   High values of WSOC/OC ratios are expected to be harmful to health (Ramgolam et al., 2009,

557   Val et al., 2013). This effect is being enhanced by the particulate size measured at this site (Kim

558   et al., 2003; Wilson et al., 2002). Indeed, the relative mass distribution of PM and OC particle

559   sizes shows a major contribution of particles less than 1 µm (as high as 85% of PM). This could

560   be due to the fact that carbonaceous aerosols are formed near emission sources and are mainly

561   of submicron size (Boucher, 2012). Nevertherless, note that EC also presents large coarse

562   particle contribution. This could be due to the importance of wood burning at this site with less

563   efficient combustion and large particle emissions (Watson et al., 2011).

564   In terms of seasonality, higher concentrations of aerosol mass, OC, WSOC, EC and total water

565   soluble ionic species (SO_4^{2-}, NH_4^+ and NO_3^-) are observed in WS2015 and WS2016 than in

566   DS2016. This may be explained by a more incomplete combustion in the wet seasons than in

567   DS2016 due to the use of moist wood for cooking and smoking fish, which leads to large

568   amount of smoke and higher particulate emission factor values. Note that DS2017 values are

569   as important as the ones of wet seasons, which will be explained later in the text. With regard

570   to WSOC, their variabilities may be also linked to meteorological factors, such as solar radiation

571   (Tang et al., 2016; Favez et al., 2008) and relative humidity (Liang et al., 2016). At ADF site,

572   temperatures are roughly similar in both seasons. However, RH variability may play a role since

573   it is higher in wet season than in dry season. Finally, our results indicate no clear seasonal cycle

574   for Cl^-, which confirms its anthropogenic origin, as previously shown.

575

4.2. Traffic sites (Abidjan traffic and Cotonou Traffic sites)

Let us recall first that the two traffic sites have been chosen since they are representative of the traffic diversity in West Africa. At CT site, both personal cars, taxis and an important two-wheel fleet may be found whereas at AT site, there are buses, taxis and personal cars. Also, the distance between the site and the traffic sources is the same for the two traffic sites, slightly larger than the distance between the site and the wood burning sources at ADF site.

In these two sites, concentrations are high with PM2.5 values well above the WHO guidelines. Average aerosol mass, EC, OC, dust and water soluble ionic concentrations (with NO_3^- and Ca^{2+} maximum at AT and CT sites respectively) are higher at CT than at AT site by a factor of 1.5 to 2. Note that this poor air quality found in Cotonou has been reported by Cachon et al. (2014). The higher values found in Cotonou could be due to more intense traffic in Cotonou than in Abidjan. Also in Cotonou, this traffic is associated with the lack of public transportation and the use of highly polluted mopeds (aged over 15 years) (Gounougbe, 1999; Avogbe et al., 2011), despite the effort in the last 10 years to restrict their use. Several studies such as MMEH (2002) have shown that more than 94,000 mopeds and 350,000 second-hand vehicles are in circulation in Cotonou. Other factors contributing to the local pollution include outdoor restaurants using charcoal and motorcycle garages, which are more present around the Cotonou traffic site compared to Abidjan site. It also includes anthropogenic dust. Indeed, at Cotonou, the lack of road infrastructure favours the resuspention of dust particles. Finally, other sources may potentially influence aerosol seasonal composition in these two sites, including marine aerosols, transported dust and biomass burning particles as well as anthropogenic aerosols from the surrounding countries (Figure 5). Note also that source enrichment factor values show that about 17% of trace element concentrations are of anthropogenic origin at both traffic sites and that the relative importance of total carbon in mass is higher at AT than at CT sites.

Aerosol mass, composition and size depend on the season and the two traffic sites are differently affected. The EC and OC concentrations measured in both traffic sites and averaged per season are higher in dry than in wet season. Such variations may be explained by several factors: particulate wet deposition occurring during the wet season, reduction of traffic flow due to school vacations and meteorological influence. Higher EC and OC concentrations are obtained at CT than at AT sites in dry seasons whereas no statistical difference may been found between the two sites in wet seasons. Such a result is mainly explained by figures 5. In wet seasons, similar backtrajectory pattern may be observed for both sites whereas in dry seasons, CT traffic site only would be influenced by Nigerian anthropogenic sources.

609   In terms of WSOC concentrations, concentrations at the AT site are on average higher than

610   those recorded at the CT site in the wet season, but lower in dry season. The presence of dust

611   can produce semi-volatile organic gas scavenging and therefore WSOC and OC enhancement.

612   Such a phenomenon can explain the highest WSOC concentrations observed in dry season at

613   the CT site where dust concentrations are highest (see dust paragraph). Moreover, this can also

614   explain why the maximum WSOC are in coarse particles at CT, while at AT maximum values

615   are in ultra-fine particles.

616   Total WSI concentrations are larger at AT site in the wet than in the dry season with higher

617   values in coarse particles. At CT site, total WSI concentrations in fine particles are higher in

618   the dry than in the wet season whereas same values are obtained in coarse particles for both

619   seasons. Note that CT values are generally higher than AT values with a more important

620   contribution of fine particles in the dry season. These WSI variations can be explained by the

621   relative importance of Ca^{2+}, SO_4^{2-} and NO_3^- in both sites.

622   First, Ca^{2+} contribution to total WSI is higher in CT site than in AT site with no clear seasonal

623   variation at CT site and higher values in dry season than in wet season at AT site. Also at CT,

624   fine and coarse Ca^{2+} particles are in the same range, whereas coarse Ca^{2+} particles are

625   predominant at AT site. Such feature may be explained by the impact of dust sources including

626   long-range dust transport at Abidjan and a combination of long-range dust transport and road

627   resuspension at Cotonou.

628   Second, the relative contribution of SO_4^{2-}, NH_4^+ and NO_3^- as a percentage of total WSI in the

629   different particle modes is reduced in the wet season. During the wet season, the clean winds

630   surrounding the ocean before reaching the measurement sites could contribute to lower the

631   proportion of these species, in addition to the scavenging processes during the rainy days.

632   Unlike the wet season, a relatively good correlation with r^2 of 0.87 (SO_4^{2-} versus NH_4^+), 0.73

633   (NO_3^- versus NH_4^+) and 0.87 (SO_4^{2-} versus NO_3^-) has been found in coarse particles, indicating

634   similar sources for these three species during the dry season. In order to try to identify these

635   sources, the ratio of SO_4^{2-}/Ca^{2+} and NO_3^-/Ca^{2+} has been determined. The average SO_4^{2-}/Ca^{2+}

636   and NO_3^-/Ca^{2+} ratios in combined coarse particles (1.07 and 2.58 during the wet season and 0.33

637   and 1.60 during the dry season) are higher than the corresponding ratios for typical soil (0.026

638   and 0.003, respectively). On the other hand, the SO_4^{2-}/Ca^{2+} ratio increases in the fine particles

639   (5.07 during the wet season and 2.53 during the dry season), while that of NO_3^-/Ca^{2+} remains

640   almost constant (2.86 during the wet season and 1.65 during the dry season). This implies that

641   the atmosphere at AT and CT sites is enriched by SO_4^{2-} formed as anthropogenic secondary

642   particles, possibly from sulfur containing pollution sources (Seinfield and Pandis, 1998),

particularly in fine particle mode, and by NO_3^- mostly coming from nitrogen containing sources in all particle sizes. The higher contributions of these elements during the dry season could result from a combination of several factors: 1) an atmosphere loaded with dust favoring heterogeneous chemistry to obtain secondary aerosol and the rise of biomass burning emissions; 2) the increase of photochemical activity and higher concentrations of hydroxyl radicals in the dry season, which can oxidize SO_2 from combustion (Arndt et al., 1997) to SO_4^{2-} (Li et al., 2014) ; and 3) the wind transport of anthropogenic secondary particles from the industrial zone located upstream from our sites. Finally, the proportion of Cl^- relative to the total mass of ions is highest for coarse particles at both traffic sites especially during the wet season, suggesting that Cl^- at AT and CT sites if from natural origin and probably from sea salt emissions.

If we focus now on dust during the two wet seasons, concentrations are higher in 2016 than in 2015 at CT and AT sites for coarse particles (no data of fine particles are available in WS2016). This is consistent with observed aerosol optical depth (AOD) values at CT, which increased by a factor of 2 between 2015 and 2016. No AOD value is given by Léon et al. (2019) at Abidjan in WS2015 to allow such comparison in Abidjan. Moreover, during the wet season, an Angström coefficient (AE) on the order of 1 has been found at CT site, indicating smaller particles that could be due to road resuspension. It is interesting to note that during WS2016, AOD and AE are respectively higher and lower at Abidjan than at Cotonou. Again, this is consistent with our dust concentrations at CT site. In Abidjan, we could assume that another source of Ca^{2+}, which is not taken into account in our dust calculations, may explain our dust concentration data. That may be the result of anthropogenic Ca^{2+} emissions from residential combustion, more important in 2016 than in 2015 as shown earlier (http://naei.beis.gov.uk/overview/pollutants?pollutant_id=84).

The relative contribution of dust generally peaks in the coarse mode and, to a lesser extent, in the fine mode, reflecting their natural origin. It is interesting to note that the dust contribution observed in this study for the year 2016 at the Abidjan site is in agreement with the results of Xu et al. (2019) which show a PM2.5 dust contribution of 35-50% compared to our values of 18-52%.

4.3. Abidjan Waste Burning site

Concentrations measured at AWB site are slightly lower than values found in the other sites. This can be explained by the larger distance of the site to the main studied source (here waste burning source) than in the other sites. However, PM2.5 values are also higher than WHO guidelines. +

677 Aerosol mass, EC and OC concentrations are higher in dry than in wet season, which suggests

678 less waste burning activities during the wet season or impacts of other local anthropogenic

679 sources or long-range biomass burning sources. Highest values are found in DS2017 with the

680 lowest OC/EC ratio, as at AT site. OC/EC ratio is highly variable at AWB (1-10) which

681 confirms that AWB site may be impacted by different types of sources as well as by secondary

682 aerosol organic formation which can be detected for OC/EC higher than 2 (Turpin et al. 1990;

683 Hildermann et al. 1991; Chow et al. 1996). Note that OC/EC typical for waste burning source

684 is of the order of 8 (Keita et al., 2018).

685 It is also observed that at the AWB site, PM mass concentrations are mainly distributed in C

686 mode (30-44%) over the entire period of study, excepted during the WS2015, and to a lesser

687 extend in F mode (21-44%). EC and OC being mainly distributed in C and UF modes. Water-

688 soluble fraction of organic carbon is important (32%) and on the order of the one found at AT

689 site. Same for WSI concentrations and WSI composition. At AWB, WSI values are globally

690 slightly higher in wet than in dry season. However, it is interesting to underline that Ca^{2+} is

691 much higher in dry season than in wet season, especially in DS2017. This is in agreement with

692 dust concentrations and trace element concentrations, which have been found to be maximum

693 at AWB, reaching 35.8% of the total PM mass in the dry season. These maximum percentages

694 are due to the large contribution of both Al and Na crustal elements which account for about

695 26%. Also note that Cu/Sb of 0.08 in DS2017, which indicate an influence of re-suspended

696 particles. A Zn/Cd value of 56 is obtained for the AWB site which is in close agreement with

697 values reported for oil burning (Watson et al., 2001, Samara et al., 2003). That could indicate

698 that oil might be one of the waste burning materials.

699 Our result suggests that AWB aerosol mass is influenced by a mix of sources, including fuel

700 combustion and mineral salt from sources around the measurement site, associated to long-

701 range source impact of dust and biomass burning which will be further discussed in the next

702 paragraph.

703

704 **4.4. Interannual variability of aerosols in Abidjan and Cotonou**

705 EC and OC concentrations are generally higher in DS2017 than in DS2016 for all the sites. This

706 is not due to the meteorological condition, which is similar in both years. This is also not due

707 to biomass burning impacts. Indeed, when looking at MODIS burnt areas for our period of study

708 (http://www.aeris-data.fr/redirect/MODIS-MCD64A1), burnt areas of west African savannas

709 are higher in 2016 than in 2017. Therefore, carbonaceous aerosol concentrations should be

710 higher in 2016. Then, this could be due to a counter effect between biomass burning emission

711   strength and air mass transport efficiency. As a result, biomass burning impact could not explain

712   the difference in EC and OC during the dry season between 2016 and 2017. Rather, this is due

713   to the variability of local sources. In DS2016 in Abidjan, there was a general strike of civil

714   servants of the State with important consequences on urban activities. Lower activities were

715   observed (lower fish smoking emissions, lower traffic ..) in DS2016 compared to DS2017, thus

716   explaining the lower EC and OC concentrations at Abidjan sites. In Cotonou, highest

717   carbonaceous aerosol values in DS2017 may be explained by backtrajectory patterns: Cotonou

718   would be impacted by air masses coming from the high polluted Lagos (Nigeria) area in that

719   period whereas from less polluted northern areas in DS2016. Such an assumption is validated

720   by the AOD values at 550nm from MODIS satellite images (http://www.aeris-

721   data.fr/redirect/MODIS-MCD64A1), which show very high particulate concentrations in the

722   Guinean Golf (Figure 14).

723   This figure also shows the AOD difference between Cotonou and Abidjan for DS2017, with

724   higher values at Cotonou than in Abidjan for the campaign period, in agreement with our

725   measurements of aerosol mass, EC, OC and dust. This is confirmed by the DACCIWA

726   sunphotometer AOD and Angström coefficient (AE) measurements at Abidjan and Cotonou

727   (Léon et al., 2019; Djossou et al., 2018). Indeed, in DS2017, during our period of

728   measurements, mean AOD in Cotonou is of the order of 1.3 versus 0.9 in Abidjan for an AE of

729   0.6 for both sites, which clearly indicates the presence of coarse dust particles.

730   Finally, aerosol mass and dust concentrations have been seen to be higher in DS2016 than in

731   DS2017 in Abidjan whereas values are on the same order of magnitude at Cotonou. Such high

732   values at Abidjan in DS2016 can be explained by the back-trajectory pattern with air-masses

733   all coming from northern dusty areas in DS2016 (Bodélé depression in Tchad, Prospero et al.

734   (2002), Washington et al., (2003), Knippertz et al. (2011), Balarabe et al., (2016)) and/or from

735   northern dusty countries (Mali, Niger) (Ozer, 2005), whereas in DS2017, contribution of

736   southern marine clean air-masses may also be noted.

737   In the wet season, aerosol mass, EC and OC are higher in WS2015 than in WS2016. This may

738   be due to particulate wet deposition, more efficient in WS2016 which have been seen earlier to

739   be more rainy (4.7mm) than in WS2015 (2mm). Moreover, at AT site, dust concentrations are

740   higher for coarse particles in WS2016 than in WS2015. Such variations may be explained by

741   long-range dust sources and/or road dust resuspension processes. As no dust event has been

742   noticed, local source explanation seems to be more evident.

743   In AT, CT and AWB, OC/EC ratios are globally on the same order for WS2015, WS2016 and

744   DS2016, with values lower than for DS2017. This could be due to lower traffic activities linked

745   to the DS2016 strike and the wet season vacation periods. Indeed, much higher OC/EC ratios

746   measured in DS2017 are typical of those of diesel vehicles (Mmari et al., 2013; Keita et al.,

747   2018). Finally, it is interesting to note that OC/EC ratios measured in this study are in the range

748   of those previously reported for other megacities such as Agra in India with 6.7 (Pachauri et al.,

749   2013), Helsinki in Finland with 2.7 (Viidanoja, 2002), Cairo in Egypt with 2.9 (Favez, 2008),

750   Paris in France with 3.5 (Favez, 2008), and Milan in Italy with 6.6 (Lonati et al., 2007).

751

752   **4.5. Comparison with literature data**

753   Firstly, the comparison between our data and other DACCIWA results including other time

754   sampling focuses on PM2.5 levels, since these particle sizes are relevant for health impact

755   studies (Xing et al., 2016). In addition to our values, Figure 7 presents data from Xu et al. (2019)

756   using personal samplers collected in the same area and at the same dates in 2016 during 12h on

757   women at the ADF site, students at the AWB site and drivers at the CT site, and from Djossou

758   et al. (2018) study based on one week exposed filters collected at the same areas and for the

759   same periods as this study. We note that PM2.5 directly measured on women are 2.3 and 0.9

760   times our values obtained at the ADF site in dry and wet seasons, respectively, and 3.4 and 4.9

761   times higher on students than at the AWB site, and 1.6 and 2.1 times higher on drivers than at

762   the CT site. Also, our values are on average 1.6, 3, 5 and 8 times higher than weekly-integrated

763   values of Djossou et al. (2018) including our 3 days of measurements at the AWB, ADF, AT

764   and CT sites respectively. As it may be seen, the lowest concentrations are observed in Djossou

765   et al. (2018), whereas the highest concentrations are recorded in Xu. et al. (2019). This is valid

766   for all sites, seasons and campaigns. Differences between our values and Djossou values may

767   be explained by the sampling times of the two studies. Indeed, as recalled, Djossou

768   measurements are weekly integrated, taking into account diurnal activities during all the week,

769   including week-end and nights which have expected lower PM2.5 concentrations. Our study

770   includes only maximum pollution conditions for each site. The highest differences occur for

771   the traffic sites. This may be clearly understood since diurnal and weekly variations of traffic

772   sources are the most variable. Comparison between our values and Xu et al. (2019) values is

773   also interesting. Indeed, it is at the ADF site that on-site and women PM2.5 concentrations are

774   the closest, which shows that this site is the most representative of the pollution exposure to

775   women. The biggest differences are found at the AWB site. As already mentioned, distance

776   from the site to the waste burning source is more important than for other sites, which explains

777   why concentrations obtained on students who are leaving close to the sources are much higher

778   than on-site concentrations. At the Cotonou traffic site, measurements taken from people are

also higher than on site measurements. Such differences can be explained by additional pollution exposure as people move around. Note that the sampling technique may also play a role in such a comparison. In terms of seasonal variation, our results are in agreement with long-term EC measurements obtained by Djossou et al. (2018) for the same sites and period. Finally, Table 4 compares our mean PM2.5 results obtained from 3-hour sampling for three consecutive days to literature data for different traffic sites in the world given at a daily scale. It is interesting to note that our values are situated at the higher end of the range of PM2.5 data observed from the other sites.

Secondly, Table 5 compares our OC and EC values to those obtained by Djossou et al. (2018) and Xu et al. (2019) as previously described for the same period and the same sites. Again, it is interesting to note that Djossou's values are in general lower than ours. Indeed, for the wet and dry seasons, our OC measurements are 4 and 1.4 times higher than Djoussou's at the AT site, 2.1 and 5.7 times higher at the CT site, and 2.5 and 2.5 times higher at the ADF site, respectively. As for PM2.5, this can be explained by the different sampling times between our experiments that were performed at the peak of urban activities, while Djossou's dataset represents weekly integrated values. Differences at the ADF site are largely explained by the temporal pattern of fish smoking activities which take place every day, only in the morning, as such the associated pollution is not well represented in the weekly sampling. Finally, there are less differences at the AWB site between both datasets. As above explained, there are no marked temporal variations of concentrations at AWB site. The predominant waste burning emissions impacting our site can occur night and day, week-days and week-end since origin of such burning can be either anthropogenic or from spontaneous combustion. It may be also recalled that another reason of agreement between both datasets may come from the large distance between the site and the local and regional sources. Comparisons made between our values and those of Xu's personal data show that both OC and EC are of the same order at the ADF site, whereas Xu values are higher than ours at the CT and AWB sites. This result is in agreement with what we found with PM2.5 concentrations as detailed above. Finally, Table 6 presents OC and EC for the PM2.5 comparison between our values and other recent studies dealing with traffic sites in other regions of the world and with similar operational conditions. We find that our values are situated in the middle of the range observed in these different studies. Briefly, as presented in Table 7, it is interesting to compare our WSOC concentrations to literature data for different traffic sites of the world. We note that our values are on the same order as values found in Asia and higher than those found in Europe.

812   Thirdly, the percentages of the total WSI to PM mass (15-20%) at the three Abidjan sites (ADF,

813   AWB and AT) are in the same order of magnitude than the data from PM2.5 personal exposure

814   samples collected at the same locations in 2016 by Xu et al. (2019). Our results also are very

815   close to the ionic contribution of 9% of the PM10 mass found at the urban curbside site in Dar

816   es Salaam in Tanzania during the wet season 2005 by Mkoma (2008).

817

818   **5. Conclusion**

819   This paper presents the mass and the size-speciated chemical composition of particulate matter

820   (PM) obtained during the dry and wet seasons in 2015, 2016 and 2017. During each campaign,

821   3-hour sampling at the peak period of pollution for three consecutive days was performed at

822   three sites in Abidjan, representative of domestic fire (ADF), waste burning (AWB) and traffic

823   (AT) sources, and at one traffic site in Cotonou (CT).

824   It is important to underline that our results and their temporal variations are very sensitive to

825   (1) the source activities whose pollution levels are highly linked to socio-economic status of

826   each city; (2) the impact of imported pollution (sea-salt, biomass burning, dust, anthropogenic

827   emissions from neighboring countries), according to air mass origins; and (3) the particle wet

828   deposition.

829   The comparison between our results and other DACCIWA measurements underlines the

830   importance of the distance of the chosen site to the sources. At the source level (such as ADF),

831   pollution results at the site are in agreement with exposure of people living at this site. However,

832   at the other sites, comparison is more difficult since the sites are under the influence of a mix

833   of transported sources. That shows the key importance of exposure studies to estimate air

834   quality and health impacts. That shows also the need of long-term studies to really understand

835   role of imported sources in urban air quality.

836   The main striking feature is that PM2.5 values are well above the annual and daily WHO

837   guidelines of 25 and 10 $\mu g.m^{-3}$, respectively, whatever the site and the season. Also, measured

838   concentrations from this study are situated in the middle to the high part of the range of

839   worldwide urban aerosol concentrations given at a daily scale. In addition, we have stressed the

840   importance of ultra-fine and fine particles in the studied aerosol and of species such as

841   particulate organic matter and water soluble organic carbon, which are well known to be

842   particularly harmful. This is again a warning signal for pollution levels in African capitals if

843   nothing is done to reduce emissions in the future.

844   Our study constitutes an original database to characterize urban air pollution from

845   specific African combustion sources. The next step will be to cross such an exhaustive aerosol

chemical characterization to biological data in order to evaluate the impact of aerosol size and chemical composition on aerosol inflammatory properties.

Acknowledgements. The research leading to these results has received funding from the European Union 7th Framework Programme (FP7/2007-2013) under Grant Agreement no. 603502 (EU project DACCIWA: Dynamics-aerosol-chemistry-cloud interactions in West Africa). The authors greatly thank all the colleagues and operators who contribute to sampling during the different campaigns.

Author Contributions

J.A. and C.L. conceived and designed the study. J.A., C.L. and E.T.D. contributed to the literature search, data analysis/interpretation and manuscript writing. J.A., C.L., A.B. and E.T.D. contributed to manuscript revision. J.A., C.L., J.F.L, H.C, V.Y., A.A, C.G, C.Z, E.C and S.K. carried out the particulate samples collection and chemical experiments, analyzed the experimental data.

Additional Information

Figure S1 and Appendix A-D accompany this manuscript can be found in SupplementaryInformation.

Competing financial interests

The authors declare no competing financial interests

References

Adon, M., Galy-Lacaux, C., Yoboué, V., Delon, C., Lacaux, J. P., Castera, P., Gardrat, E., Pienaar, J., Al Ourabi, H., Laouali, D., Diop, B., Sigha-Nkamdjou, L., Akpo, A., Tathy, J. P., Lavenu, F. and Mougin, E.: Long term measurements of sulfur dioxide, nitrogen dioxide, ammonia, nitric acid and ozone in Africa using passive samplers, Atmos. Chem. Phys., 10(15), 7467-7487, doi:10.5194/acp-10-7467-2010, 2010.

Alastuey, A., Querol, X., Castillo, S., Escudero, M., Avila, A., Cuevas, E., Torres, C., Romero, P., Exposito, F. and Garcia, O.: Characterisation of TSP and PM2.5 at Izaña and Sta. Cruz de Tenerife (Canary Islands, Spain) during a Saharan Dust Episode (July 2002),

Atmospheric Environment, 39(26), 4715-4728, doi: 10.1016/j.atmosenv.2005.04.018, 2005.

Arditsoglou, A. and Samara, C.: Levels of total suspended particulate matter and major trace elements in Kosovo: a source identification and apportionment study, Chemosphere, 59(5), 669-678, doi: 10.1016/j.chemosphere.2004.10.056, 2005.

Arndt, R. L., Carmichael, G. R., Streets, D. G. and Bhatti, N.: Sulfur dioxide emissions and sectorial contributions to sulfur deposition in Asia, Atmospheric Environment, 31(10), 1553-1572, doi: 10.1016/S1352-2310(96)00236-1, 1997.

Avogbe, P. H., Ayi-Fanou, L., Cachon, B., Chabi, N., Debende, A., Dewaele, D., Aissi, F., Cazier, F. and Sanni, A.: Hematological changes among Beninese motor-bike taxi drivers exposed to benzene by urban air pollution, African Journal of Environmental Science and Technology, 5(7), 464-472, 2011.

Balarabe, M., Abdullah, K. and Nawawi, M.: Seasonal Variations of Aerosol Optical Properties and Identification of Different Aerosol Types Based on AERONET Data over Sub-Sahara West-Africa, ACS, 06(01), 13-28, doi:10.4236/acs.2016.61002, 2016.

Belis, C. A., Karagulian, F., Larsen, B. R. and Hopke, P. K.: Critical review and meta-analysis of ambient particulate matter source apportionment using receptor models in Europe, Atmospheric Environment, 69, 94-108, doi: 10.1016/j.atmosenv.2012.11.009, 2013.

Bisht, D.S., Dumka, U.C., Kaskaoutis, D.G., Pipal, A.S., Srivastava, A. K., Soni, V.K., Attri, S.D., Sateesh, M., Tiwari, S.: Carbonaceous aerosols and pollutants over Delhi urban environment: Temporal evolution, source apportionment and radiative forcing, Science of the Total Environment, 521-522: 431-445, 2015.

Bouhila, Z., Mouzai, M., Azli, T., Nedjar, A., Mazouzi, C., Zergoug, Z., Boukhadra, D., Chegrouche, S. and Lounici, H.: Investigation of aerosol trace element concentrations nearby Algiers for environmental monitoring using instrumental neutron activation analysis, Atmospheric Research, 166, 49-59, doi: 10.1016/j.atmosres.2015.06.013, 2015.

Cachier, H., Brémond, M.-P. and Buat-Ménard, P.: Carbonaceous aerosols from different tropical biomass burning sources, Nature, 340(6232), 371-373, doi:10.1038/340371a0, 1989.

Cachon, B. F., Firmin, S., Verdin, A., Ayi-Fanou, L., Billet, S., Cazier, F., Martin, P. J., Aissi, F., Courcot, D., Sanni, A. and Shirali, P.: Proinflammatory effects and oxidative stress within human bronchial epithelial cells exposed to atmospheric particulate matter (PM2.5 and PM$_{>2.5}$) collected from Cotonou, Benin, Environmental Pollution, 185, 340-351, doi: 10.1016/j.envpol.2013.10.026, 2014.

Cao, J.J., Lee, S.C., Zhang, X.Y., Chow, J.C., An, Z.S., Ho, K.F., Watson, J.G., Fung, K., Wang, Y.Q. and Shen, Z.X.: Characterization of airborne carbonate over a site near Asian dust source regions during spring 2002 and its climatic and environmental significance, J. Geophys. Res., 110(D3), D03203, doi: 10.1029/2004JD005244, 2005.

Cassee, F. R., Héroux, M.-E., Gerlofs-Nijland, M. E. and Kelly, F. J.: Particulate matter beyond mass: recent health evidence on the role of fractions, chemical constituents and sources of emission, Inhalation Toxicology, 25(14), 802–812, doi:10.3109/08958378.2013.850127, 2013.

Celo, V., Dabek-Zlotorzynska, E., Mathieu, D., Okonskaia, I.: Validation of simple microwave-assisted acid digestion method using microvessels for analysis of trace elements in atmospheric PM2.5 in monitoring and fingerprinting studies, The Open Chemical & Biomedical Methods Journal 3., 141-150, 2010.

Cesari, D., Donateo, A., Conte, M., Merico, E., Giangreco, A., Giangreco, F. and Contini, D.: An inter-comparison of PM2.5 at urban and urban background sites: Chemical characterization and source apportionment, Atmospheric Research, 174-175, 106-119, doi: 10.1016/j.atmosres.2016.02.004, 2016.

Cheng, Z., Jiang, J., Chen, C., Gao, J., Wang, S., Watson, J. G., Wang, H., Deng, J., Wang, B., Zhou, M., Chow, J. C., Pitchford, M. L. and Hao, J.: Estimation of Aerosol Mass Scattering Efficiencies under High Mass Loading: Case Study for the Megacity of Shanghai, China, Environ. Sci. Technol., 49(2), 831-838, doi: 10.1021/es504567q, 2015.

Chiapello, I., Bergametti, G., Chatenet, B., Bousquet, P., Dulac, F. and Soares, E. S.: Origins of African dust transported over the northeastern tropical Atlantic, J. Geophys. Res., 102(D12), 13701-13709, doi: 10.1029/97JD00259, 1997.

Chow, J. C., Watson, J. G., Lu, Z., Lowenthal, D. H., Frazier, C. A., Solomon, P. A., Thuillier, R. H. and Magliano, K.: Descriptive analysis of PM2.5 and PM10 at regionally representative locations during SJVAQS/AUSPEX, Atmospheric Environment, 30(12), 2079-2112, doi:10.1016/1352-2310(95)00402-5, 1996.

Colbeck, I., Nasir, Z. A., Ahmad, S. and Ali, Z.: Exposure to PM10, PM2.5, PM1 and Carbon Monoxide on Roads in Lahore, Pakistan, Aerosol Air Qual. Res., 11(6), 689-695, doi:10.4209/aaqr.2010.10.0087, 2011.

Colette, A., Menut, L., Haeffelin, M. and Morille, Y.: Impact of the transport of aerosols from the free troposphere towards the boundary layer on the air quality in the Paris area, Atmospheric Environment, 42(2), 390-402, doi: 10.1016/j.atmosenv.2007.09.044, 2007.

Dieme, D., Cabral-Ndior, M., Garçon, G., Verdin, A., Billet, S., Cazier, F., Courcot, D., Diouf, A. and Shirali, P.: Relationship between physicochemical characterization and toxicity of fine particulate matter (PM2.5) collected in Dakar city (Senegal), Environmental Research, 113, 1-13, doi:10.1016/j.envres.2011.11.009, 2012.

Ding, A., Huang, X. and Fu, C.: Air Pollution and Weather Interaction in East Asia, Oxford Research Encyclopedias-Environmental Sience, doi: 10.1093/acrefore/9780199389414.013. 536, 2017.

Djossou, J., Léon, J.-F., Akpo, A. B., Liousse, C., Yoboué, V., Bedou, M., Bodjrenou, M., Chiron, C., Galy-Lacaux, C., Gardrat, E., Abbey, M., Keita, S., Bahino, J., Touré N'Datchoh, E., Ossohou, M. and Awanou, C. N.: Mass concentration, optical depth and

carbon composition of particulate matter in the major southern West African cities of Cotonou (Benin) and Abidjan (Côte d'Ivoire), Atmos. Chem. Phys., 18(9), 6275-6291, doi:10.5194/acp-18-6275-2018, 2018.

Doumbia, E.H.T., Liousse, C., Galy-Lacaux, C., Ndiaye, S.A., Diop, B., Ouafo, M., et al. Real time black carbon measurements in West and Central Africa urban sites. Atmospheric Environment. 2012;54(0):529-37.

Draxler, R. R., and G. D. Rolph: Evaluation of the Transfer Coefficient Matrix (TCM) approach to model the atmospheric radionuclide air concentrations from Fukushima, J. Geophys. Res., 117, D05107, doi:10.1029/2011JD017205, 2012.

Du, Z., He, K., Cheng, Y., Duan, F., Ma, Y., Liu, J., Zhang, X., Zheng, M. and Weber, R.: A yearlong study of water-soluble organic carbon in Beijing I: Sources and its primary vs. secondary nature, Atmospheric Environment, 92, 514-521, doi:10.1016/j.atmosenv.2014.04. 060, 2014.

Favez, O.: Caractérisation physico-chimique de la pollution particulaire dans des mégapoles contrastées, Thèse de l'Université PARIS.DIDEROT (Paris 7), France, 2008.

Favez, O., Sciare, J., Cachier, H., Alfaro, S. C. and Abdelwahab, M. M.: Significant formation of water-insoluble secondary organic aerosols in semi-arid urban environment, Geophys. Res. Lett., 35(15), L15801, doi:10.1029/2008GL034446, 2008.

Feng, J., Guo, Z., Chan, C. K. and Fang, M.: Properties of organic matter in PM2.5 at Changdao Island, China - A rural site in the transport path of the Asian continental outflow, Atmospheric Environment, 41(9), 1924-1935, doi: 10.1016/j.atmosenv.2006.10.064, 2007.

Feng, J., Hu, M., Chan, C. K., Lau, P. S., Fang, M., He, L. and Tang, X.: A comparative study of the organic matter in PM2.5 from three Chinese megacities in three different climatic zones, Atmospheric Environment, 40(21), 3983-3994, doi: 10.1016/j.atmosenv.2006.02.017, 2006.

Freitas, M.C., Pacheco, A.M.G., Baptista, M.S., Dionísio, I., Vasconcelos, M.T.S.D. and Cabral, J.P.: Response of exposed detached lichens to atmospheric elemental deposition, Proc. ECOpole., 1(1/2), 15-21, 2007.

Gaga, E. O., Arı, A., Akyol, N., Üzmez, Ö. Ö., Kara, M., Chow, J. C., Watson, J. G., Özel, E., Döğeroğlu, T. and Odabasi, M.: Determination of real-world emission factors of trace metals, EC, OC, BTEX, and semivolatile organic compounds (PAHs, PCBs and PCNs) in a rural tunnel in Bilecik, Turkey, Science of The Total Environment, 643, 1285-1296, doi: 10.1016/j.scitotenv.2018.06.227, 2018.

Gao, Y., Nelson, E. D., Field, M. P., Ding, Q., Li, H., Sherrell, R. M., Gigliotti, C. L., Van Ry, D. A., Glenn, T. R. and Eisenreich, S. J.: Characterization of atmospheric trace elements on PM2.5 particulate matter over the New York–New Jersey harbor estuary, Atmospheric Environment, 36(6), 1077–1086, doi:10.1016/S1352-2310(01)00381-8, 2002.

Genga, A., Ielpo, P., Siciliano, T. and Siciliano, M.: Carbonaceous particles and aerosol mass closure in PM2.5 collected in a port city, Atmospheric Research, 183, 245-254, doi: 10.1016/j.atmosres.2016.08.022, 2017.

Gounougbe, F.: Pollution atmosphérique par les gaz d'échappement et état de santé des conducteurs de taxi-moto (Zemidjan) de Cotonou (Bénin), Thèse de doctorat en Médecine (832), 1999.

Guinot, B., Cachier, H. and Oikonomou, K.: Geochemical perspectives from a new aerosol chemical mass closure, Atmos. Chem. Phys., 7(6), 1657-1670, doi: 10.5194/acp-7-1657-2007, 2007.

Guttikunda, S. K. and Calori, G.: A GIS based emissions inventory at 1 km × 1 km spatial resolution for air pollution analysis in Delhi, India, Atmospheric Environment, 67, 101-111, doi:10.1016/j.atmosenv.2012.10.040, 2013.

Hara, K., Osada, K., Kido, M., Hayashi, M., Matsunaga, K., Iwasaka, Y., Yamanouchi, T., Hashida, G. and Fukatsu, T.: Chemistry of sea-salt particles and inorganic halogen species in Antarctic regions: Compositional differences between coastal and inland stations, J. Geophys. Res., 109, D20208, doi:10.1029/2004JD004713, 2004.

He, K., Yang, F., Ma, Y., Zhang, Q., Yao, X., Chan, C. K., Cadle, S., Chan, T. and Mulawa, P.: The characteristics of PM2.5 in Beijing, China, Atmospheric Environment, 35(29), 4959-4970, doi: 10.1016/S1352-2310(01)00301-6, 2001.

Hildemann, L. M., Markowski, G. R. and Cass, G. R.: Chemical composition of emissions from urban sources of fine organic aerosol, Environ. Sci. Technol., 25(4), 744-759, doi: 10.1021/es00016a021, 1991.

Huang, H., Ho, K. F., Lee, S. C., Tsang, P. K., Ho, S. S. H., Zou, C. W., Zou, S. C., Cao, J. J. and Xu, H. M.: Characteristics of carbonaceous aerosol in PM2.5: Pearl Delta River Region, China, Atmospheric Research, 104-105, 227-236, doi: 10.1016/j.atmosres.2011.10.016, 2012.

Jaffrezo, J.-L., Aymoz, G., Delaval, C., and Cozic, J.: Seasonal variations of the Water Soluble Organic Carbon mass fraction of aerosol in two valleys of the French Alps, Atmos. Chem. Phys., 5, 2809-2821, 2005.

Keita, S., Liousse, C., Yoboué, V., Dominutti, P., Guinot, B., Assamoi, E.-M., Borbon, A., Haslett, S. L., Bouvier, L., Colomb, A., Coe, H., Akpo, A., Adon, J., Bahino, J., Doumbia, M., Djossou, J., Galy-Lacaux, C., Gardrat, E., Gnamien, S., Léon, J. F., Ossohou, M., N'Datchoh, E. T. and Roblou, L.: Particle and VOC emission factor measurements for anthropogenic sources in West Africa, Atmos. Chem. Phys., 18(10), 7691-7708, doi:10.5194/acp-18-7691-2018, 2018.

Khan, Md. F., Shirasuna, Y., Hirano, K. and Masunaga, S.: Characterization of PM2.5, PM2.5-10 and PM>10 in ambient air, Yokohama, Japan, Atmospheric Research, 96(1), 159-172, doi:10.1016/j.atmosres.2009.12.009, 2010.

Kim, H., Liu, X., Kobayashi, T., Kohyama, T., Wen, F.-Q., Romberger, D. J., Conner, H., Gilmour, P. S., Donaldson, K., MacNee, W. and Rennard, S. I.: Ultrafine Carbon Black Particles Inhibit Human Lung Fibroblast-Mediated Collagen Gel Contraction, Am J Respir. Cell. Mol. Biol., 28(1), 111-121, doi:10.1165/rcmb.4796, 2003.

Knippertz, P., Tesche, M., Heinold, B., Kandler, K., Toledano, C. and Esselborn, M.: Dust mobilization and aerosol transport from West Africa to Cape Verde - a meteorological overview of SAMUM-2, Tellus B: Chemical and Physical Meteorology, 63(4), 430-447, doi:10.1111/j.1600-0889.2011. 00544.x, 2011.

Kouassi, K. S., Billet, S., Garçon, G., Verdin, A., Diouf, A., Cazier, F., Djaman, J., Courcot, D. and Shirali, P.: Oxidative damage induced in A549 cells by physically and chemically characterized air particulate matter ($PM_{2.5}$) collected in Abidjan, Côte d'Ivoire, J. Appl. Toxicol., doi:10.1002/jat.1496, 2009.

Lamaison, L. : Caractérisation des particules atmosphériques et identification de leurs sources dans une atmosphère urbaine sous influence industrielle, Thèse Doctorat, Univ des Sciences et Technologies, Lille, 2006.

Léon, J.F., Akpo, A., Bedou, M., Djossou, J., Bodjrenou, M., Yoboué, V., et Liousse, C.: Profondeur optique des aérosols sur le sud de l'Afrique de l'Ouest, soumis à ACPD, 2019.

Li, T.-C., Yuan, C.-S., Hung, C.-H., Lin, H.-Y., Huang, H.-C. and Lee, C.-L.: Chemical Characteristics of Marine Fine Aerosols over Sea and at Offshore Islands during Three Cruise Sampling Campaigns in the Taiwan Strait-Sea Salts and Anthropogenic Particles, Atmos. Chem. Phys. Discuss., 1-27, doi:10.5194/acp-2016-384, 2016.

Li, Y., Schwandner, F. M., Sewell, H. J., Zivkovich, A., Tigges, M., Raja, S., Holcomb, S., Molenar, J. V., Sherman, L., Archuleta, C., Lee, T. and Collett, J. L.: Observations of ammonia, nitric acid and fine particles in a rural gas production region, Atmospheric Environment, 83, 80-89, doi:10.1016/j.atmosenv.2013.10.007, 2014.

Liang, L., Engling, G., Du, Z., Cheng, Y., Duan, F., Liu, X. and He, K.: Seasonal variations and source estimation of saccharides in atmospheric particulate matter in Beijing, China, Chemosphere, 150, 365-377, 2016.

Liousse, C., Assamoi, E., Criqui, P., Granier, C., Rosset, R.: Explosive growth in African combustion emissions from 2005 to 2030, Environ. Res. Lett., 9, 035003, 2014.

Lonati, G., Ozgen, S. and Giugliano, M.: Primary and secondary carbonaceous species in $PM_{2.5}$ samples in Milan (Italy), Atmospheric Environment, 41(22), 4599-4610, doi:10.1016/j.atmosenv.2007.03.046, 2007.

Lowenthal, D., Zielinska, B., Samburova, V., Collins, D., Taylor, N. and Kumar, N.: Evaluation of assumptions for estimating chemical light extinction at U.S. national parks, Journal of the Air & Waste Management Association, 65(3), 249-260, doi:10.1080/10962247.2014.986307, 2015.

1069 Mason, B., Moore, B.C.: Principles of Geochemistry, fourth ed. John Wiley and Sons, New
1070   York, pp. 46-47, 1982.

1071 Minguillón, M. C., Cirach, M., Hoek, G., Brunekreef, B., Tsai, M., de Hoogh, K., Jedynska, A.,
1072   Kooter, I. M., Nieuwenhuijsen, M. and Querol, X.: Spatial variability of trace elements and
1073   sources for improved exposure assessment in Barcelona, Atmospheric Environment, 89,
1074   268-281, doi: 10.1016/j.atmosenv.2014.02.047, 2014.

1075 Mkoma, S. L.: Physico-Chemical characterisation of atmospheric aerosols in Tanzania, with
1076   emphasis on the carbonaceous aerosol components and on chemical mass closure, PhD,
1077   Ghent University, Ghent, Belguim, 2008.

1078 Mmari, A. G., Potgieter-Vermaak, S. S., Bencs, L., McCrindle, R. I. and Van Grieken, R.:
1079   Elemental and ionic components of atmospheric aerosols and associated gaseous pollutants
1080   in and near Dar es Salaam, Tanzania, Atmospheric Environment, 77, 51-61, doi:
1081   10.1016/j.atmosenv.2013.04.061, 2013.

1082 MMEH (Ministère des Mines de l'Energie et d'Hydraulique): Tableau de bord de l'Energie 2002
1083   au Bénin, Direction Générale de l'Energie, 2002.

1084 Ngo, N. S., Asseko, S. V. J., Ebanega, M. O., Allo'o Allo'o, S. M. and Hystad, P.: The
1085   relationship among PM2.5, traffic emissions, and socioeconomic status: Evidence from
1086   Gabon using low-cost, portable air quality monitors, Transportation Research Part D:
1087   Transport and Environment, 68, 2-9, doi: 10.1016/j.trd.2018.01.029, 2019.

1088 Ozer, P.: Estimation de la pollution particulaire naturelle de l'air en 2003 à Niamey (Niger) à
1089   partir de données de visibilité horizontale, 2005.

1090 Pachauri, T., Singla, V., Satsangi, A., Lakhani, A. and Kumari, K. M.: Characterization of
1091   carbonaceous aerosols with special reference to episodic events at Agra, India,
1092   Atmospheric Research, 128, 98-110, doi: 10.1016/j.atmosres.2013.03.010, 2013.

1093 Park, J. H., Mudunkotuwa, I. A., Mines, L. W. D., Anthony, T. R., Grassian, V. H. and Peters,
1094   T. M.: A Granular Bed for Use in a Nanoparticle Respiratory Deposition Sampler, Aerosol
1095   Science and Technology, 49(3), 179-187, doi:10.1080/02786826.2015.1013521, 2015.

1096 Person, A. and Tymen, G.: Mesurage des particules en suspension dans l'air en relation avec la
1097   santé. Pollution atmosphèrique, 271-285, 2005.

1098 Pipal, A. S., Jan, R., Satsangi, P. G., Tiwari, S. and Taneja, A.: Study of Surface Morphology,
1099   Elemental Composition and Origin of Atmospheric Aerosols (PM2.5 and PM10) over
1100   Agra, India, Aerosol Air Qual. Res., 14(6), 1685-1700, doi:10.4209/aaqr.2014.01.0017,
1101   2014.

1102 Pipal, A. S., Singh, S. and Satsangi, G. P.: Study on bulk to single particle analysis of
1103   atmospheric aerosols at urban region, Urban Climate, 27, 243-258, doi:
1104   10.1016/j.uclim.2018.12.008, 2019.

1105 Prospero, J.M., Ginoux, P., Torres, O., Nicholson, S.E., Gill, T.E.: Environmental
1106   characterization of global sources of atmospheric soil dust identified with the NIMBUS 7

Total Ozone Mapping Spectrometer (TOMS) absorbing aerosol product, Rev. Geophys., 40, 2-1-31, 2002.

Qin, Y., Chan, C. K. and Chan, L. Y.: Characteristics of chemical compositions of atmospheric aerosols in Hong Kong: spatial and seasonal distributions, Science of The Total Environment, 206(1), 25-37, doi: 10.1016/S0048-9697(97)00214-3, 1997.

Ramgolam K, Favez O, Cachier H, Gaudichet A, Marano F, Martinon L, Baeza-Squiban A: Size-partitioning of an urban aerosol to identify particle determinants involved in the proinflammatory response induced in airway epithelial cells. Part Fibre Toxicol 2009, 6: 10. 10.1186/1743-8977-6-10.

Rengarajan, R., Sudheer, A. K. and Sarin, M. M.: Aerosol acidity and secondary organic aerosol formation during wintertime over urban environment in western India, Atmospheric Environment, 45(11), 1940-1945, doi: 10.1016/j.atmosenv.2011.01.026, 2011.

Samara, C., Kouimtzis, T., Tsitouridou, R., Kanias, G. and Simeonov, V.: Chemical mass balance source apportionment of PM10 in an industrialized urban area of Northern Greece, Atmospheric Environment, 37(1), 41-54, doi:10.1016/S1352-2310(02)00772-0, 2003.

Satsangi, A., Pachauri, T., Singla, V., Lakhani, A. and Kumari, K. M.: Organic and elemental carbon aerosols at a suburban site, Atmospheric Research, 113, 13-21, doi: 10.1016/j.atmosres.2012.04.012, 2012.

Saxena, P., and Hildemann, L.M.: Water-soluble organics in atmospheric particles: a critical review of the literature and application of thermodynamics to identify candidate compounds, J. Atmos. Chem., 24(1), 57-109, 1996.

Sciare, J., Oikonomou, K., Cachier, H., Mihalopoulos, N., Andreae, M. O., Maenhaut, W. and Sarda-Estève, R.: Aerosol mass closure and reconstruction of the light scattering coefficient over the Eastern Mediterranean Sea during the MINOS campaign, Atmos. Chem. Phys., 5(8), 2253-2265, doi:10.5194/acp-5-2253-2005, 2005.

Seinfeld, J. H.   and Pandis, S. N.: Atmospheric Chemistry and Physics: from Air Pollution to Climate Change, John Wiley and Sons, Inc. New York, 1998.

Shahsavani, A., Naddafi, K., Jaafarzadeh Haghighifard, N., Mesdaghinia, A., Yunesian, M., Nabizadeh, R., Arhami, M., Yarahmadi, M., Sowlat, M. H., Ghani, M., Jonidi Jafari, A., Alimohamadi, M., Motevalian, S. A. and Soleimani, Z.: Characterization of ionic composition of TSP and PM10 during the Middle Eastern Dust (MED) storms in Ahvaz, Iran, Environ Monit Assess, 184(11), 6683-6692, doi:10.1007/s10661-011-2451-6, 2012.

Stone, R. S., Herber, A., Vitale, V., Mazzola, M., Lupi, A., Schnell, R. C., Dutton, E. G., Liu, P. S. K., Li, S.-M., Dethloff, K., Lampert, A., Ritter, C., Stock, M., Neuber, R. and Maturilli, M.: A three-dimensional characterization of Arctic aerosols from airborne Sun photometer observations: PAM-ARCMIP, April 2009, J. Geophys. Res., 115(D13), D13203, doi: 10.1029/2009JD013605, 2010.

Sullivan, A. P., Weber, R. J., Clements, A. L., Turner, J. R., Bae, M. S. and Schauer, J. J.: A method for on-line measurement of water-soluble organic carbon in ambient aerosol particles: Results from an urban site: on-line measurement of WSOC in aerosols, Geophys. Res. Lett., 31(13), doi: 10.1029/2004GL019681, 2004.

Sun, Y., Zhuang, G., Wang, Y., Han, L., Guo, J., Dan, M., Zhang, W., Wang, Z. and Hao, Z.: The airborne particulate pollution in Beijing - concentration, composition, distribution and sources, Atmospheric Environment, 38(35), 5991-6004, doi: 10.1016/j.atmosenv.2004.07.009, 2004.

Tang, X., Zhang, X., Ci, Z., Guo, J. and Wang, J.: Speciation of the major inorganic salts in atmospheric aerosols of Beijing, China: Measurements and comparison with model, Atmospheric Environment, 133, 123-134, doi: 10.1016/j.atmosenv.2016.03.013, 2016.

Tapsoba, D. : Caractérisation événementielle des régimes pluviométriques ouestafricains et de leur récent changement, Thèse de Doctorat, Univ.Paris-XI (Orsay). 100p, 1997.

Taylor, S. R.: Abundance of chemical elements in the continental crust: a new table, Geochimica et Cosmochimica Acta, 28(8), 1273-1285, doi: 10.1016/0016-7037(64)90129-2, 1964.

Terzi, E., Argyropoulos, G., Bougatioti, A., Mihalopoulos, N., Nikolaou, K. and Samara, C.: Chemical composition and mass closure of ambient PM10 at urban sites, Atmospheric Environment, 44(18), 2231-2239, doi: 10.1016/j.atmosenv.2010.02.019, 2010.

Tunno, B., Longley, I., Somervell, E., Edwards, S., Olivares, G., Gray, S., Cambal, L., Chubb, L., Roper, C., Coulson, G. and Clougherty, J. E.: Separating spatial patterns in pollution attributable to woodsmoke and other sources, during daytime and nighttime hours, in Christchurch, New Zealand, Environmental Research, 171, 228-238, doi: 10.1016/j.envres.2019.01.033, 2019.

Turpin, B. J., Cary, R. A. and Huntzicker, J. J.: An In Situ, Time-Resolved Analyzer for Aerosol Organic and Elemental Carbon, Aerosol Science and Technology, 12(1), 161-171, doi:10.1080/02786829008959336, 1990.

United Nations, Department of Economic and Social Affairs, Population Division (2019). World Population Prospects 2019: Volume II: Demographic Profiles. Made available under a Creative Commons license. http://creativecommons.org/licenses/by/3.0/igo/ 2019

Val, S., Liousse, C., Doumbia, E. H. T., Galy-Lacaux, C., Cachier, H., Marchand, N., Badel, A., Gardrat, E., Sylvestre, A. and Baeza-Squiban, A.: Physico-chemical characterization of African urban aerosols (Bamako in Mali and Dakar in Senegal) and their toxic effects in human bronchial epithelial cells: description of a worrying situation, Part Fibre Toxicol, 10(1), 10, doi:10.1186/1743-8977-10-10, 2013.

Viana, M., López, J. M., Querol, X., Alastuey, A., García-Gacio, D., Blanco-Heras, G., López-Mahía, P., Piñeiro-Iglesias, M., Sanz, M. J., Sanz, F., Chi, X. and Maenhaut, W.: Tracers and impact of open burning of rice straw residues on PM in Eastern Spain, Atmospheric Environment, 42(8), 1941-1957, doi: 10.1016/j.atmosenv.2007.11.012, 2008.

1183 Viana, M., Maenhaut, W., ten Brink, H. M., Chi, X., Weijers, E., Querol, X., Alastuey, A.,
1184   Mikuška, P. and Večeřa, Z.: Comparative analysis of organic and elemental carbon
1185   concentrations in carbonaceous aerosols in three European cities, Atmospheric
1186   Environment, 41(28), 5972-5983, doi: 10.1016/j.atmosenv.2007.03.035, 2007.

1187 Viidanoja, J., Sillanpää, M., Laakia, J., Kerminen, V.-M., Hillamo, R., Aarnio, P. and
1188   Koskentalo, T.: Organic and black carbon in PM2.5 and PM10: 1 year of data from an
1189   urban site in Helsinki, Finland, Atmospheric Environment, 36(19), 3183-3193, doi:
1190   10.1016/S1352-2310(02)00205-4, 2002.

1191 Wang, X., Bi, X., Sheng, G. and Fu, J.: Chemical Composition and Sources of PM10 and PM2.5
1192   Aerosols in Guangzhou, China, Environ Monit Assess, 119(1-3), 425-439, doi:
1193   10.1007/s10661-005-9034-3, 2006.

1194 Washington, R., Todd, M., Middleton, N. J. and Goudie, A. S.: Dust-Storm Source Areas
1195   Determined by the Total Ozone Monitoring Spectrometer and Surface Observations,
1196   Annals of the Association of American Geographers, 93(2), 297-313, doi:10.1111/1467-
1197   8306.9302003, 2003.

1198 Watson, J. G. and Chow, J. C.: Estimating middle-, neighborhood-, and urban-scale
1199   contributions to elemental carbon in Mexico City with a rapid response aethalometer, J.
1200   Air Waste Manag. Assoc., 51(11), 1522-1528, 2001.

1201 Watson, J. G., Chow, J. C. and Houck, J. E.: PM2.5 chemical source profiles for vehicle exhaust,
1202   vegetative burning, geological material, and coal burning in Northwestern Colorado during
1203   1995, Chemosphere, 43(8), 1141-1151, doi:10.1016/S0045-6535(00)00171-5, 2001.

1204 WHO (World Health Organization), 7 million premature deaths annually linked to air pollution.
1205   Media Centre news release. Geneva: World Health Organization. (http: //www.who.int/
1206   mediacentre/news/releases/2014/airpollution/en/, 2014.

1207 Wilson, M. R., Lightbody, J. H., Donaldson, K., Sales, J. and Stone, V.: Interactions between
1208   ultrafine particles and transition metals in vivo and in vitro, Toxicol. Appl. Pharmacol.,
1209   184(3), 172-179, 2002.

1210 Xiang, P., Zhou, X., Duan, J., Tan, J., He, K., Yuan, C., Ma, Y. and Zhang, Y.: Chemical
1211   characteristics of water-soluble organic compounds (WSOC) in PM2.5 in Beijing, China:
1212   2011-2012, Atmospheric Research, 183, 104-112, doi: 10.1016/j.atmosres.2016.08.020,
1213   2017.

1214 Xie, Y., Wang, Y., Bilal, M. and Dong, W.: Mapping daily PM2.5 at 500 m resolution over
1215   Beijing with improved hazy day performance, Science of The Total Environment, 659,
1216   410-418, doi: 10.1016/j.scitotenv.2018.12.365, 2019.

1217 Xu, H., Léon, J.-F., Liousse, C., Guinot, B., Yoboué, V., Akpo, A. B., Adon, J., Ho, K. F., Ho,
1218   S. S. H., Li, L., Gardrat, E., Shen, Z. and Cao, J.: Personal exposure to PM2.5 emitted from
1219   typical anthropogenic sources in Southern West Africa (SWA): Chemical characteristics
1220   and associated health risks, Atmos. Chem. Phys. Discuss., 1-68, doi:10.5194/acp-2018-
1221   1060, 2019.

1222 Xu, J., Zhang, Y., Zheng, S. and He, Y.: Aerosol effects on ozone concentrations in Beijing: a
1223   model sensitivity study, J Environ Sci (China), 24(4), 645-656, 2012.

1224 Yu, P., Froyd, K. D., Portmann, R. W., Toon, O. B., Freitas, S. R., Bardeen, C. G., Katich, J.
1225   M., Schwarz, J. P., Williamson, C., Kupc, A., Brock, C., Liu, S., Gao, R.-S., Schill, G.,
1226   Fan, T., Rosenlof, K. H., and Murphy, D. M.: An improved treatment of aerosol convective
1227   transport and removal in a chemistry-climate model, Geophys. Res. Lett., submitted, 2018.

1228 Zghaid, M., Noack, Y., Bounakla, M., and Benyaich, F.: Pollution atmosphérique particulaire
1229   dans la ville de Kenitra (Maroc), Pollution atmosphérique [En ligne], N° 203, mis à jour le
1230   12/10/2015,URL:http://lodel.irevues.inist.fr/pollution-atmospherique/index.php?id=1184,
1231   https://doi.org/10.4267/pollution-atmospherique.1184

1232 Zhang, X. Y., Gong, S. L., Shen, Z. X., Mei, F. M., Xi, X. X., Liu, L.C., Zhou, Z. J., Wang, D.,
1233   Wang, Y. Q., and Cheng, Y.: Characterization of soil dust aerosol in China and its transport
1234   and distribution during 2001 ACE-Asia: 1. Network observations, J. Geophys. Res.
1235   Atmos., 108(D9), 4261, doi:10.1029/2002JD002632, 2003.

1236

1237

1238

1239

1240

1241

1242

1243

1244

1245

1246

1247

1248

1249

1250

1251 **Figure caption**

1252 Figure 1: Map of the city of Abidjan reporting the geographical location of DACCIWA urban
1253   sampling sites.

1254   Figure 2: Map of the city of Cotonou reporting the geographical location of DACCIWA urban
1255   sampling site.

1256   Figure 3: Pictures of the different sampling sites: (a) Traffic in Cotonou (Benin, CT station),
1257   (b) Waste burning in Abidjan (Côte d'Ivoire, AWB station), (c), Domestic fire, showing
1258   smoking activity in Yopougon, Abidjan (Côte d'Ivoire, ADF station), (d) '' woro-woro
1259   and Gbaka '' traffic in Abidjan (Côte d'Ivoire, AT station).

1260   Figure 4: Wind, pressure and temperature diagram at Abidjan and Cotonou during the different
1261   campaigns.

1262   Figure 5: Back trajectories arriving at Abidjan (a) and Cotonou (b) for each season (WS2015,
1263   WS2016, DS2016 and DS2017).

1264   Figure 6: Aerosol Mass concentrations at the different study sites for each campaign and for the
1265   different sizes (C in black, Fine in light Grey, Ultra-fine in grey). Bulk aerosol mass is
1266   indicated in boxes.

1267   Figure 7: Comparison of PM2.5 mass concentrations in $\mu g.m^{-3}$ at the four sites with those
1268   obtained by Djossou et al. (2018) and Xu et al. (2019) for the same sites and periods.
1269   Data for the following weeks were then selected in Djossou et al. (2018): 20-27/07/2015
1270   for WS15, 4-11/01/2016 for DS16, 4-11/07/2016 for WS16 and 9-16/01/2017 for DS17.

1271   Figure 8: EC relative concentrations in each size classes (C in black, Fine in light grey, Ultra-
1272   fine in grey) at the different study sites for each campaign. Bulk EC concentration for
1273   each site is indicated in boxes.

1274   Figure 9: OC relative concentrations in each size classes (C in black, Fine in light grey, Ultra-
1275   fine in grey) at the different study sites for each campaign. Bulk OC concentration for
1276   each site is indicated in boxes.

1277   Figure 10: OC/ EC ratio for the different campaigns and sites for each aerosol size (C in black,
1278   Fine in light grey, Ultra-fine in grey). Each box shows the median and the first and the
1279   third quartiles.

1280   Figure 11: Water-soluble ionic species speciation for each site, each campaign and each aerosol
1281   size.

1282   Figure 12: Dust concentrations at the different study sites for each campaign and for the
1283   different sizes (C in black, Fine in light grey, Ultra-fine in grey).

1284   Figure 13: Size-speciated aerosol chemical composition for each site, for each campaign and
1285   each aerosol size.

1286   Figure 14: MODIS Aerosol optical depth regional distribution over West Africa. Data are for
1287   2017, focusing on our campaign date at Abidjan (a-c 01/11-12-left part) and Cotonou
1288   (b-d 01/6-7, right part).

1289

1290

1291

1292

1293

1294

1295

1296
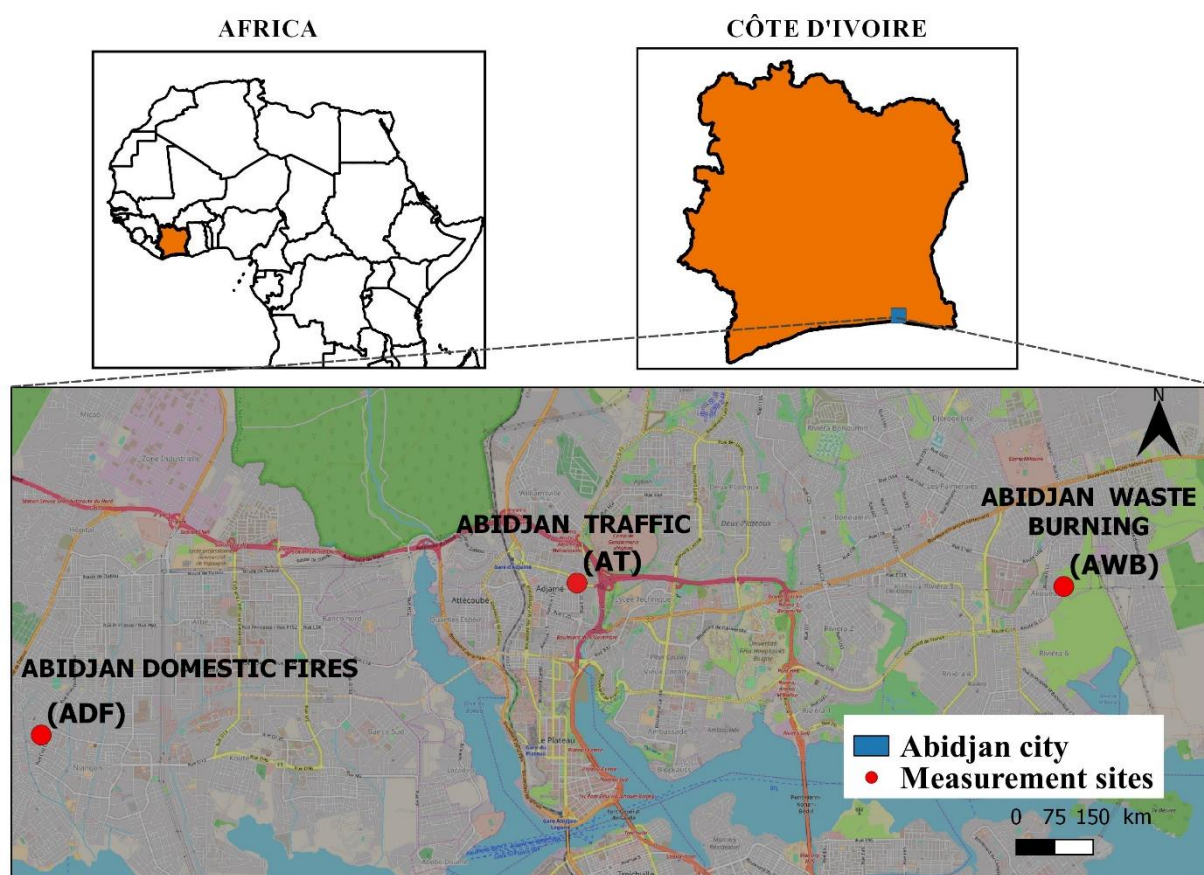
1297

1298

1299   Figure1

1300

1301

1302

1303
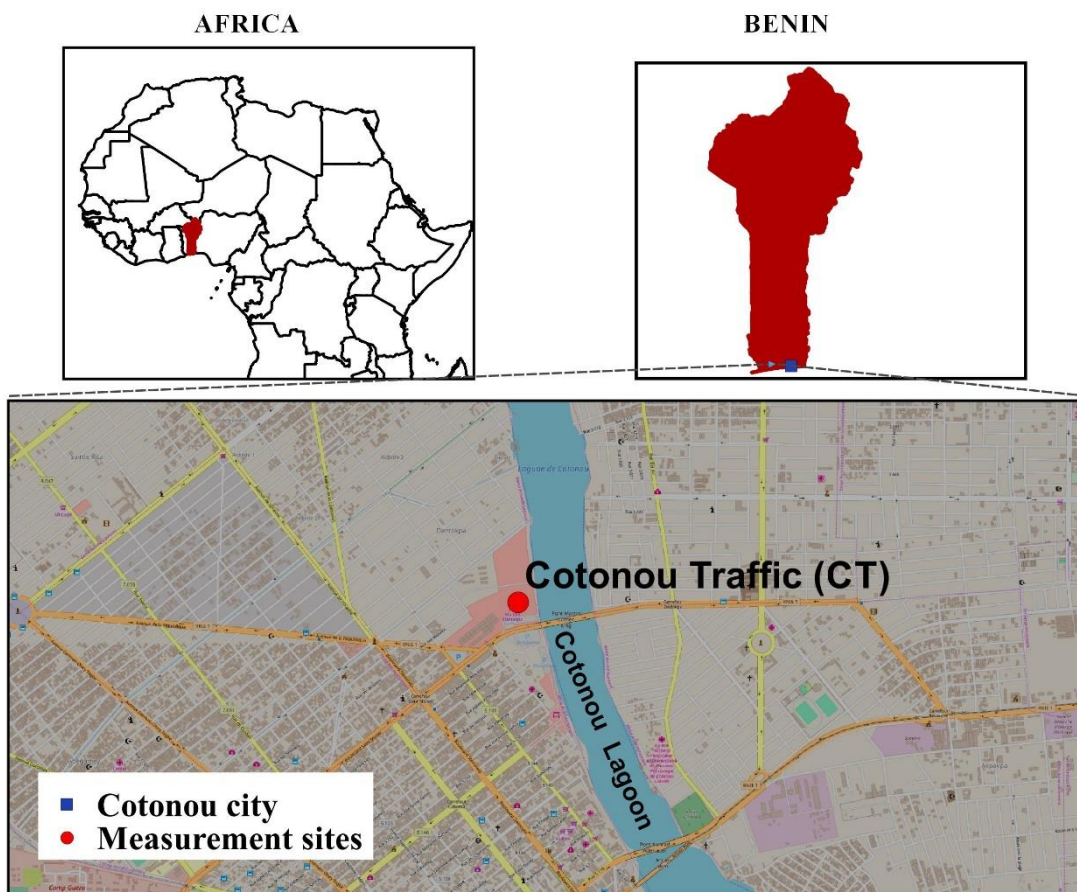
1304

1305

1306   **Figure 2**

1307

1308

1309

1310

1311

1312

1313

1314 **Figure 3**

1315

1316

1317

1318

1319

1320

1321

1322

1323
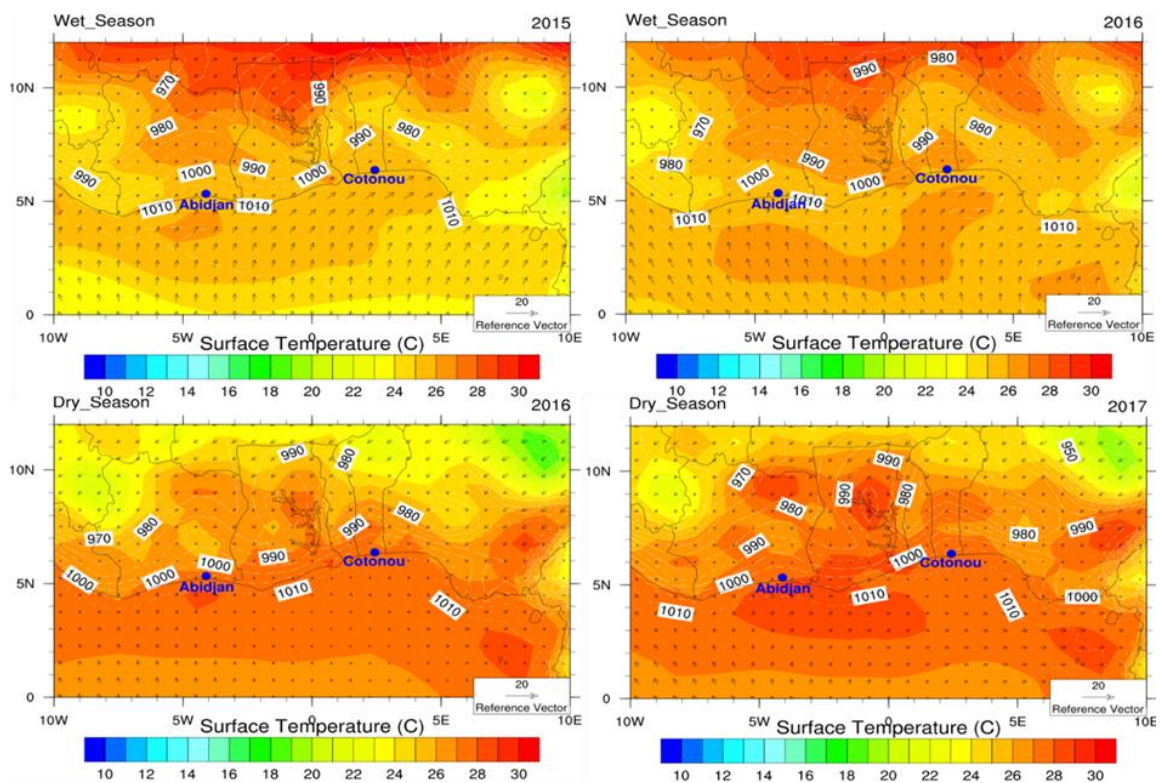
1324

1325

Figure 4

1327

1328

1329

1330

1331

1332

1333

1334

1335

1336

1337

1338

1339

1340

1341

1342

Wet season 2015 Wet season 2016

Dry season 2016 Dry season 2017

1343

1344 **Figure 5-a**

Wet season 2015 Wet season 2016

Dry season 2016 Dry season 2017
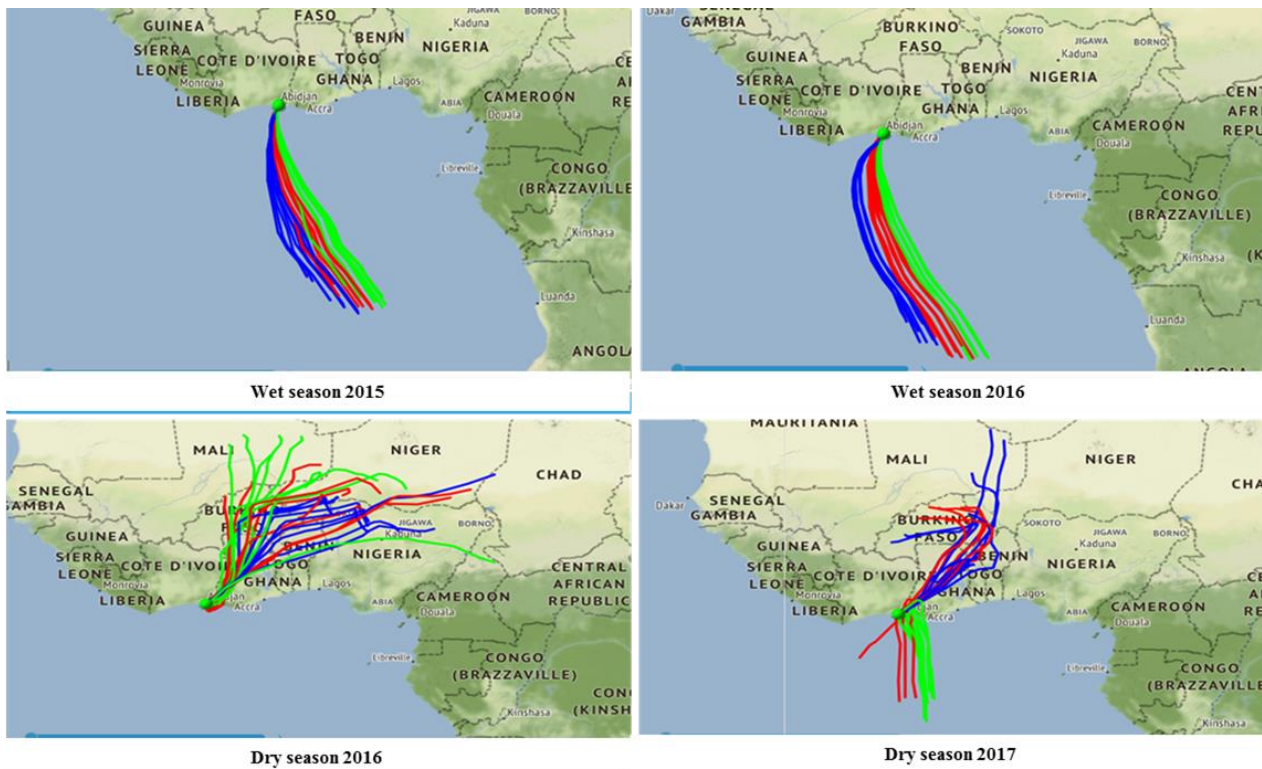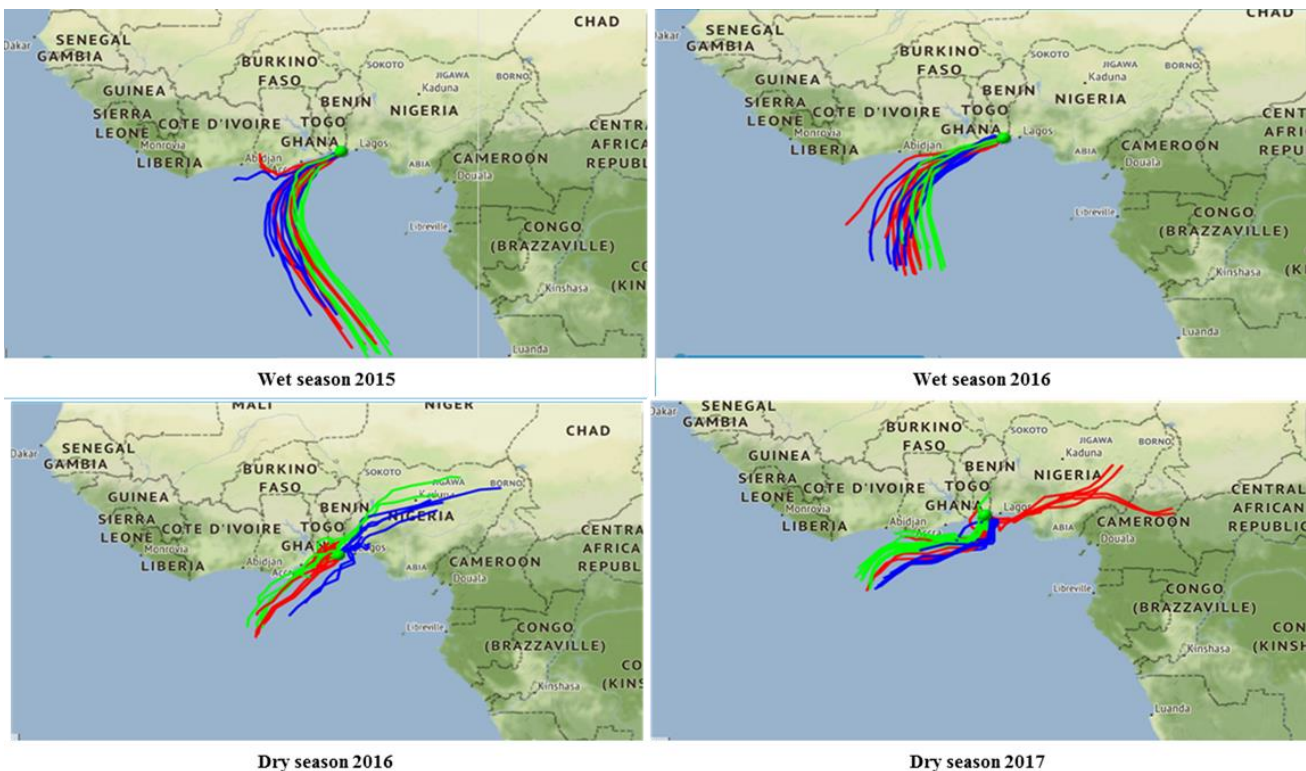
1345

1346 **Figure 5-b**

1347

1348

1349

1350
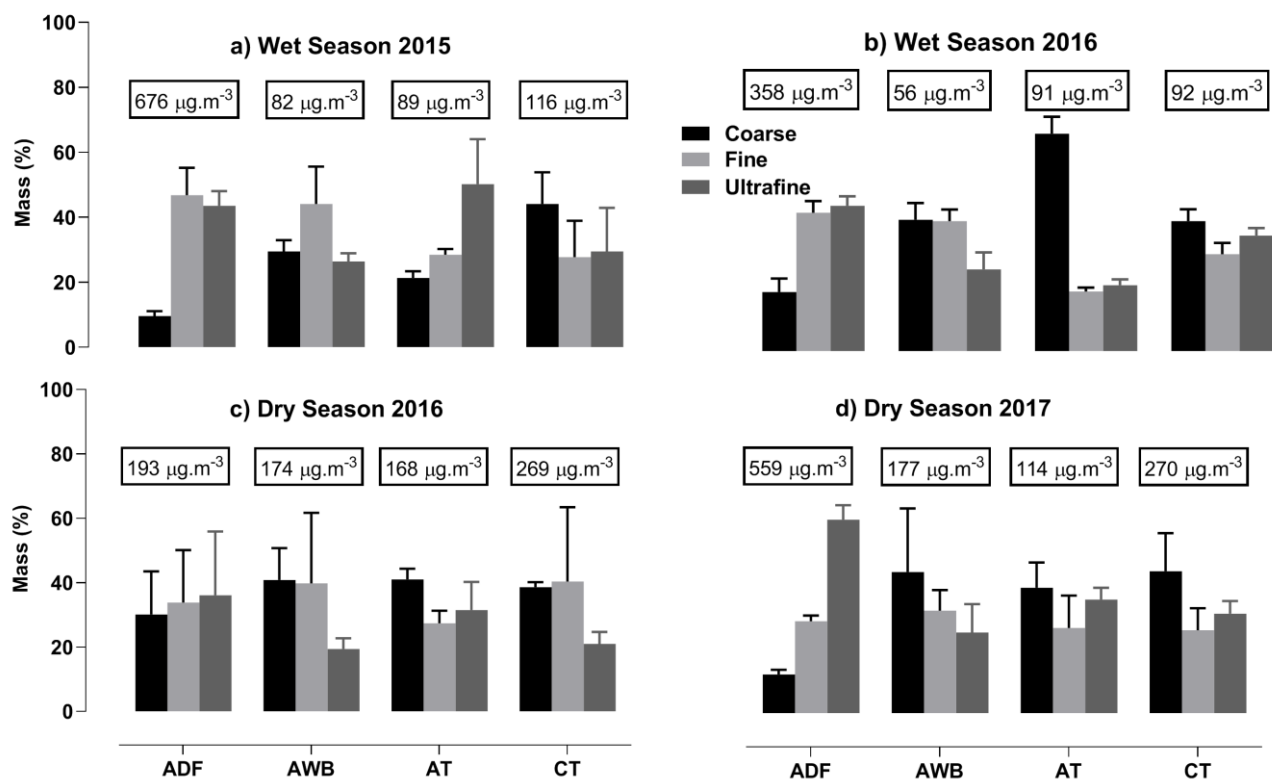
1351

1352   **Figure 6**

1353

1354
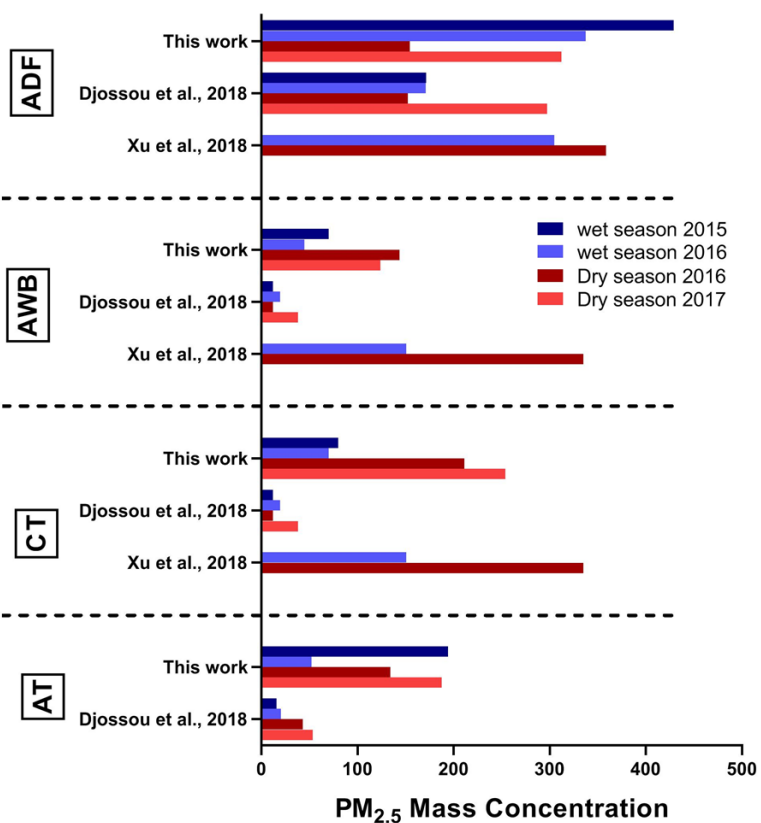
1355

1356   **Figure 7**

1357

1358

1359

1360
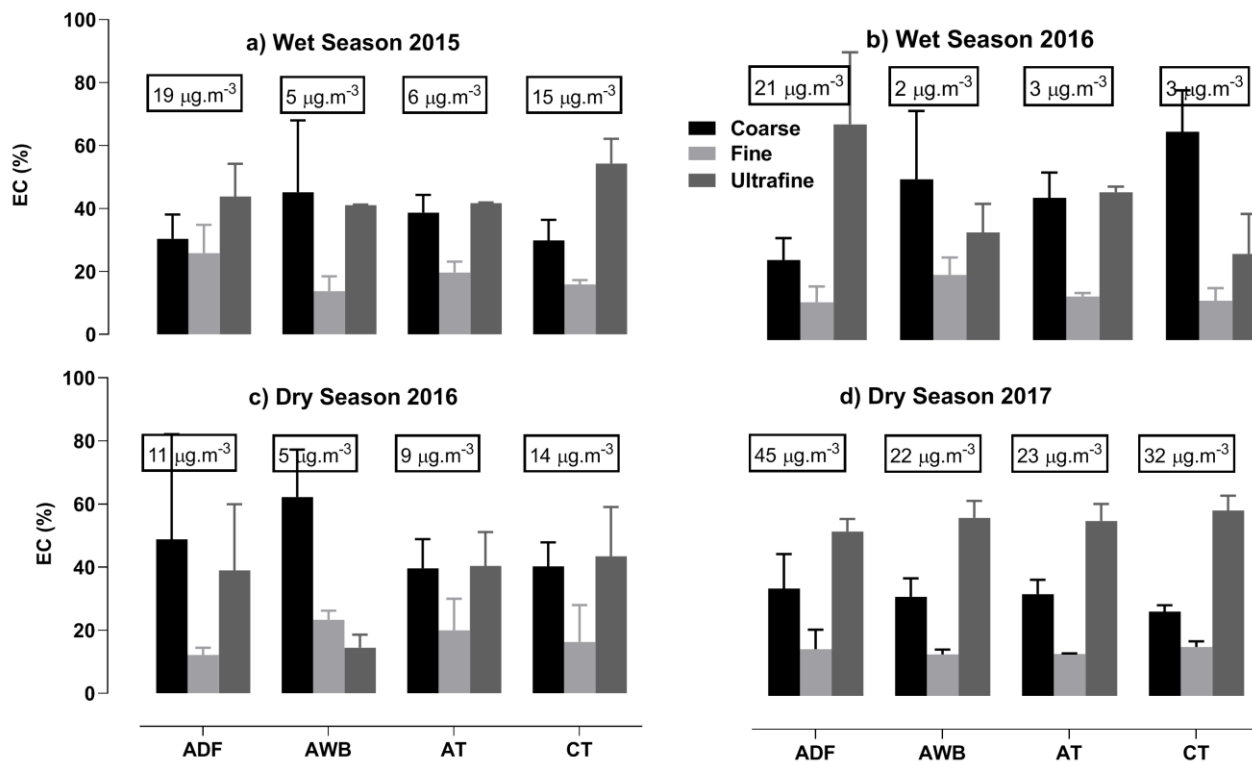
1361

1362   **Figure 8**

1363

1364

1365

1366

1367
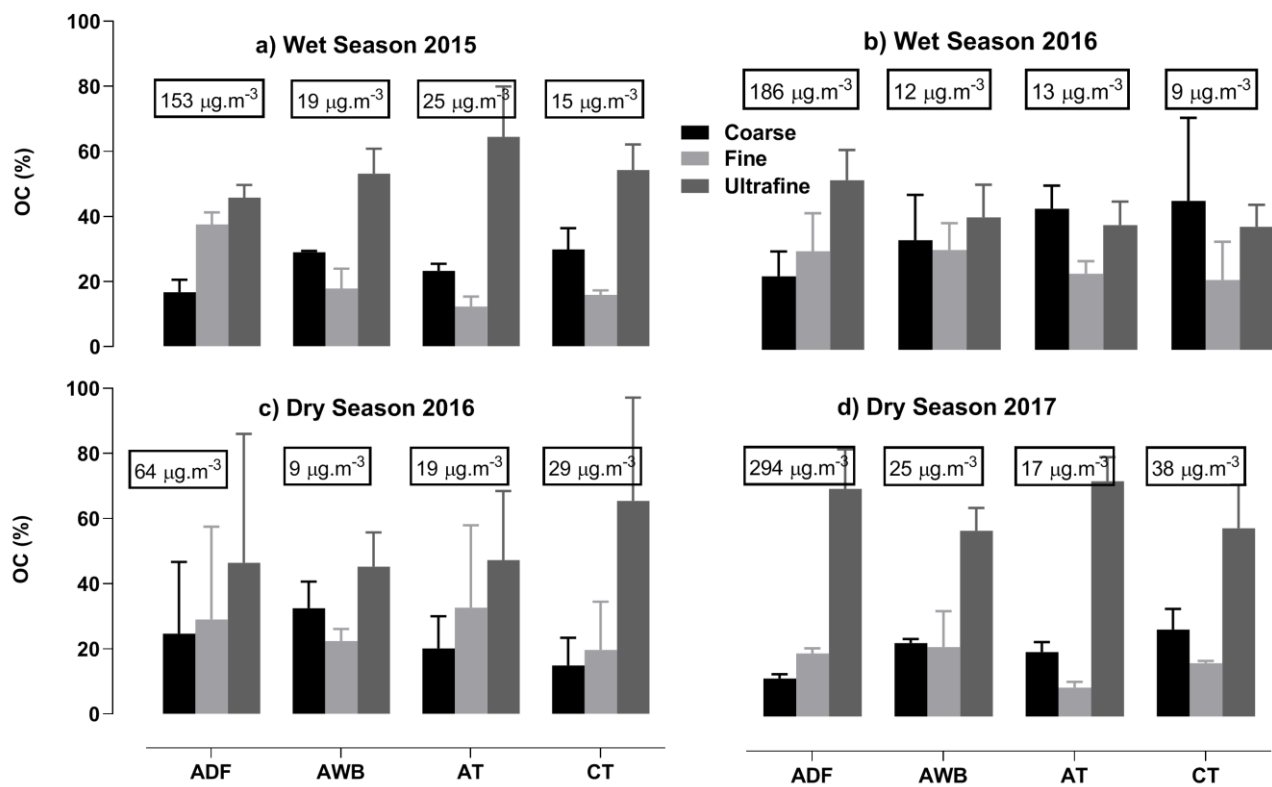
1368

1369   **Figure 9**

1370

1371

1372

1373

1374
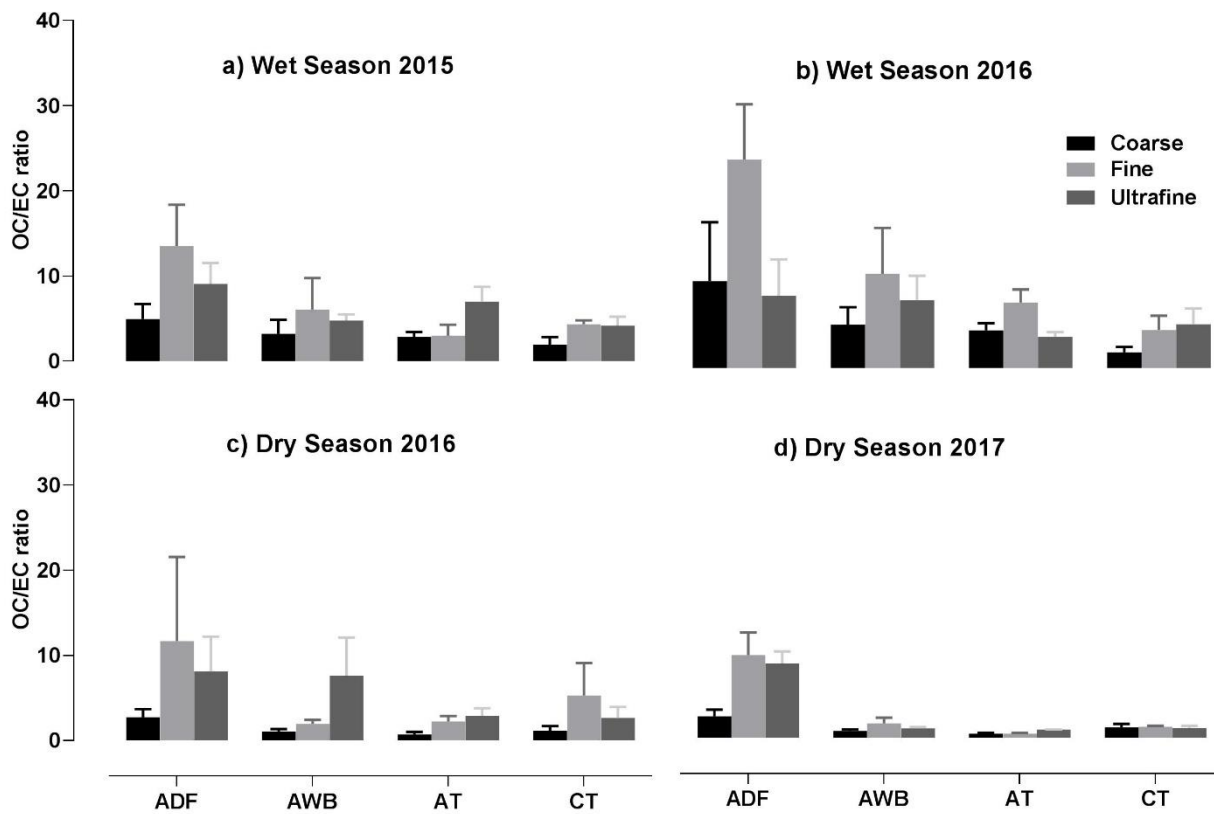
1375

1376   **Figure 10**

1377

1378
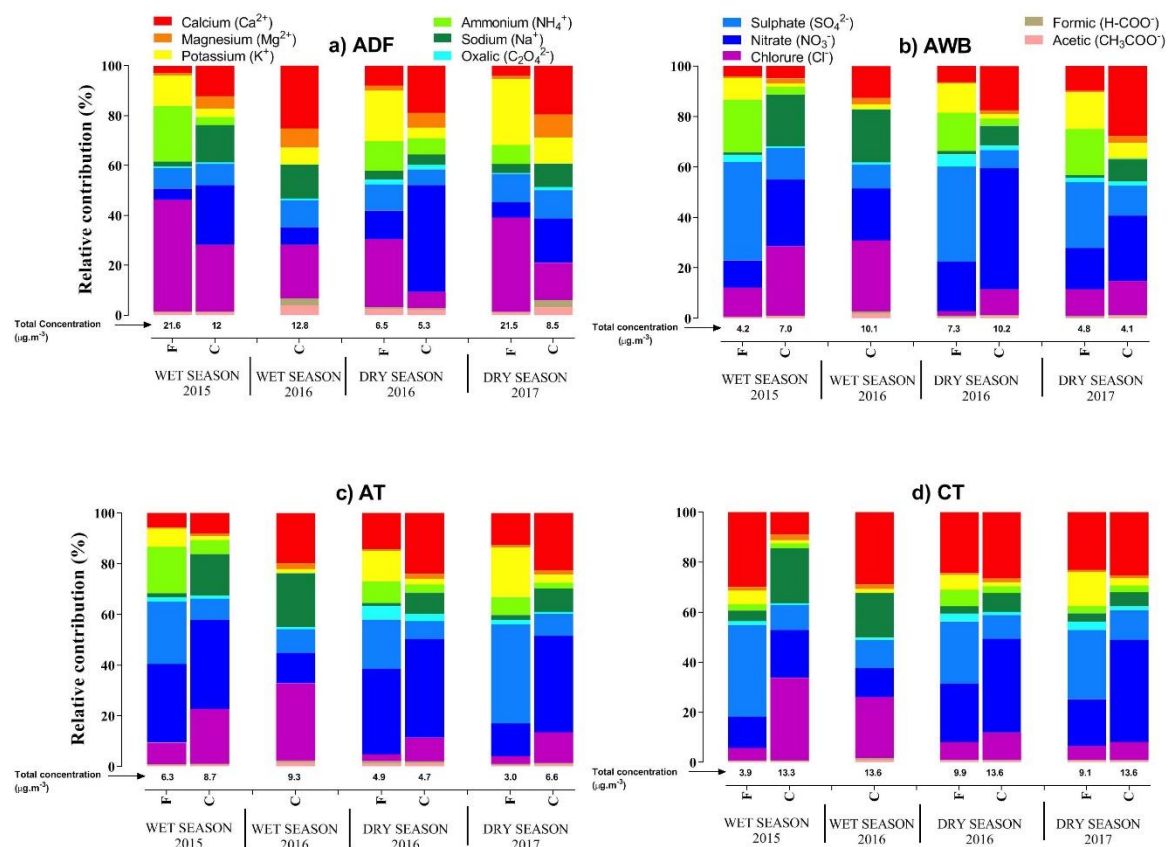
1379

1380   **Figure 11**

1381

1382
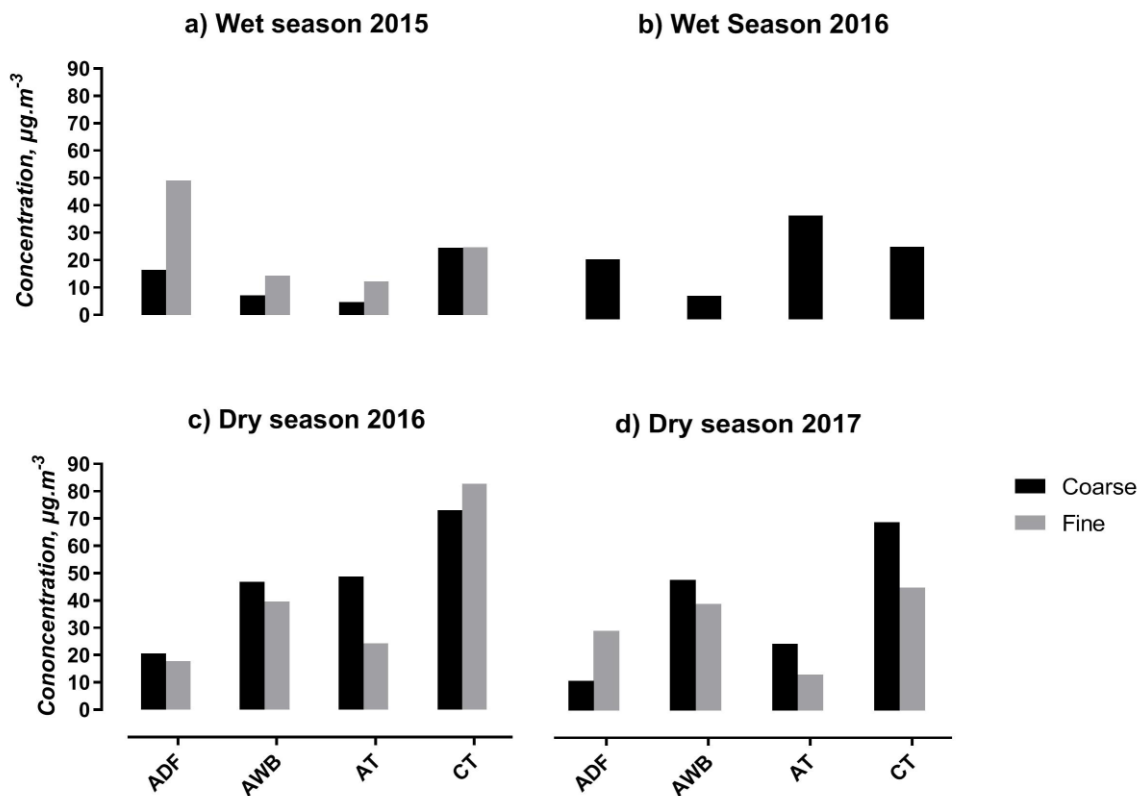
1383

1384   **Figure 12**

1385
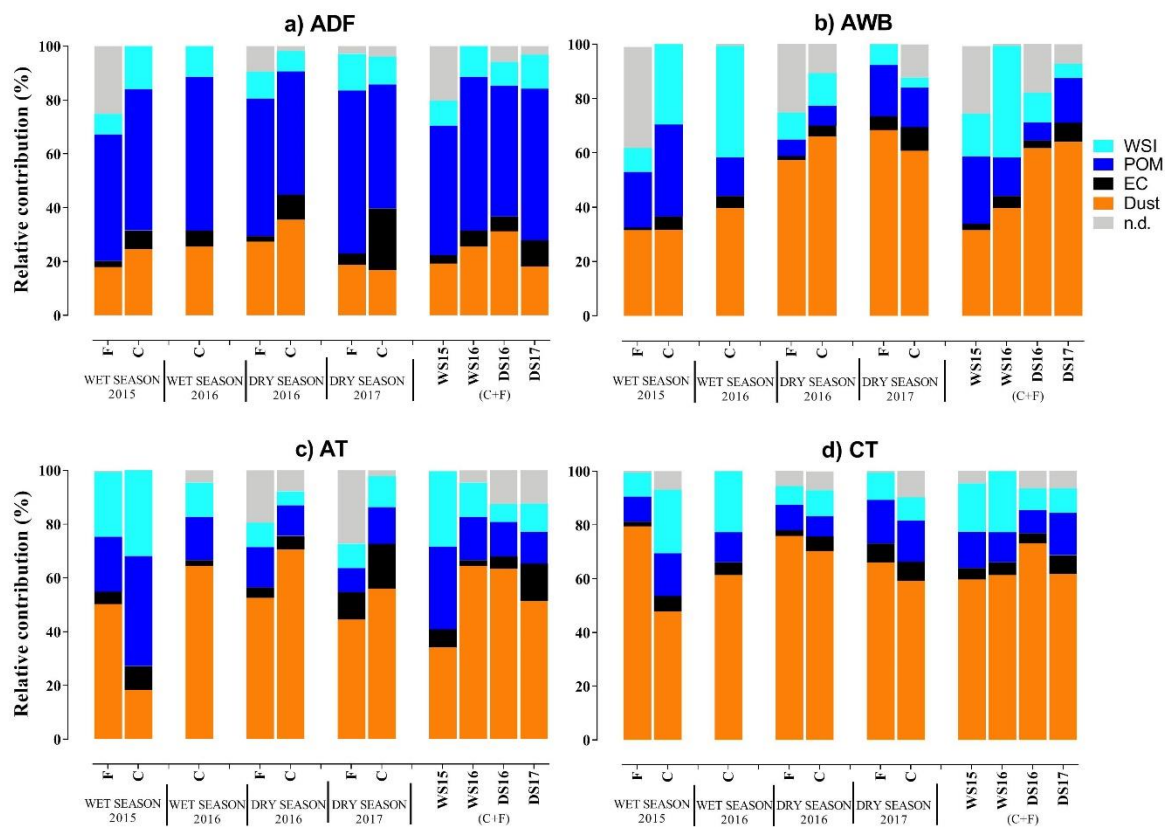
1386

1387   **Figure 13**

1388

1389

1390

1391
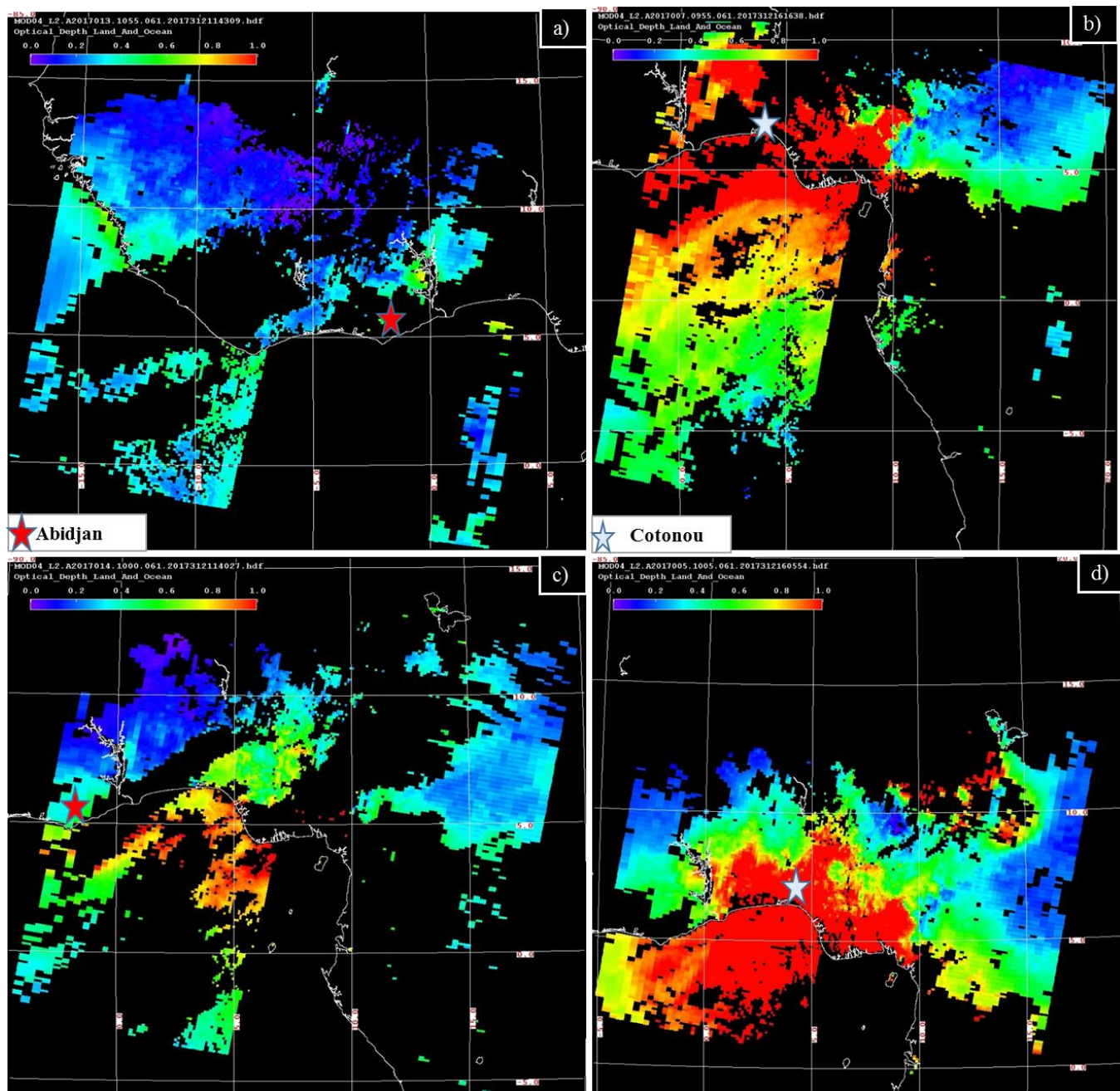
1392

Figure 14

1393

1394

1395

1396

1397

1398

1399

1400

1401

1402

1403   List of table

1404

1405   Table 1: Comparison of dust concentrations obtained from different methodologies

1406   Table 2: WSOC concentrations (μg.m^{-3}) and WSOC/OC ratios (%) for each site, each campaign and
1407   each aerosol size

1408   Table 3: Trace element concentrations for bulk aerosol for each site and for DS2017 and WS2016.

1409   Table 4: Comparison of PM2.5 concentrations with literature data. Only literature data given at a daily
1410   scale have been selected.

1411   Table 5: PM2.5-EC and PM2.5-OC comparison with Djossou et al. (2018) and Xu et al. (2019) values.
1412   Units are μgC.m^{-3}

1413   Table 6: EC and OC comparison with literature values. Only literature data given at a daily scale have
1414   been selected.

1415   Table 7: Comparison of WSOC concentrations with literature data. Only literature data given at a daily
1416   scale have been selected.

1417

1418

1419

1420

1421

1422

1423

1424

1425

1426

1427

1428

1429

1430

1431

1432

1433

1434

1435

1436

1437

1438

1439

1440   Table 1: Comparison of dust concentrations obtained from different methodologies in µg.m^{-3}

Dry 2017		Sciare et al. (2005)	Guinot et al. (2007)	Terzi et al. (2010)
ADF	C	18.5	11.2	86.9
	F	9.3	29.7	22.2
	bulk	27.7	40.9	109.1
AWB	C	12.3	48.5	126.4
	F	5.2	39.7	106.4
	bulk	17.6	88.2	232.8
AT	C	16.4	24.8	98.5
	F	4.3	13.4	34.2
	bulk	20.7	38.2	132.7
CT	C	37.9	70.0	98.4
	F	23.4	45.6	55.8
	bulk	61.3	115.6	154.2

1441

Wet 2016		Sciare et al., 2005	Guinot et al., 2007	Terzi et al.(2010)
ADF	C	35.34	21.5	27.9
AWB	C	13.46	8.6	21.1
AT	C	19.65	37.5	21.4
CT	C	42.98	26.2	52.5
	Bulk	42.98	26.2	52.5

1442

1443

1444

1445

1446

1447

1448

1449

1450 Table 2: WSOC concentrations (µg.m^{-3}) and WSOC/OC ratios (%) for each site, each campaign and

1451 each aerosol size

Site		Abidjan Waste Burning		Abidjan Domestic Fire	
Period	Size	WSOC	WSOC/OC	WSOC	WSOC/OC
Wet season 2015	Coarse	1.3	24,6	8.2	32.5
	Fine	0.7	19.9	12.8	22.7
	Ultra fine	4.1	43.6	51.3	72.5
	PM2.5	5.5	33.7	69.5	47.2
Dry season 2016	Coarse	0.4	12.3	4.4	18.8
	Fine	0.9	46.9	7.0	20.4
	Ultra fine	1.5	38.4	21.9	61.5
	PM2.5	2.7	32.7	31.0	32.0
Wet season 2016	Coarse	1.3	42.5	16.5	44.3
	Fine	0.8	26.3	17.1	33.0
	Ultra fine	2.0	41.2	79.7	84.5
	PM2.5	3.5	37.1	106.0	52.0
Dry season 2017	Coarse	1.9	32.9	12.1	36.0
	Fine	1.4	38.4	19.9	35.0
	Ultra fine	1.6	11.5	38.6	19.0
	PM2.5	4.0	30.0	65.8	29.0

1452

1453

1454 Table 2 (suite): WSOC concentrations (µg.m^{-3}) and WSOC/OC ratios (%) for each site, each campaign

1455 and each aerosol size

Site		Abidjan Traffic		Cotonou Traffic	
Period	Size	WSOC	WSOC/OC	WSOC	WSOC/OC
Wet season 2015	Coarse	2.4	39.6	1.1	23.3
	Fine	1.3	46.7	0.5	22.1
	Ultra fine	4.7	29.0	0.4	12.7
	PM2.5	6.9	34.0	2.2	18.0
Dry season 2016	Coarse	1.4	43.0	2.3	64.1
	Fine	1.9	59.0	0.6	10.5
	Ultra fine	4.9	62.0	6.3	42.9
	PM2.5	7.5	49.4	8.0	29.0
Wet season 2016	Coarse	1.1	23.1	1.2	34.7
	Fine	0.5	16.8	0.5	32.2
	Ultra fine	1.4	34.8	0.9	23.0
	PM2.5	2.4	26.0	1.9	28.0
Dry season 2017	Coarse	0.9	24.0	3.5	37.8
	Fine	0.3	24.3	2.4	39.6
	Ultra fine	1.8	14.8	1.9	10.4
	PM2.5	2.6	16.0	6.0	18.2

1456   Table 3: Trace element concentrations for bulk aerosol for each site and for DS2017 and WS2016.

	Bulk ng.m⁻³ (%)							
	DRY 2017				WET 2016			
	ADF	AWB	AT	CT	ADF	AWB	AT	CT
Al	10050.8 (1.8)	25186.1 (13.7)	14015.8 (12.26)	15480.4 (5.7)	1370.5 (0.4)	1990.1 (3.5)	2191.4 (2.4)	4010.5 (4.4)
K	8634.3 (1.5)	6093.7 (3.3)	3677.7 (3.22)	5068.9 (1.9)	1105.0 (0.3)	472.0 (0.8)	275.9 (0.3)	1076.0 (1.2)
Na	6847.8 (1.2)	23430.5 (12.8)	15372.1 (13.44)	11529.3 (4.3)	2070.6 (0.6)	3735.4 (6.6)	2861.5 (3.1)	5310.2 (5.8)
Ca	4321.2 (0.8)	2923.7 (1.6)	4117.6 (3.60)	6233.5 (2.3)	4124.7 (1.1)	447.5 (0.8)	374.7 (0.4)	4954.02 (5.4
Mg	1940.6 (0.3)	384.0 (0.2)	410.3 (0.36)	823.2 (0.3)	1524.7 (0.4)	294.9 (0.5)	283.5 (0.3)	619.2 (0.7)
Fe	1709.9 (0.3)	3807.9 (2.1)	1628.1 (1.42)	3406.8 (1.3)	1314.0 (0.4)	709.3 (1.3)	987.3 (1.1)	1549.4 (1.7)
P	1521.9 (0.3)	696.0 (0.4)	147.8 (0.13)	207.4 (0.1)	605.4 (0.2)	8.6	13.2	81.4 (0.1)
Ti	488.9 (0.1)	2270.3 (1.2)	282.8 (0.25)	457.9 (0.17)	170.8 (0.05)	75.7 (0.13)	96.8 (0.11)	154.7 (0.17)
Zn	189.7 (0.03)	80.9 (0.04)	57.9 (0.05)	149.4 (0.06)	60.3 (0.02)	1.9	41.1 (0.04)	36.2 (0.04)
Zr	172.1 (0.03)	390.3 (0.21)	217.9 (0.19)	145.3 (0.05)	-	22.4 (0.04)	36.7 (0.04)	31.2 (0.03)
Pb	87.1 (0.02)	11.0 (0.01)	4.8	11.5	8.3	2.1	2.3	9.3 (0.01)
Sn	79.7 (0.01)	38.4 (0.02)	21.6 (0.02)	37.4 (0.01)	0.77	0.09	0.0006	9.ç (0.01)
Mn	74.2 (0.01)	35.2 (0.02)	33.7 (0.03)	160.6 (0.06)	48.9 (0.01)	12.01 (0.02)	9.1 (0.01)	41.41 (0.05)
Rb	52.4 (0.01)	8.7	5.9 (0.01)	8.5	4.47	0.71	0.85	1.9
Sb	59.9 (0.01)	201.2 (0.11)	123.6 (0.11)	149.04 (0.06)	24.4 (0.01)	0	0.0006	2.9
Ba	37.3 (0.01)	53.3 (0.03)	47.4 (0.04)	65.8 (0.02)	18.5	8.02 (0.01)	9.9 (0.01)	32.0 (0.03)
Ni	36.5 (0.01)	34.5 (0.02)	27.9 (0.02)	50.2 (0.02)	18.00)	33.1 (0.06)	9.7 (0.01)	14.9 (0.02)
Cr	29.4 (0.01)	53.8 (0.03)	35.8 (0.03)	28.6 (0.01)	41.9 (0.01)	47.7 (0.08)	24.3 (0.03)	29.7 (0.03)
Sr	28.1 (0.01)	15.5 (0.01)	21.2 (0.02)	34.02 (0.01)	17.02	0	0.19	8.1 (0.01)
Cu	24.0	12.3 (0.01)	3.6	9.6	3.99	0.26	0.87	2.8)
Sr	12.6	-	-	-	17.1	-	0.22	8.9 (0.01)
Li	7.3	15.5 (0.01)	7.8 (0.01)	7.39	0.36	0.32	0.23	0.75
Cd	6.1	1.6	1.0	0.83	1.18	0.05	0.02	0.17
V	5.5	12.4 (0.01)	5.1	10.62	2.14	1.84	2.0	3.35
Mo	5.5	8.0	4.9	3.19	4.56	6.84 (0.01)	2.04	3.2
Cs	5.4	0.9	1.2	0.94	0.11	0.12	0.01	0.17
Hf	4.5	10.8 (0.01)	6.8 (0.01)	4.63	0	0.67	1.03	0.97
As	4.2	4.5	3.1	1.22	0	0 (0)	0.05	0.60
Li	4.0	9.8	5.9 (0.01)	5.82	0.27	0.37	0.16	0.93
Co	3.8	1.1	2.1	35.67 (0.01)	0.86	0.49	0.13	0.33
Ce	3.7	6.8	6.0 (0.01)	9.85	1.06	0.50	0.42	2.03
La	1.8	3.5	2.9	4.78	0.54	0.24	0.25	0.92
Nb	1.5	2.6)	1.4	2.48	0.98	0.46	0.5	0.63
Nd	1.5	2.5	2.4	4.15	0.05	0 (0)	-	0.40
Sc	0.69	1.4	1.1)	1.31		0,00		0.02
Be	0.13	0.19	0.2	0.28	0.003	-	-	0.03
Ga	0.61	1.15	0.8	0.98	0.2	0.11	0.12	0.37
Ge	0.42	1.02	0.8	0.68	0.01	0.07	0.02	0.11
Se	0.91	-	-	0.02	0.59	-	0.20	0.18
Rh	0.02	0.02	0.00002	0.002	-	0.002		0.0002
Te	0.06	0.08	0.08	0.05	0.02	0.02	0.02	0,00
Pr	0.40	0.74	0.7	1.13	0.06	0.01	0.004	0.15
Sm	0.27	0.46	0.45	0.76	0.01	0,00	-	0.07
Eu	0.05	0.08	0.08	0.15	0.01	0.003	-	0.0
Gd	0.31	0.57	0.54	0.86	0.05	0.02	0.001	0.15
Tb	0.04	0.07	0.07	0.10	0.005	-	-	0.02
Dy	0.24	0.42	0.40	0.57	0.001	-	-	0.05
Ho	0.05	0.09	0.09	0.12	0.01	0.008	0.01	0.03
Er	0.16	0.31	0.28	0.35	0.02	0.03	0.02	0.09

Tm	0.02	0.05	0.05	0.05	0.002	0.003	0.001	0.01
Yb	0.18	0.38	0.32	0.34	0.01	0.02	0.03	0.09
Lu	0.03	0.06	0.08	0.06	0.003	0.005	0.005	0.02
Ta	0.07	0.14	0.09	0.16	0.06	0.02	0.02	0.03
W	0.80	1.63	0.69	0.54	0.26	0.41	0.4	0.3
Tl	0.22	0.01	0.03	0.06		0.009		
Bi	0.32	0.26	0.02	0.08	0.06	-	-	0.08
Th	0.41	0.88	0.79	1.29	0.15	0.09	0.09	0.24
U	0.22	0.43	0.49	0.51	0.03	0.03	0.02	0.09
Total	36459.9	65817.6	40312.2	44159.2	12562.9	7874.7	7227.2	18001.1
Mass(µg/m^3)	558.8	183.6	114.4	270.0	374.7	56.3	91.6	91.9

1457

1458

1459

1460

1461

1462

1463

1464

1465

1466

1467

1468

1469

1470

1471

1472

1473

1474

1475

1476

1477

1478

1479

1480

1481

1482

1483

Table 4: Comparison of PM2.5 concentrations with literature data. Only literature data given at a daily scale have been selected.

Location	PM2.5 ($\mu g.m^{-3}$)	Reference
Abidjan, Côte d'Ivoire	142	This work
Cotonou, Benin	154	This work
Beijing, China	81.4	Xie et al., 2019
Christchurch, New Zealand	9.2	Tunno et al., 2019
Pune, India	98 ± 28	Pipal et al., 2019
Delhi, India	123	Guttikunda and Calori, 2013
Lahore, Pakistan	91	Colbeck et al., 2011
Ahvaz, Iran	69	Shahsavani et al., 2012
Hong Chong, Hong Kong	54.7 ± 25.6	Cheng et al., 2015
Lecce, Italia	16	Cesari et al., 2016
Libreville, Gabon	35.8	Ngo et al., 2019
Port Gentille, Gabon	60.9	Ngo et al., 2019
Kenitra, Morocco	51.3	Zghaid et al., 2009
Bilecik, Turkey	247	Gaga et al., 2018
Algiers, Algeria	34.8	Bouhila et al., 2015
Shobra, Egypt	216	Lowenthal et al.,2015

1504

1505 Table 5: PM2.5-EC and PM2.5-OC comparison with Djossou et al. (2018) and Xu et al. (2019) values.
1506 Units are $\mu gC.m^{-3}$.

Location	Period	PM2.5 OC	PM2.5 EC	References
Traffic Abidjan. Cote d'Ivoire	July 2015	22.6 ± 3.4	4.3 ± 0.2	This Work
	January 2016	15.2 ± 5.3	7.0 ± 2.6	
	July 2016	9.3 ± 1.3	2.2 ± 0.1	
	January 2017	16.1 ± 1.7	18.9 ± 1.4	
	July 2015	3.3 ± 0.2	2.3 ± 0.2	Djossou et al. 2018
	January 2016	7.7 ± 0.0	3.9 ± 0.0	
	July 2016	7.6 ± 0.2	4.9 ± 0.0	
	January 2017	19.1 ± 6.2	13.9 ± 5.5	
Traffic Cotonou. Benin	July 2015	13.1 ± 1.2	3.5 ± 0.7	This Work
	January 2016	27.8 ± 11.3	10.9 ± 2.6	
	July 2016	6.7 ± 1.9	2.0 ± 0.5	
	January 2017	33.1 ± 4.6	27.3 ± 0.9	
	July 2015	4.2 ± 0.7	1.5 ± 0.1	Djossou et al. 2018
	January 2016	3.0 ± 0.3	1.5 ± 0.2	
	July 2016	6.7 ± 0.2	1.6 ± 0.1	
	January 2017	14.5 ± 0.8	4.4 ± 0.7	
	January 2016	49.5 ± 12.5	13.6 ± 3.6	Xu et al. 2019
	July 2016	37.0 ± 3.5	9.3 ± 0.8	
Domestic fire Abidjan. Cote d'Ivoire	July 2015	147.2 ± 14.5	16.1 ± 1.6	This Work
	January 2016	56.5 ± 51.5	7.4 ± 3.1	
	July 2016	172.3 ± 39.0	17.9 ± 4.8	
	January 2017	283.9 ± 34.9	37.9 ± 4.3	
	July 2015	80.5 ± 1.1	32.2 ± 1.6	Djossou et al. 2018
	January 2016	76.3 ± 13.7	11.4 ± 0.2	
	July 2016	68.4 ± 16.5	17.4 ± 2.1	
	January 2017	66.4 ± 7.5	21.1 ± 6.6	
	January 2016	72.4 ± 24.6	19.5 ± 7.3	Xu et al. 2019
	July 2016	189.3 ± 197.8	11.5 ± 10.8	
Waste Burning Abidjan. Cote d'Ivoire	July 2015	14.8 ± 1.1	4.4 ± 0.1	This Work
	January 2016	7.7 ± 1.3	3.0 ± 0.3	
	July 2016	10.0 ± 2.4	1.5 ± 0.3	
	January 2017	21.9 ± 4.2	19.2 ± 2.4	
	July 2015	3.7 ± 2.2	4.3 ± 0.3	Djossou et al. 2018
	January 2016	13.9 ± 9.0	3.6 ± 1.8	
	July 2016	9.8 ± 4.4	2.8 ± 0.9	
	January 2017	22.4 ± 7.8	8.7 ± 3.0	
	January 2016	85 ± 57.4	15 ± 4.7	Xu et al. 2019
	July 2016	65.2 ± 65.2	12.3 ± 11.4	

1507

1508

1509

1510 Table 6: EC and OC comparison with literature values. Only literature data given at a daily scale have
1511 been selected.

1512

Location	OC (µg.m^{-3})	BC (µg.m^{-3})	Reference
Abidjan (Côte d'Ivoire)	16	8.1	This study
Cotonou (Benin)	20.2	11	This study
Bilecik (Turkey)	49.6-62.8	38.8-58.1	Gaga et al., 2018
Pune (India)	30	5	Pipal et al., 2019
Shanghai (China)	4.9-13.1	1.9-5	Ding et al., 2017
Lahore (Pakistan)	85.7-152	13.8-21	Stone et al., 2010
Agra (India)	25.4-70	3.3-9.5	Satsangi et al., 2012, Pipal et al., 2014
Delhi (India)	34.1-50	5.3-10.6	Bisht et al., 2015a, Pipal et al., 2014
Ahmedabad (India)	18.3	3	Rengarajan et al., 2011
Yokohama (Japan)	4	2	Khan et al., 2010
Beijing (China)	2.9-28.2	1.2-16.3	Guinot et al., 2007

1513

1514

1515

1516

1517

1518

1519

1520

1521

1522

1523

1524

1525

1526

1527

1528

1529

1530

1531

1532

1533

1534 Table 7: Comparison of WSOC concentrations with literature data. Only literature data given at a daily
1535 scale have been selected.

1536

Location	WSOC ($\mu g.m^{-3}$)	Reference
Abidjan, Côte d'Ivoire	2-8	This work
Cotonou, Benin	2-8	This work
Beijing, China	9-27	Yu et al., 2018
Beijing, China	4-6	Xiang et al., 2017
Beijing, China	8-12	Tang et al., 2016
Beijing, China	7	Du et al., 2014
Beijing, China	6-8	Feng et al., 2006
Shanghai, China	2-7	Feng et al., 2006, Huang et al., 2012
Guangzhou, Hong Kong	2	Huang et al., 2012
Guangzhou, Hong Kong	5-10	Feng et al., 2006
Gwangju, Korea	2-3.5	Park et al., 2015
Tokyo, Japan	3-23	Sempere and Kawamura, 1994
Cairo, Egypt	3	Favez et al., 2008
Amsterdam, Netherland	1-2	Feng et al., 2007
Barcelone, Spain	1-2	Viana et al., 2007 and 2008
Brindisi, Italy	1.5	Genga et al., 2017
Saint Jean de Maurienne, France	1-5	Sullivan et al., 2004, Jaffrezo et al., 2005a

1537

Physico-chemical characterization of urban aerosols from specific combustion sources in West Africa at Abidjan in Côte d'Ivoire and Cotonou in Benin in the frame of the DACCIWA program

Aka Jacques Adon[1], Catherine Liousse[1], Elhadji Thierno Doumbia[2], Armelle Baeza-Squiban[3], Hélène Cachier[1], Jean-Francois Léon[1], Veronique Yoboué[4], Aristique Barthel Akpo[5], Corinne Galy-Lacaux[1], Benjamin Guinot[1], Cyril Zouiten[6], Hongmei Xu[1, 7], Eric Gardrat[1], Sekou. Keita[8].

[1] Laboratoire d'Aérologie, Université de Toulouse, CNRS, UPS, Toulouse, France

[2] Centre National de Recherche Météorologique (CNRM)/Groupe d'étude de l'Atmosphère Météorologique, CNRS-Météo-France, Toulouse, France

[3] Université Paris Diderot, Unité de Biologie Fonctionnelle et Adaptative-RMCX, CNRS, UMR 8251, Paris, France

[4] Laboratoire de Physique de l'Atmosphère, Université Félix Houphouët-Boigny, Abidjan BPV 34, Côte d'Ivoire

[5] Laboratoire de Physique du Rayonnement, Université d'Abomey-Calavi, Abomey-Calavi, Bénin

[6] Géosciences Environnement Toulouse, Université de Toulouse, CNRS, UPS, Toulouse, France

[7] Department of Environmental Science and Engineering, Xi'an Jiaotong University, Xi'an, China

[8] Université de Khorogo, Khorogo, Côte d'Ivoire.

Correspondence to: adonjacks@gmail.com (J. Adon) and lioc@aero.obs-mip.fr (C. Liousse)

Abstract

Urban air pollution in West Africa has yet to be well characterized. **In the frame of** DACCIWA (Dynamics-Aerosol-Chemistry-Cloud Interactions in West Africa) program, intensive measurement campaigns were performed in Abidjan (Côte d'Ivoire) and Cotonou (Benin), in dry (January 2016 and 2017) and wet (July 2015 and 2016) seasons, at different sites chosen to be representative of African urban combustion sources (i.e. domestic fires (ADF), traffic (AT) and waste burning (AWB) sources in Abidjan and traffic source in Cotonou (CT)). Both the size distribution of particulate matter (PM) and their chemical composition including elemental carbon (EC), organic carbon (OC), water-soluble organic carbon (WSOC), water-soluble inorganic ions (WSI) and trace metals were examined. Results show very high PM concentrations at all sites and a well-marked seasonality as well as a strong spatial variation. The average $PM_{2.5}$ mass concentrations during the wet season are 517.3, 104.1, 90.3 and 69.1 $\mu g.m^{-3}$ at the ADF, CT, AT and AWB sites, respectively. In the dry season, $PM_{2.5}$ concentrations decrease to 375.7 $\mu g.m^{-3}$ at the ADF site, while they increase to 269.7, 141.3 and 175.3 $\mu g.m^{-3}$ at the CT, AT and AWB sites, respectively. The annual $PM_{2.5}$ levels at almost all sites are significantly higher than the WHO guideline level of 10 $\mu g.m^{-3}$. As for PM mass, (EC) and (OC) concentrations are also maximum at ADF site, accounting up to 69% of the total PM mass. Such high content is mainly linked to wood burning for domestic cooking and commercial food smoking activities. Dust contributions are dominant at CT (57-80%), AT (20-70%) and AWB (30-69%) sites and specially in the coarse and fine particle modes at CT and in the coarse fraction at AT site, which may be explained by the impact of long-range desert-dust transport and re-suspended particles from the roads, in addition to anthropogenic sources. The contributions of WSI to the total PM mass, mainly driven by chloride, nitrate and calcium in the fine and/or large particles are highly variable according to the sites but remain less than 30%. Values are generally 1-3 times higher in the wet season than the dry season. This is due to anthropogenic emissions but also to nitrate formation by reaction processes and natural emissions. The concentrations of trace element well reflect the trends of dust at the traffic and AWB sites, with a predominance of Al, Na, Ca, Fe and K, keys markers of crustal dust. This study constitutes an original database that characterizes specific African combustion sources.

Keywords: atmospheric pollution, chemical composition, physicochemical characterization, Particulate matter, traffic, waste burning, domestic fires.

1.   Introduction

The impact of anthropogenic pollution on environment and health has been demonstrated by numerous studies in Europe and North America, which have contributed to the implementation of emission reduction policies. By contrast, air pollution in Africa is far from being well characterized, although it is suspected to be responsible for negative health outcomes (*WHO, 2014*). This is a major problem since Africa is an intense emitter of pollution from anthropogenic sources that includes domestic fires, vehicular traffic, waste burning as well as growing oil and mining industries. It has also one of the fastest growing urban populations in the world, especially in West and East Africa (UN, 2019). As a consequence, it has been shown that massive urbanization and rapid economic growth could be responsible for tripling anthropogenic emissions in Africa between 2000 and 2030 (*Liousse et al., 2014*). Moreover, it is important to recall the impact of biomass burning and dust sources in the African atmospheric composition, especially occurring during the dry season. All of this results in a major degradation of urban air quality and an impact on the health of exposed populations. Only a few studies on this subject have been conducted in West Africa (*Val et al., 2013*; *Dieme et al., 2012*; *Kouassi et al., 2009*) despite the high atmospheric pollutant concentrations already measured to be of the same order as in Asian megacities and well above WHO international standards (*WHO, 2014*).

West Africa is then an "unique laboratory" to study urban pollution. Previous studies conducted under the framework of the AMMA (Analyses Multidisciplinaires de la Mousson Africaine) and POLCA (POLlution des Capitales Africaines) programs, have revealed very high average particulate mass concentrations in Cotonou (Benin), Bamako (Mali), Dakar (Senegal) and Yaoundé (Cameroun) during the dry season (*Doumbia et al., 2012; Val et al., 2013*), suggesting that the population may be affected by negative health outcomes. For example, during the dray season in Bamako (Mali) and Dakar (Senegal), *Val et al. (2013)* showed that the inflammatory impact of combustion aerosol depends on the type of emission sources and determined the predominant role of particulate organic matter. This is consistent with global findings showing that fine and ultrafine aerosol fractions, as well as their content in trace metals and organic compounds, induce biological effects due to their ability to reach the distal lung (*Cassee et al., 2013*). Such reasons highlight the need to better understand the size-speciation of aerosol chemical composition for the main West African anthropogenic sources during the different seasons. Within this context, the DACCIWA (Dynamics-Aerosol-Chemistry-Cloud Interactions in West Africa) program, dedicated a specific work package to "Air Pollution and

96 Health" dealing with pollutant characterization related to health issues through toxicological
97 studies and epidemiological studies.

98 Campaigns have been organized from December 2014 to March 2017 in Abidjan and Cotonou.
99 The strategy was to measure aerosol chemical composition in different sites, representative of
100 the main prevailing urban sources in West Africa following *Liousse et al. (2014)* and *Keita et*
101 *al. (2018)*. Two typical traffic-sampling sites were chosen, one in Abidjan (Côte d'Ivoire) and
102 another one in Cotonou (Benin), to take into account differences in terms of fleets, type of fuel
103 used and quality of roads. Indeed, in Cotonou, the majority of population uses two-wheel
104 vehicles susing gasoline fuel or gasoline and oil fuel, whereas in Abidjan, the vehicle fleet is
105 dominated by four-wheel engines using diesel fuel. Measurements were also performed at
106 domestic fire and waste burning sites, both located in Abidjan.

107 For a period of two years, $PM_{2.5}$ mass and carbonaceous aerosol were weekly measured and
108 results are discussed in *Djossou et al. (2018)*. In this paper, we focus on the results from the
109 intensive campaigns. We present measurements obtained at each site during the wet and dry
110 seasons of the studied periods: (i) PM size distribution and mass concentrations and (ii) PM
111 chemical composition including carbonaceous aerosol, water-soluble organic carbon, water-
112 soluble inorganic ions, dust and trace elements in different size fractions. Experimental method
113 including description of sites, types of measurements and analyses, meteorological conditions,
114 will be presented in the section 2, whereas results and discussion are discussed in the sections
115 3 and 4 of the paper, respectively.

2. Experimental method

2.1. Description of sites

119   Measurement campaigns have been performed in wet season (July 20-26, 2015 and July
120 4-13, 2016) and dry seasons (January 7-15, 2016 and January 5-14, 2017) at three sites in
121 Abidjan (Côte d'Ivoire), representative of different sources, i.e. ADF for Abidjan Domestic
122 Fires, AWB for Abidjan Waste Burning and AT for Abidjan Traffic (Figure 1), as well as one
123 traffic site in Cotonou (Benin) (Figure 2).

124 As shown in Figure 3 which presents pictures of the different sampling sites, the ADF site (5˚
125 19' 44 "N, 4˚ 06' 21" W) is situated on a platform, 5 m above ground level, in Yopougon

126   Bracody district near a market (Figure 1). This geographical area is highly populated with
127   various small commercial activities such as a fish and meat-smoking by women. There are also
128   many formal and informal settlements, which mainly use wood and charcoal as a source of fuel
129   for private and professional combustion activities. Other sources of concern contributing to the
130   mix of pollutant emissions in the area include transportation-related emissions, biomass
131   burning, garbage bins or small landfills and various other fugitive sources. The AT site (5° 21'
132   14" N, 4° 01' 04" W) is located in Adjamé, on the roof of « 220 pharmacie logement building »,
133   about 7 m above ground level and roughly 10 m away from the main road. This site, close to
134   the Adjamé market and to a bus station, is highly affected by traffic (Gbaka, bus, taxi, woro-
135   woro, private cars…). The AWB site (5° 21' 12" N, 3° 56' 16" W) is located at Akouédo in the
136   district of Cocody, on the roof of « Talafiguié », a building 15 m above ground level. This site
137   close to the big municipal landfill of Abidjan operational since 1965 and now covering an area
138   of 153 ha, is submitted to frequent waste burning pollution. The Cotonou Traffic (CT) (6° 22'
139   19" N, 2° 26' 5" E) site is located in Cotonou, on the «Sogema» building roof, about 7 m above
140   ground level. This site is close to the Dantokpa market and also to the biggest crossroad of
141   Cotonou (intersection of 4 main roads). This site is highly influenced by intense traffic
142   activities. As previously mentioned, such a site is interesting because the vehicle fleet and fuels
143   are different in Cotonou compared to Abidjan: (1) there are many two-wheel vehicles in
144   Cotonou whereas a few only in Abidjan; (2) in Cotonou, gasoline is of poor quality due to the
145   illegal fuel transport from Nigeria and (3) the roads are in worse conditions in Cotonou than in
146   Abidjan.

147   **2.2. Measurements**

148   During each intensive campaign and on each site, two 3-hour samples collected with
149   cascade impactors operating in parallel are obtained for three consecutive days (i.e. six size-
150   resolved samples per site during each campaign), to allow size-speciated characterization of the
151   aerosol chemical composition. Note that the choice of the 3-hour periods is linked to the period
152   of maximum pollution for each site as shown by preliminary studies (e.g. morning at ADF site
153   (7-10am), afternoon at AT site (4-7pm, morning at CT site (7-10am)). There is no specific
154   period at AWB site since the activities are roughly the same during the day. The first impactor
155   with 4 stages ($PM_{>2.5}$; $PM_{2.5-1}$; $PM_{1-0.2}$; $PM_{<0.2}$) includes 4 quartz fiber filters (QMA, Whatman)
156   for mass and carbonaceous aerosol (EC, OC and WSOC analysis). The second impactor with 3
157   stages ($PM_{>2.5}$; $PM_{2.5-1}$; $PM_{1-0.1}$) is equipped with three Teflon filters (Zefluor, Pall
158   Corporation®), dedicated for water-soluble ions species and trace elements. Due to operational

159 problems in july 2016, this second 3-stage cascade impactor is replaced by another 3-stage

160 cascade impactor with different size cuts ($PM_{>10}$, $PM_{10-2.5}$, $PM_{2.5-1}$). For consistency, results will

161 be presented as an ultrafine (UF), fine (F) and coarse (C) classification. The two first stages

162 ($PM_{>2.5}$ and $PM_{2.5-1}$) being considered as the coarse particulate fraction, the $PM_{1-0.1}$ or $PM_{1-0.2}$

163 stage, the fine particulate fraction and the $PM_{<0.2}$ stage, the ultrafine fraction.

164 All the filters are prepared and analyzed at the Laboratoire d'Aerologie in Toulouse under

165 different protocols described in the following paragraphs. Note that the quartz filters are

166 prefired before sampling.

2.3. Analyses

2.3.1. Gravimetric analyses

169 Aerosol mass concentrations are obtained using a high-precision balance (SARTORIUS

170 MC21S), placed under a controlled temperature and humidity atmosphere (Person and Tymen,

171 2005). Before weighing, the filters are kept 24 hours in the weighing room at an ambient relative

172 humidity of 30 ±15%. The filters are weighed before and after sampling. Result of a gravimetric

173 measurement consists of the average of 2 to 4 weighing whose differences do not exceed 5μg.

174 The standard error on a gravimetric measurement is therefore less than 10 μg, typically

175 representing less than 5% of the particles mass.

2.3.2. Carbonaceous aerosols

177 Carbonaceous aerosol is determined with thermal analysis with a two-step method

178 adapted from Cachier et al. (1989). Two aliquots of the same filter are separately analyzed.

179 One portion is directly analyzed for its total carbon content (TC). The other portion is

180 first submitted to a pre-combustion step (2 h at 340°C under pure oxygen) in order to eliminate

181 Organic Carbon (OC), and then analyzed for its Elemental Carbon (EC) content. Organic

182 carbon (OC) concentrations are calculated as the differences between TC and EC. Note that the

183 aerosol carbon content is quantified by a non-dispersive infrared (NDIR) detector with G4

184 ICARUS instrument with a detection limit of the order of 2 $\mu gC.cm^{-2}$. Uncertainty is in the

185 order of 5% for TC, while being in the range of 5-20%, for EC and OC.

2.3.3 Water Soluble Organic Carbon analysis

187 WSOC measurements are performed using a total organic carbon analyzer (Sievers M9).

188 A detailed description of this technique is reported in Favez et al. (2008). Briefly, the full

189 oxidation of total organic carbon into CO_2 is obtained by coupling chemical oxidation (with

190 ammonium persulphate) and UV light. CO_2 is then quantified by conductivity. Analyses are

191 conducted on 20 ml of solution extracts. For UF samples, solutions to be analyzed are obtained

192 using a total filter surface of 3cm² (6x0.5 cm² punches symmetrically taken out of each QMA

193 filter), whereas, for C and F sizes, due to the geometry of the spots at the surface of the filters,

194 samples are divided into equivalent parts (1/2 or 1/4 of 47 mm filters, rest of the filters being

195 used for carbonaceous analysis). The extraction protocol consists of 16h soaking under soft

196 shaking in an Erlen-Meyer containing 20mL of ultra-pure water. Prior to WSOC analysis, water

197 extracts are filtered through Teflon (PTFE) filters (0.2μm pore size diameter) in order to remove

198 any suspended particle. Measurement uncertainty, given by the manufacturer, is of the order of

199 7%. The overall calculated blank value is of the order of $2.27 \pm 0.33\,\mu gC.cm^{-2}$, which represents

200 $16.4 \pm 8.5\%$ of the mean WSOC content. For each sample, duplicate analyses show a good

201 reproducibility.

202 ### 2.3.4. Water-soluble ionic species

203 Water-soluble ionic species (Na^+, NH_4^+, K^+, Mg^{2+}, Ca^{2+}, SO_4^{2-}, NO_3^- and Cl^-) are

204 analyzed using ion chromatograph (IC), following the analytical protocol described in Adon et

205 al. (2010). Briefly, the aerosol water-soluble fraction is first extracted from half-sampled Teflon

206 filter (the other part being used for trace element analysis), with a 10-min sonication in plastic

207 vials including 6 ml or 10 ml of purified water with a controlled resistivity of 18.2MΩ. Then

208 these vials are subjected to ionic chromatograph analysis or stored at +4°C if not analyzed

209 immediately. Cations are analyzed with Dionex DX-100 and anions with Dionex DX-500 with

210 a detection limit of 1 to 6 ppb depending on ionic species. Uncertainties in the range of 1-50%

211 is found depending on ionic species.

212 ### 2.3.5. Trace elements

213 The protocol to measure trace element concentrations is developed and performed at the

214 Laboratory of Environmental Geosciences of Toulouse. Half-sampled Teflon filters (the other

215 part being used for water-soluble ionic species, see below) are mineralized by acid digestion

216 with a 10 ml concentrated HNO_3 and 0.5 ml HF solution (Lamaison, 2006) using a closed vessel

217 microwave accelerated reaction system (MARS 5, CEM Corporation) at high pressure (700 psi)

218 (Celo et al. 2010). The digestion is realized in 3 steps: a rise in temperature at 130°C in 3min

219 and holding for 1 min, then, a second rise at 160°C in 1 min and holding for 30 seconds and

220 finally a third rise to 180°C in 1 min and holding for 3min. After a 12 h cooling period, the

221 solutions are evaporated at 80°C, and concentrated in 7 ml of 2% concentrated HNO_3 solution,

222 before analysis by ICP-MS which are performed with a 7500 ce Agilent Technologies

223 instrument equipped with a collision cell, and using In and Re as internal standards. The

224 detection limit is less than 10 ppt. For all the samples, the final blank values and detection limit

225 on filters are taken into account for final concentrations calculations. 13 trace metals are

226 considered in this work: Al, Ti, Cr, Mn, Fe, Ni, Cu, Zn, Ba, La, Th, Pb and Cd.

227 **2.3.6. Dust calculation**

228 Many methods can be used to quantify dust concentrations. We have selected three

229 methods (Sciare et al. 2005, Guinot et al. 2007, Terzi et al. 2010) to underline the uncertainties

230 linked to dust estimates.

231 (1) Sciare et al. (2005) method consists of using soluble calcium data obtained with Ionic

232 Chromatography (IC), to estimate the dust concentrations following the relationship:

233 dust = 10.96*nss-Ca^{2+}, where nss-Ca^{2+} (=1.02*Ca^{2+}-0.038*Na^+) refers to non-sea-salt

234 calcium concentration.

235 (2) Guinot et al. (2007) method is based on a chemical closure where fine and coarse

236 particle aerosols are separated in 4 components (EC, POM, WSI and dust). EC, WSI,

237 and total aerosol mass are directly experimentally determined (see below paragraphs).

238 POM concentrations are obtained from OC concentrations experimentally determined

239 and k, the OC/POM conversion factor. Dust concentrations are obtained from measured

240 Ca^{2+} concentrations and f, the abundance of calcium in dust. The k and f values are

241 obtained from a linear regression (L) between the reconstructed and the weighed aerosol

242 mass concentrations. Briefly, first step consists of focusing on the aerosol coarse

243 fraction. k is fixed to 1.8 and as a result of (L) just mentioned, f is obtained to be in the

244 range of 0.012 to 0.15 depending on our sites. Second step deals with the aerosol fine

245 fraction. The f values just obtained for the aerosol coarse fraction are applied to the fine

246 fraction and k ratios are estimated using (L) to be in the range of 1.2 to 2.1. Note that at

247 all of our sites, the correlation between Ca^{2+} and the missing mass between the weighed

248 and the reconstructed aerosol mass is sufficiently good (r^2=0.9) to support the

249 consistency of this simple approach for the evaluation of dust. Also, f and k values are

250 included in the range of values provided in the literature (He et al. 2001; Sun et al. 2004;

251 Guinot et al. 2007). However, it is important to mention that the range of f and k

252 coefficients are large which is due to the source mixing observed in this study.

253   (3) In Terzi et al. (2010) method, dust is obtained with the following relationship: dust =

254   1.89[Al] + 1.21[K] + 1.95[Ca] +1.66[Mg] + 1.7 [Ti] +2.14[Si] + 1.42[Fe]. In our study,

255   all these elements are determined except Silica (Si). Consequently, we used mean Si

256   values obtained from different relationships available in the literature ($SiO_2 = 3*Al_2O_3$

257   for Alastuey et al., 2005, $Si = 4.0*Al$ for Zhang et al., 2003 and $Si = 2.03*Al$ for

258   Chiapello et al., 1997).

259   The results of dust concentrations estimated from the three methodologies above described are

260   summarized in the Table 1 for wet season (WS) 2016 and dry season (DS) 2017. Indeed, Ca,

261   Al, and Fe concentrations measured by ICP-MS are only available in WS2016 and DS2017 due

262   to experimental problems, whereas Ca^{2+} concentrations measured by IC are available for all

263   campaigns. As shown in table 1, the dust obtained from Ca^{2+} measured by IC (Sciare et al.,

264   2005) and by the Guinot et al. (2007) method is lower than that obtained from trace elements

265   (Terzi et al., 2010) for DS2017 whereas in the same order of magnitude in WS2016. Such

266   results are in agreement with methodological aspects. Indeed, Al, Fe, Ca … obtained by ICP-

267   MS include both soluble and insoluble particles whereas Ca^{2+} measured by IC only include

268   soluble particles. During the dry season, comparison of Ca measured by ICP-MS (not shown

269   here) is higher than that of the IC, by a factor of 1.7, 1.8, 2.2 and 1.1, at the ADF, AWB, AT,

270   and CT sites respectively. By contrast, this factor is low and constant (1.3) in the wet season

271   for all the sites. In our study, due to the lack of trace element data for WS2015 and DS2016,

272   dust estimations are performed from Guinot et al. (2007) method. This choice globally implies

273   an underestimate of dust concentrations by a factor of 1.5 to 3.5 in DS2017 as shown in Table

274   1.

275

276   **2.3.7. Aerosol chemical closure methodology**

277   As previously mentioned and detailed, aerosol chemical closure is performed following

278   the Guinot et al. (2007) methodology.

279

280   **2.4. Meteorological conditions**

281   In Figure 4, meteorological data (surface temperature, wind directions and speed) issued

282   from the NOAA Integrated Surface database (ISD; see https:// www.ncdc.noaa.gov/isd) and the

283   ASECNA (Agence pour la Sécurité de la Navigation Aérienne en Afrique et à Madagascar) are

284   presented for the South-West Africa region including Abidjan and Cotonou. As expected, this

area is under the influence of the Convergence Zone of two air masses of a different nature, i.e. Harmattan (hot and dry continental trade winds) from the north and Monsoon (humid maritime trade winds) from the south (Figure 4). Ground contact between these two air masses constitutes the intertropical front (ITF) of which the fluctuations during the year determine the seasons in the Gulf of Guinea (Tapsoba, 1997). During the dry season (from November to March), temperatures are relatively high with maximum around 30°C on the coast. The humidity is low, since the prevailing Harmattan wind blows from the desert, usually bringing dust (Figure 4, lower line). The period from June to September, especially in July is the wet season period when daytime temperatures are slightly lower, with maximum around 26/28°C on the coast (Figure 4, upper line). At this season, the humidity level is high across the region. On the coast, rains may occur from March to November.

During our campaigns (not shown here), temperatures are roughly the same at Abidjan and Cotonou, reaching 28°C and 26°C in the dry and wet seasons, respectively. Gentle to moderate wind speeds are observed during the measurement campaigns at the two cities, with average values of 15-20 and 15-22 km.h^{-1} at Abidjan and Cotonou, respectively. There is no precipitation at CT site during the studied periods. In Abidjan on the contrary, low rains occur both in wet and dry periods with cumulative precipitation higher in DS2017 (7mm), than in WS2016 (4.7mm) and WS2015 (2mm). There is no rain in DS2016 (https://www.historique-meteo.net/afrique/).

2.5. Backward trajectories

The Hybrid Single-Particle Lagrangian Integrated Trajectory (HYSPLIT) modelling system (Air resources laboratory, Draxler and Rolph, 2012) is used for the trajectory analysis. HYSPLIT model is run to compute 120 h back trajectories ending at Abidjan and Cotonou at 50 m a.g.l. (Figure 5). Global Data Assimilation System reanalysis database is used as meteorological input, with a 0.25×0.25 degrees horizontal resolution. Results presented in Figure 5, confirm that air masses mainly come from the north with a few from the south-west in dry season (January), whereas from the south-west and the south in wet season (July). Therefore, in January, Abidjan and Cotonou are mainly impacted by polluted air masses from surrounding areas and northern countries with possible dust and west African biomass burning influences, whereas in July, the impact of oceanic sources possibly polluted by long-range south African biomass burning aerosols may be observed.

3. Results

318 **3.1. Aerosol size distribution and mass concentration**

319   In Figure 6, the relative mass distribution of PM for Coarse (C), Fine (F) and Ultra-Fine
320   (UF) particle sizes in percentages are presented with bulk mass concentration averages
321   indicated in the black boxes for each site and for each campaign. As it may be seen, bulk
322   concentrations vary widely from site to site and from campaign to campaign. During the wet
323   season, the average total concentrations range from 82 to 676 $\mu g.m^{-3}$ in 2015 and 56 to 358
324    $\mu g.m^{-3}$ in 2016, with the maximum at the Abidjan Domestic Fire (ADF) site. While during the
325   dry season, values range from 168 to 269 $\mu g.m^{-3}$ in 2016 and from 114 to 559 $\mu g.m^{-3}$ in 2017,
326   with maximum concentration obtained at the Cotonou Traffic (CT) and ADF sites. In terms of
327   size distribution, concentration peaks may be observed for all aerosol size-fractions which are
328   found to exhibit different seasonal patterns. UF particles (<0.2 µm) represent the highest
329   contributor to the bulk mass at the ADF site, by up to 60 % (335.3 $\mu g.m^{-3}$) in DS2017. F particles
330   (1-0.2 µm) are the second most important contributor and both combined particle sizes account
331   for more than 85 % of the total mass at the ADF site. In this site, ultra-fine and fine fractions
332   are also found to be maximum during WS2015 and WS2016 by up to 90 and 83%, respectively.
333   Let us note that C particle contribution in bulk is relatively higher in the traffic and waste
334   burning sites than in ADF site (40%) whereas F and UF particle contributions are on the order
335   of 60%.

336   In terms of PM2.5, the results of this work are presented in Figure 7. The mass
337   concentration of PM2.5 averaged over DS2016 and DS2017 are 154 ± 74, 144 ± 42, 134 ± 7
338   and 211 ± 51 $\mu g.m^{-3}$ at the ADF, AWB, AT and CT sites, respectively and 338 ± 24, 45 ± 3, 52
339   ± 4 and 70 ± 1 $\mu g.m^{3}$ over the wet seasons (2015-2016). The increase in PM2.5 is of the order
340   of 54% at ADF from dry to wet season, whereas a sharp reduction (more than 60%) is obtained
341   at AWB, AT, and CT sites.

342 **3.2. Carbonaceous aerosol**

343 **3.2.1. EC and OC concentrations**

344   In Figure 8, EC relative mass contributions are presented for each size, site and
345   campaign: wet season 2015 (WS2015), wet season 2016 (WS2016), dry season 2016 (DS2016)
346   and dry season 2017 (DS2017). Mean EC bulk mass concentrations are added in the black boxes
347   for each size and for each campaign. The most striking feature is that the ADF site
348   concentrations are higher than at the other sites in WS2016 and in DS2017, whereas of the same

349   order of CT site concentrations in the other seasons. Mean concentration at the CT site ($16\mu g.m^{-3}$)

350   is slightly higher than at the AT site ($10\mu g.m^{-3}$), whereas the lowest concentrations are found

351   at the AWB site. Results of the EC size distribution are very consistent among the different

352   sites (Figure 8). Whatever the site and the season, higher EC concentrations are found in C

353   (42%) and UF (43%) particles compared to F particles.

354   Same data are presented for OC concentrations in Figure 9. It may be underlined that

355   ADF OC values are always higher than in the other sites by a factor ranging from 6 to 30, for

356   all seasons and particle sizes, with highest and lowest values respectively in DS2017 and DS

357   2016. In terms of size distribution, maximum OC concentrations at the ADF site may be found

358   in UF (53%), then F (29%) and finally C (18%) particles. The same distribution is observed for

359   the traffic sites in DS2016, however, for the other campaigns, OC size distribution looks like

360   the EC ones with higher concentrations in UF and C particles than in F particles.

361   As shown in Figure 10, the highest OC/EC ratios are always obtained at the ADF site

362   with a value as high as 25 for F particles in WS2016 whereas the lowest values are found in

363   DS2017. This is the same feature for the other sites with ratios lower than 2 in DS2017. OC/EC

364   ratios in AWB site are higher than in the traffic sites. Note that values at AT site are higher than

365   CT values in the wet season whereas lower in the dry season. Finally, it is interesting to

366   underline that linear correlations between EC and OC are obtained in the ultrafine and fine

367   modes in all campaigns, particularly in DS2017 (r^2 = 0.8, 0.8, 0.9 and 0.9) at the ADF, AWB,

368   AT and CT sites, respectively. This suggests that different studied sources can be assessed as

369   significant sources of both EC and OC.

370

371   **3.2.2. Water-Soluble Organic Carbon**

372   Concentrations of WSOC and WSOC/OC ratios are presented in Table 2 for each size

373   (UF, F, C and PM2.5) and campaign. As seen, WSOC are always higher at the ADF site than

374   in other sites, at least by a factor of 12. Maximum values are obtained in WS2016 with an

375   average of 16.47, 17.08 and 79.68 $\mu gC.m^{-3}$ for coarse, fine and ultra-fine fractions, respectively,

376   followed by WS2015 and DS2017. WSOC concentrations are the lowest in DS2016, with an

377   average of 4.14, 6.95 and 21.89 $\mu g.m^{-3}$ for coarse, fine and ultrafine fractions, respectively. In

378   terms of seasonality, there is not a clear trend in WSOC values at the AWB and AT sites,

379   whereas at the CT and ADF sites, WSOC values are found to be respectively higher and lower

380 in dry seasons compared to wet seasons. It is also interesting to note that WSOC are maximum

381 in UF sizes in the AT, ADF and AWB sites. At the CT site, the highest values are found in the

382 coarse particulate fractions, except in DS2016.

383 As expected, WSOC is strongly correlated with OC (r=0.7 at ADF, 0.8 at AT, 0.5 at

384 AWB and 0.7 at CT), whereas correlations with EC are weaker, especially at the AWB and CT

385 sites with values ranging from 0.1 to 0.4, respectively. Finally, when looking at WSOC/OC

386 ratios (Table 2), maximum values are obtained at the ADF site with PM2.5 ratios as high as

387 43%, followed by the AT and AWB sites with 32%. The lowest value (23%) is found at the CT

388 site. Also, Table 2 shows that there is no clear seasonality in WSOC/OC values, excepted at

389 ADF where maximum values occur during the wet season. Note as for WSOC, that ratios are

390 maximum in UF and F fractions for all sites except at the CT site where the ratio for coarse

391 fraction is the highest.

392 ### 3.3. Water-soluble ionic species

393 Figure 11 shows the relative contribution of the major ions to the total concentration

394 (also given) of the ions in the different particle modes (C and F) at the ADF, AWB, AT and CT

395 sites for the different measurement campaigns. Let us recall here that only C and F fractions

396 may be documented due to the our experimental protocol. Total concentrations present

397 maximum values in ADF and CT sites. Values in AWB and AT sites are of the same order of

398 magnitude and lower by a factor of 2 than in ADF and CT sites. The contribution of different

399 ions show significant variations from site to site. The dominant ionic species at the ADF site

400 over all campaigns is chloride (Cl^-), with a 26% contribution, followed by nitrate (NO_3^-) (16%),

401 calcium (Ca^{2+}) (13%) and potassium (K^{2+}) (12%). Sulfate (SO_4^{2-}), ammonium (NH_4^+), sodium

402 (Na^+) and to a lesser extent magnesium (Mg^{2+}) contributions are lower, ranging from 4 to 7%

403 of the total ion species. The lowest contribution is for organic acids with their total value lower

404 than 5%. NO_3^- is the major ionic component at the AWB and AT sites, representing 24% and

405 29% of the total water soluble inorganic concentration, respectively. The second major

406 contributor in AWB and AT is SO_4^{2-}, accounting for 21% and 17% of the ion mass, respectively

407 followed by Ca^{2+} (12% and 15%) and Cl^- (15% and 13%). In CT, Ca^{2+} is predominant with a

408 relative abundance of 24%, followed by NO_3^- (23%), SO_4^{2-} (19%) and Cl^- (13%). Na^+, NH_4^+

409 and K^+ contributions are lower and in the same order of magnitude in AT, AWB and CT sites,

410 ranging from 4 to 9% of the total ion species. Note that organic ion contributions at AT, CT and

411 AWB is of the same order than in ADF, with lower values at CT. It is interesting to underline

412 in the Figure 11, that NO_3^- contribution is always higher in the coarse than in the fine size.

413 Conversely, K^+ is always higher in the fine than in the coarse size. In CT, Ca^{2+} in the fine

414 fraction is as high as in the coarse fraction whereas in AT, AWB and ADF, Ca^{2+} coarse fraction

415 is predominant. Fine particle contribution may be noticed for Cl^- in ADF whereas in the other

416 sites, Cl^- is most likely dominated by coarse particles. Finally, SO_4^{2-} is mainly found in the fine

417 mode at the AT, AWB and CT sites, but in the coarse mode in ADF site.

418 In terms of seasonal variations, it may be shown in Figure 11 that higher Cl^- values are found

419 in wet seasons than in the dry seasons everywhere, except in ADF site where there is no marked

420 difference between seasons. For example, the mean relative total percentages of Cl^- at the CT

421 site are 38 and 24% in the WS2015 and WS2016, respectively, while these percentages decrease

422 significantly to 18 and 13% in the DS2016 and DS2017, respectively. The Cl^-/Na^+ ratios are

423 about 1.5 everywhere in both seasons, in agreement with the typical sea water ratio (1-1.2)

424 (Hara et al.,2004), except at the ADF site where these ratios increase to 4 and 5 in wet and dry

425 season, respectively and at the AWB site in the dry season (2). K^+ and Ca^{2+} are always higher

426 in dry season than in wet season except for Ca^{2+} in ADF where values are of the same order.

427 Finally, the same trend is observed for NO_3^- and SO_4^{2-} with higher values in dry than in wet

428 seasons at AWB and CT sites whereas values at ADF and AT sites are of the same order of

429 magnitude for the two seasons.

430 **3.4. Trace element concentrations**

431 Table 3 shows the mean values of the major trace elements in bulk aerosol at the

432 different studied sites in WS2016 and DS2017, with their corresponding relative abundances in

433 the total aerosol mass into brackets. Let us recall that data are not available in WS2015 and

434 DS2016. The concentrations of trace elements span a wide range, from 0.2 to 25.2 $\mu g.m^{-3}$.

435 Among the measured elements, Al, K, Na and Ca are the most abundant, followed by Fe and

436 Mg. In DS2017, Al and Na concentrations are higher in AWB than in the other sites. The

437 minimum value for these species is found in ADF site. Values in traffic sites are of the same

438 order of magnitude and higher than in ADF site. Maximum of Ca and K values may be found

439 in CT and ADF site respectively. It is interesting to note that Al, K, Na concentrations are higher

440 in the dry season than in the wet season. Such feature is less clear for Ca, whose seasonal

441 variability is less marked except in AWB and AT sites. In terms of Mg, maximum values are

442 observed in ADF site and of the same order of magnitude whatever the season. Fe abundance

443 is higher in AWB and CT sites than in ADF and AT sites and higher in DS2017 than in WS2016

444 everywhere. The other metals (Ti, P, Zr, Zn, Cr, Mn, Pb and Ni) represent less than 0.5% and

445   2% of the total mass in WS2016 and DS2017, respectively, at all sites, with Cr, Mn, Pb and Ni

446   exhibiting less seasonal variability compared to the rest of the metal elements.

447   To assess the relative contribution of crustal and non-crustal origin of elemental aerosol

448   loadings, source enrichment factor (EF) of a trace element X have been first calculated with the

449   following formula using both literature data of the typical elemental composition of the upper

450   continental crust (Mason and Moore, 1982; Taylor, 1964), measured elemental composition

451   from this study and Al as a reference element :

452
$$EF_X = \frac{\dfrac{[X]_{atm}}{[Al]_{atm}}}{[X]_{soil}\Big/[Al]_{soil}}$$

453   Where $[X]_{atm}$ and $[Al]_{atm}$ are the concentrations of the chemical element X and Al in the

454   atmosphere, respectively, and $[X]_{soil}$ and $[Al]_{soil}$ are the typical concentrations of the element

455   X and Al in the earth's crust, respectively. Al is frequently used as a reference element assuming

456   that its anthropogenic sources in the atmosphere are negligible (Gao et al., 2002; Cao et al.,

457   2005; Xu et al., 2012). In all sampling sites, EF values typically lower than 5 are obtained for

458   several trace elements (Be, Sc, Ti, V, Fe, Ga, Sr, Nb, Rh, Ba, La, Ce, Pr, Nd, Sm, Eu, Gd, Tb,

459   Dy, Ho, Er, Tm, Yb, Lu, Ta, Th and U). This suggests a natural origin of these species (Freitas

460   et al., 2007; Gao et al., 2002). The most enriched elements (EF>100) are Sb, Sn, Zn, Se, Te,

461   Cd, Pb, Bi and Mo at nearly all of the sites, indicating significant anthropogenic origin (Wang

462   et al., 2006). These elements are mainly emitted into the atmosphere through fossil fuel

463   combustion, traffic emission, wear of brake lining materials and industrial processes (Watson

464   and Chow, 2001; Samara and al., 2003). Secondly, source contributions have been estimated

465   from these EF values following the method described by Arditsoglou and Samara (2005). Note

466   that this study refers to ratios for a limited list of sources, perhaps not including the African

467   source specificities. As a result, it may be seen that 30% of trace element concentrations is of

468   anthropogenic origin at ADF site whereas about 17 % at the others sites.

469   **3.5. Dust**

470   Figure 12 shows dust concentrations calculated from Guinot et al. (2007) methodology

471   (see paragraph 2.3.6) for C and F particle sizes at the different sites for each season. Note that

472   as for WSI and trace element and due to our sampling procedure, there are values for fine and

473   coarse particles for all seasons excepted for WS2016 with values for coarse particles only.

474   During the wet season, coarse dust concentrations range from 5 to 25 µg.m^{-3} in 2015 and 9 to

475   37 µg.m^{-3} in 2016, with higher values at the CT and ADF sites in 2015 and at AT, CT and ADF

476 in 2016. In WS2015, fine dust concentrations range from 12 to 49 with maximum values at

477 ADF and CT sites also. During the dry season, values range from 38 to 156 μg.m^{-3} in 2016 and

478 from 41 to 116 μg.m^{-3} in 2017, with maximum concentrations obtained at the CT site, followed

479 by AWB site. When considering mean values of the dry seasons, total dust at CT is 2.4 times

480 the values found at AT, 1.6 times at AWB and 3.4 times at ADF. Seasonal comparison shows

481 that total dust concentration is higher in the dry seasons than in WS2015 by a factor of 3 in AT,

482 2.6 in CT and 4 in AWB, but of the same order of magnitude in ADF site.

483 **3.6. Aerosol chemical closure**

484 The aerosol chemical closure obtained using the Guinot et al. (2007) method (see below)

485 at the different sites for each season is presented in Figure 13. Results show clear intra- and

486 inter-annual variations at all of the sites, as well as significant differences among the sites. In

487 total, dust accounts for 39 to 75% of the bulk PM mass at both traffic sites, with no clear

488 seasonal cycle and higher contributions in Cotonou (Figures 13c and 13d). These percentages

489 vary from 32 to 64% at the AWB site, and from 18 to 35% at the ADF site, with percentages

490 1.8 times higher in the dry season than in the wet season in AWB and no clear seasonal

491 difference in ADF (Figures 13a and 13b). Carbonaceous aerosol, the sum of EC and POM,

492 show large contributions at the ADF site (from 49 to 69% of the total PM mass), with relatively

493 similar proportions in each season (Figure 13a). The absence of a clear seasonal pattern is also

494 observed in CT whereas carbonaceous aerosol is slightly higher in WS than in DS in AWB (23

495 and 16% respectively) and AT (37 and 21% respectively) (Figures 13b-d). Carbonaceous

496 aerosol contribution accounts for about 11- 49% of the total mass at both traffic sites with higher

497 values in AT (mean of 30%) than in CT (13%). The ion percentages in PM fractions present

498 the same pattern at AT, CT and AWB sites with higher values in wet than in dry seasons. In

499 these sites, we may notice that mass concentration in coarse particles is larger in the wet season

500 whereas of the same order of magnitude than the one in fine particles in the dry season. In ADF,

501 no marked difference may be found between the seasons and the sizes (Figure 13).

502

503 **4. Discussion**

504 A discussion of the results site by site (Abidjan domestic fire site, traffic sites both together and

505 waste burning site) will be first proposed. We will scrutinize (1) the proximity between the sites

506 and the sources; (2) the source specificity with more or less incomplete combustion (e.g. wood

507 combustion and two-wheel vehicle emission factors are higher than gasoline emission factors

508 (Keita et al., 2018); (3) the relative influence of other local sources or transported sources to

509 the studied sites such as dust and biomass burning; (4) the occurrence of continental air masses;

510 (5) the variation of the boundary layer height (as reported by Colette et al., 2007); and (6) the

511 meteorological parameters (e.g. temperature, relative humidity and wet deposition) to explain

512 the differences of pollutant concentrations and their seasonal and inter-annual variabilities.

513 In a second part, we will present comparison of our values with other DACCIWA values and

514 also with literature values for other intensive campaigns in Africa.

515

4.1. Abidjan Domestic Fires (ADF)

517 As shown in the above paragraphs, maximum values are obtained at the ADF site, for aerosol

518 mass, EC, OC, WSOC, water-soluble ionic species (e.g. Cl^-, NO_3^-, Ca^{2+} and K^+) and some trace

519 elements such as Mg and K (whereas Al, Na and Fe are lower than in the other sites). Also,

520 aerosol PM2.5 values are well above the annual and daily WHO guidelines of 25 and 10 μg.m$^-$

521 ^{3} respectively, whatever the season.

522 Such pattern is due to the proximity of the ADF site to the studied combustion source: in that

523 area, the use of wood combustion is very active due to commercial activities of women drying

524 fish and meat and domestic cooking. This is also confirmed by the high relative importance of

525 total carbon in aerosol mass whatever the size (49 to 69%) and by values of source enrichment

526 factor. Indeed, at least 30% of trace element concentrations are of anthropogenic origin at ADF

527 site. In addition, wood combustion is well known to be highly polluting due to incomplete

528 combustion: this is shown here by the measurements of very high OC/EC ratios at ADF, on the

529 order of the one measured at the source level by Keita et al. (2018). This is also shown by

530 WSOC relative importance which is expected for wood burning following Yu et al. (2018),

531 Tang et al. (2016), Feng (2006) and Saxena and Hildemann (1996) and by the strong correlation

532 of WSOC with biomass burning K^+ tracer.

533 Chloride is most likely associated with sea salt origin (normal chloride concentrations represent

534 at least 55% of marine aerosols following Goldberg (1963)) or secondary aerosol production

535 (Li et al., 2016). Since chloride relative concentration at the ADF site remains lower than the

536 that of sea-sal aerosols, the secondary production source would be the better explanation for

537 high chloride concentrations observed at ADF. The size distributions of Cl^-, K^+, NH_4^+ and SO_4^{2-}

538 support this conclusion : the predominance of these elements in fine particle mode at the ADF

539 site would be associated with anthropogenic emissions, particularly biomass combustion and

540 domestic fires, or with secondary inorganic aerosols origin. This is confirmed by Cl^-/Na^+ ratio

541 values as shown earlier. Contrarily, Ca^{2+} and NO_3^- contributions to the total ions at the ADF

site peak mainly in the large particle fraction and may be attributed to quasi natural origin, primarily to dust emissions and nitrate formation by reaction processes, respectively. In addition, Na^+ and Mg^{2+} display similar size distributions at the ADF site, with the major contribution in the coarse particle fraction, suggesting the common sea salt origin of these two elements (Belis et al., 2013).

As we have shown above, the lower proportion of metal elements at the ADF site (6.5% of the bulk concentration) can be explained by the less dominant influence of re-suspended dust particles compared to traffic sources. Elements such as Cr, Mn, Pb and Ni have less seasonal variability than other metallic elements. These small proportions of these non-crust elements suggest a low contribution of elements emitted mainly by anthropogenic activities such as industrial processes (Viana et al., 2007 and 2008; Minguillón et al., 2014). Finally, the Zn/Cd ratio has been also examined. A value of 29 close to ratio reported for gasoline vehicle (27, Qin et al., 1997) is obtained for the ADF site, indicating that this site is also impacted by traffic sources.

High values of WSOC/OC ratios are expected to be harmful to health (Ramgolam et al., 2009, Val et al., 2013). This effect is being enhanced by the particulate size measured at this site (Kim et al., 2003; Wilson et al., 2002). Indeed, the relative mass distribution of PM and OC particle sizes shows a major contribution of particles less than 1 µm (as high as 85% of PM). This could be due to the fact that carbonaceous aerosols are formed near emission sources and are mainly of submicron size (Boucher, 2012). Nevertherless, note that EC also presents large coarse particle contribution. This could be due to the importance of wood burning at this site with less efficient combustion and large particle emissions (Watson et al., 2011).

In terms of seasonality, higher concentrations of aerosol mass, OC, WSOC, EC and total water soluble ionic species (SO_4^{2-}, NH_4^+ and NO_3^-) are observed in WS2015 and WS2016 than in DS2016. This may be explained by a more incomplete combustion in the wet seasons than in DS2016 due to the use of moist wood for cooking and smoking fish, which leads to large amount of smoke and higher particulate emission factor values. Note that DS2017 values are as important as the ones of wet seasons, which will be explained later in the text. With regard to WSOC, their variabilities may be also linked to meteorological factors, such as solar radiation (Tang et al., 2016; Favez et al., 2008) and relative humidity (Liang et al., 2016). At ADF site, temperatures are roughly similar in both seasons. However, RH variability may play a role since it is higher in wet season than in dry season. Finally, our results indicate no clear seasonal cycle for Cl^-, which confirms its anthropogenic origin, as previously shown.

4.2. Traffic sites (Abidjan traffic and Cotonou Traffic sites)

Let us recall first that the two traffic sites have been chosen since they are representative of the traffic diversity in West Africa. At CT site, both personal cars, taxis and an important two-wheel fleet may be found whereas at AT site, there are buses, taxis and personal cars. Also, the distance between the site and the traffic sources is the same for the two traffic sites, slightly larger than the distance between the site and the wood burning sources at ADF site.

In these two sites, concentrations are high with PM2.5 values well above the WHO guidelines. Average aerosol mass, EC, OC, dust and water soluble ionic concentrations (with NO_3^- and Ca^{2+} maximum at AT and CT sites respectively) are higher at CT than at AT site by a factor of 1.5 to 2. Note that this poor air quality found in Cotonou has been reported by Cachon et al. (2014). The higher values found in Cotonou could be due to more intense traffic in Cotonou than in Abidjan. Also in Cotonou, this traffic is associated with the lack of public transportation and the use of highly polluted mopeds (aged over 15 years) (Gounougbe, 1999; Avogbe et al., 2011), despite the effort in the last 10 years to restrict their use. Several studies such as MMEH (2002) have shown that more than 94,000 mopeds and 350,000 second-hand vehicles are in circulation in Cotonou. Other factors contributing to the local pollution include outdoor restaurants using charcoal and motorcycle garages, which are more present around the Cotonou traffic site compared to Abidjan site. It also includes anthropogenic dust. Indeed, at Cotonou, the lack of road infrastructure favours the resuspention of dust particles. Finally, other sources may potentially influence aerosol seasonal composition in these two sites, including marine aerosols, transported dust and biomass burning particles as well as anthropogenic aerosols from the surrounding countries (Figure 5). Note also that source enrichment factor values show that about 17% of trace element concentrations are of anthropogenic origin at both traffic sites and that the relative importance of total carbon in mass is higher at AT than at CT sites.

Aerosol mass, composition and size depend on the season and the two traffic sites are differently affected. The EC and OC concentrations measured in both traffic sites and averaged per season are higher in dry than in wet season. Such variations may be explained by several factors: particulate wet deposition occurring during the wet season, reduction of traffic flow due to school vacations and meteorological influence. Higher EC and OC concentrations are obtained at CT than at AT sites in dry seasons whereas no statistical difference may been found between the two sites in wet seasons. Such a result is mainly explained by figures 5. In wet seasons, similar backtrajectory pattern may be observed for both sites whereas in dry seasons, CT traffic site only would be influenced by Nigerian anthropogenic sources.

609 In terms of WSOC concentrations, concentrations at the AT site are on average higher than

610 those recorded at the CT site in the wet season, but lower in dry season. The presence of dust

611 can produce semi-volatile organic gas scavenging and therefore WSOC and OC enhancement.

612 Such a phenomenon can explain the highest WSOC concentrations observed in dry season at

613 the CT site where dust concentrations are highest (see dust paragraph). Moreover, this can also

614 explain why the maximum WSOC are in coarse particles at CT, while at AT maximum values

615 are in ultra-fine particles.

616 Total WSI concentrations are larger at AT site in the wet than in the dry season with higher

617 values in coarse particles. At CT site, total WSI concentrations in fine particles are higher in

618 the dry than in the wet season whereas same values are obtained in coarse particles for both

619 seasons. Note that CT values are generally higher than AT values with a more important

620 contribution of fine particles in the dry season. These WSI variations can be explained by the

621 relative importance of Ca^{2+}, SO_4^{2-} and NO_3^- in both sites.

622 First, Ca^{2+} contribution to total WSI is higher in CT site than in AT site with no clear seasonal

623 variation at CT site and higher values in dry season than in wet season at AT site. Also at CT,

624 fine and coarse Ca^{2+} particles are in the same range, whereas coarse Ca^{2+} particles are

625 predominant at AT site. Such feature may be explained by the impact of dust sources including

626 long-range dust transport at Abidjan and a combination of long-range dust transport and road

627 resuspension at Cotonou.

628 Second, the relative contribution of SO_4^{2-}, NH_4^+ and NO_3^- as a percentage of total WSI in the

629 different particle modes is reduced in the wet season. During the wet season, the clean winds

630 surrounding the ocean before reaching the measurement sites could contribute to lower the

631 proportion of these species, in addition to the scavenging processes during the rainy days.

632 Unlike the wet season, a relatively good correlation with r^2 of 0.87 (SO_4^{2-} versus NH_4^+), 0.73

633 (NO_3^- versus NH_4^+) and 0.87 (SO_4^{2-} versus NO_3^-) has been found in coarse particles, indicating

634 similar sources for these three species during the dry season. In order to try to identify these

635 sources, the ratio of SO_4^{2-}/Ca^{2+} and NO_3^-/Ca^{2+} has been determined. The average SO_4^{2-}/Ca^{2+}

636 and NO_3/Ca^{2+} ratios in combined coarse particles (1.07 and 2.58 during the wet season and 0.33

637 and 1.60 during the dry season) are higher than the corresponding ratios for typical soil (0.026

638 and 0.003, respectively). On the other hand, the SO_4^{2-}/Ca^{2+} ratio increases in the fine particles

639 (5.07 during the wet season and 2.53 during the dry season), while that of NO_3^-/Ca^{2+} remains

640 almost constant (2.86 during the wet season and 1.65 during the dry season). This implies that

641 the atmosphere at AT and CT sites is enriched by SO_4^{2-} formed as anthropogenic secondary

642 particles, possibly from sulfur containing pollution sources (Seinfield and Pandis, 1998),

particularly in fine particle mode, and by NO_3^- mostly coming from nitrogen containing sources in all particle sizes. The higher contributions of these elements during the dry season could result from a combination of several factors: 1) an atmosphere loaded with dust favoring heterogeneous chemistry to obtain secondary aerosol and the rise of biomass burning emissions; 2) the increase of photochemical activity and higher concentrations of hydroxyl radicals in the dry season, which can oxidize SO_2 from combustion (Arndt et al., 1997) to SO_4^{2-} (Li et al., 2014) ; and 3) the wind transport of anthropogenic secondary particles from the industrial zone located upstream from our sites. Finally, the proportion of Cl^- relative to the total mass of ions is highest for coarse particles at both traffic sites especially during the wet season, suggesting that Cl^- at AT and CT sites if from natural origin and probably from sea salt emissions.

If we focus now on dust during the two wet seasons, concentrations are higher in 2016 than in 2015 at CT and AT sites for coarse particles (no data of fine particles are available in WS2016). This is consistent with observed aerosol optical depth (AOD) values at CT, which increased by a factor of 2 between 2015 and 2016. No AOD value is given by Léon et al. (2019) at Abidjan in WS2015 to allow such comparison in Abidjan. Moreover, during the wet season, an Angström coefficient (AE) on the order of 1 has been found at CT site, indicating smaller particles that could be due to road resuspension. It is interesting to note that during WS2016, AOD and AE are respectively higher and lower at Abidjan than at Cotonou. Again, this is consistent with our dust concentrations at CT site. In Abidjan, we could assume that another source of Ca^{2+}, which is not taken into account in our dust calculations, may explain our dust concentration data. That may be the result of anthropogenic Ca^{2+} emissions from residential combustion, more important in 2016 than in 2015 as shown earlier (http://naei.beis.gov.uk/overview/pollutants?pollutant_id=84).

The relative contribution of dust generally peaks in the coarse mode and, to a lesser extent, in the fine mode, reflecting their natural origin. It is interesting to note that the dust contribution observed in this study for the year 2016 at the Abidjan site is in agreement with the results of Xu et al. (2019) which show a PM2.5 dust contribution of 35-50% compared to our values of 18-52%.

4.3. Abidjan Waste Burning site

Concentrations measured at AWB site are slightly lower than values found in the other sites. This can be explained by the larger distance of the site to the main studied source (here waste burning source) than in the other sites. However, PM2.5 values are also higher than WHO guidelines. +

677 Aerosol mass, EC and OC concentrations are higher in dry than in wet season, which suggests

678 less waste burning activities during the wet season or impacts of other local anthropogenic

679 sources or long-range biomass burning sources. Highest values are found in DS2017 with the

680 lowest OC/EC ratio, as at AT site. OC/EC ratio is highly variable at AWB (1-10) which

681 confirms that AWB site may be impacted by different types of sources as well as by secondary

682 aerosol organic formation which can be detected for OC/EC higher than 2 (Turpin et al. 1990;

683 Hildermann et al. 1991; Chow et al. 1996). Note that OC/EC typical for waste burning source

684 is of the order of 8 (Keita et al., 2018).

685 It is also observed that at the AWB site, PM mass concentrations are mainly distributed in C

686 mode (30-44%) over the entire period of study, excepted during the WS2015, and to a lesser

687 extend in F mode (21-44%). EC and OC being mainly distributed in C and UF modes. Water-

688 soluble fraction of organic carbon is important (32%) and on the order of the one found at AT

689 site. Same for WSI concentrations and WSI composition. At AWB, WSI values are globally

690 slightly higher in wet than in dry season. However, it is interesting to underline that Ca^{2+} is

691 much higher in dry season than in wet season, especially in DS2017. This is in agreement with

692 dust concentrations and trace element concentrations, which have been found to be maximum

693 at AWB, reaching 35.8% of the total PM mass in the dry season. These maximum percentages

694 are due to the large contribution of both Al and Na crustal elements which account for about

695 26%. Also note that Cu/Sb of 0.08 in DS2017, which indicate an influence of re-suspended

696 particles. A Zn/Cd value of 56 is obtained for the AWB site which is in close agreement with

697 values reported for oil burning (Watson et al., 2001, Samara et al., 2003). That could indicate

698 that oil might be one of the waste burning materials.

699 Our result suggests that AWB aerosol mass is influenced by a mix of sources, including fuel

700 combustion and mineral salt from sources around the measurement site, associated to long-

701 range source impact of dust and biomass burning which will be further discussed in the next

702 paragraph.

703

704 **4.4. Interannual variability of aerosols in Abidjan and Cotonou**

705 EC and OC concentrations are generally higher in DS2017 than in DS2016 for all the sites. This

706 is not due to the meteorological condition, which is similar in both years. This is also not due

707 to biomass burning impacts. Indeed, when looking at MODIS burnt areas for our period of study

708 (http://www.aeris-data.fr/redirect/MODIS-MCD64A1), burnt areas of west African savannas

709 are higher in 2016 than in 2017. Therefore, carbonaceous aerosol concentrations should be

710 higher in 2016. Then, this could be due to a counter effect between biomass burning emission

711 strength and air mass transport efficiency. As a result, biomass burning impact could not explain

712 the difference in EC and OC during the dry season between 2016 and 2017. Rather, this is due

713 to the variability of local sources. In DS2016 in Abidjan, there was a general strike of civil

714 servants of the State with important consequences on urban activities. Lower activities were

715 observed (lower fish smoking emissions, lower traffic ..) in DS2016 compared to DS2017, thus

716 explaining the lower EC and OC concentrations at Abidjan sites. In Cotonou, highest

717 carbonaceous aerosol values in DS2017 may be explained by backtrajectory patterns: Cotonou

718 would be impacted by air masses coming from the high polluted Lagos (Nigeria) area in that

719 period whereas from less polluted northern areas in DS2016. Such an assumption is validated

720 by the AOD values at 550nm from MODIS satellite images (http://www.aeris-

721 data.fr/redirect/MODIS-MCD64A1), which show very high particulate concentrations in the

722 Guinean Golf (Figure 14).

723 This figure also shows the AOD difference between Cotonou and Abidjan for DS2017, with

724 higher values at Cotonou than in Abidjan for the campaign period, in agreement with our

725 measurements of aerosol mass, EC, OC and dust. This is confirmed by the DACCIWA

726 sunphotometer AOD and Angström coefficient (AE) measurements at Abidjan and Cotonou

727 (Léon et al., 2019; Djossou et al., 2018). Indeed, in DS2017, during our period of

728 measurements, mean AOD in Cotonou is of the order of 1.3 versus 0.9 in Abidjan for an AE of

729 0.6 for both sites, which clearly indicates the presence of coarse dust particles.

730 Finally, aerosol mass and dust concentrations have been seen to be higher in DS2016 than in

731 DS2017 in Abidjan whereas values are on the same order of magnitude at Cotonou. Such high

732 values at Abidjan in DS2016 can be explained by the back-trajectory pattern with air-masses

733 all coming from northern dusty areas in DS2016 (Bodélé depression in Tchad, Prospero et al.

734 (2002), Washington et al., (2003), Knippertz et al. (2011), Balarabe et al., (2016)) and/or from

735 northern dusty countries (Mali, Niger) (Ozer, 2005), whereas in DS2017, contribution of

736 southern marine clean air-masses may also be noted.

737 In the wet season, aerosol mass, EC and OC are higher in WS2015 than in WS2016. This may

738 be due to particulate wet deposition, more efficient in WS2016 which have been seen earlier to

739 be more rainy (4.7mm) than in WS2015 (2mm). Moreover, at AT site, dust concentrations are

740 higher for coarse particles in WS2016 than in WS2015. Such variations may be explained by

741 long-range dust sources and/or road dust resuspension processes. As no dust event has been

742 noticed, local source explanation seems to be more evident.

743 In AT, CT and AWB, OC/EC ratios are globally on the same order for WS2015, WS2016 and

744 DS2016, with values lower than for DS2017. This could be due to lower traffic activities linked

to the DS2016 strike and the wet season vacation periods. Indeed, much higher OC/EC ratios measured in DS2017 are typical of those of diesel vehicles (Mmari et al., 2013; Keita et al., 2018). Finally, it is interesting to note that OC/EC ratios measured in this study are in the range of those previously reported for other megacities such as Agra in India with 6.7 (Pachauri et al., 2013), Helsinki in Finland with 2.7 (Viidanoja, 2002), Cairo in Egypt with 2.9 (Favez, 2008), Paris in France with 3.5 (Favez, 2008), and Milan in Italy with 6.6 (Lonati et al., 2007).

4.5. Comparison with literature data

Firstly, the comparison between our data and other DACCIWA results including other time sampling focuses on PM2.5 levels, since these particle sizes are relevant for health impact studies (Xing et al., 2016). In addition to our values, Figure 7 presents data from Xu et al. (2019) using personal samplers collected in the same area and at the same dates in 2016 during 12h on women at the ADF site, students at the AWB site and drivers at the CT site, and from Djossou et al. (2018) study based on one week exposed filters collected at the same areas and for the same periods as this study. We note that PM2.5 directly measured on women are 2.3 and 0.9 times our values obtained at the ADF site in dry and wet seasons, respectively, and 3.4 and 4.9 times higher on students than at the AWB site, and 1.6 and 2.1 times higher on drivers than at the CT site. Also, our values are on average 1.6, 3, 5 and 8 times higher than weekly-integrated values of Djossou et al. (2018) including our 3 days of measurements at the AWB, ADF, AT and CT sites respectively. As it may be seen, the lowest concentrations are observed in Djossou et al. (2018), whereas the highest concentrations are recorded in Xu. et al. (2019). This is valid for all sites, seasons and campaigns. Differences between our values and Djossou values may be explained by the sampling times of the two studies. Indeed, as recalled, Djossou measurements are weekly integrated, taking into account diurnal activities during all the week, including week-end and nights which have expected lower PM2.5 concentrations. Our study includes only maximum pollution conditions for each site. The highest differences occur for the traffic sites. This may be clearly understood since diurnal and weekly variations of traffic sources are the most variable. Comparison between our values and Xu et al. (2019) values is also interesting. Indeed, it is at the ADF site that on-site and women PM2.5 concentrations are the closest, which shows that this site is the most representative of the pollution exposure to women. The biggest differences are found at the AWB site. As already mentioned, distance from the site to the waste burning source is more important than for other sites, which explains why concentrations obtained on students who are leaving close to the sources are much higher than on-site concentrations. At the Cotonou traffic site, measurements taken from people are

779   also higher than on site measurements. Such differences can be explained by additional
780   pollution exposure as people move around. Note that the sampling technique may also play a
781   role in such a comparison. In terms of seasonal variation, our results are in agreement with long-
782   term EC measurements obtained by Djossou et al. (2018) for the same sites and period. Finally,
783   Table 4 compares our mean PM2.5 results obtained from 3-hour sampling for three consecutive
784   days to literature data for different traffic sites in the world given at a daily scale. It is interesting
785   to note that our values are situated at the higher end of the range of PM2.5 data observed from
786   the other sites.

787   Secondly, Table 5 compares our OC and EC values to those obtained by Djossou et al. (2018)
788   and Xu et al. (2019) as previously described for the same period and the same sites. Again, it is
789   interesting to note that Djossou's values are in general lower than ours. Indeed, for the wet and
790   dry seasons, our OC measurements are 4 and 1.4 times higher than Djoussou's at the AT site,
791   2.1 and 5.7 times higher at the CT site, and 2.5 and 2.5 times higher at the ADF site,
792   respectively. As for PM2.5, this can be explained by the different sampling times between our
793   experiments that were performed at the peak of urban activities, while Djossou's dataset
794   represents weekly integrated values. Differences at the ADF site are largely explained by the
795   temporal pattern of fish smoking activities which take place every day, only in the morning, as
796   such the associated pollution is not well represented in the weekly sampling. Finally, there are
797   less differences at the AWB site between both datasets. As above explained, there are no marked
798   temporal variations of concentrations at AWB site. The predominant waste burning emissions
799   impacting our site can occur night and day, week-days and week-end since origin of such
800   burning can be either anthropogenic or from spontaneous combustion. It may be also recalled
801   that another reason of agreement between both datasets may come from the large distance
802   between the site and the local and regional sources. Comparisons made between our values and
803   those of Xu's personal data show that both OC and EC are of the same order at the ADF site,
804   whereas Xu values are higher than ours at the CT and AWB sites. This result is in agreement
805   with what we found with PM2.5 concentrations as detailed above. Finally, Table 6 presents OC
806   and EC for the PM2.5 comparison between our values and other recent studies dealing with
807   traffic sites in other regions of the world and with similar operational conditions. We find that
808   our values are situated in the middle of the range observed in these different studies. Briefly, as
809   presented in Table 7, it is interesting to compare our WSOC concentrations to literature data
810   for different traffic sites of the world. We note that our values are on the same order as values
811   found in Asia and higher than those found in Europe.

812   Thirdly, the percentages of the total WSI to PM mass (15-20%) at the three Abidjan sites (ADF,

813   AWB and AT) are in the same order of magnitude than the data from PM2.5 personal exposure

814   samples collected at the same locations in 2016 by Xu et al. (2019). Our results also are very

815   close to the ionic contribution of 9% of the PM10 mass found at the urban curbside site in Dar

816   es Salaam in Tanzania during the wet season 2005 by Mkoma (2008).

817

818   **5. Conclusion**

819   This paper presents the mass and the size-speciated chemical composition of particulate matter

820   (PM) obtained during the dry and wet seasons in 2015, 2016 and 2017. During each campaign,

821   3-hour sampling at the peak period of pollution for three consecutive days was performed at

822   three sites in Abidjan, representative of domestic fire (ADF), waste burning (AWB) and traffic

823   (AT) sources, and at one traffic site in Cotonou (CT).

824   It is important to underline that our results and their temporal variations are very sensitive to

825   (1) the source activities whose pollution levels are highly linked to socio-economic status of

826   each city; (2) the impact of imported pollution (sea-salt, biomass burning, dust, anthropogenic

827   emissions from neighboring countries), according to air mass origins; and (3) the particle wet

828   deposition.

829   The comparison between our results and other DACCIWA measurements underlines the

830   importance of the distance of the chosen site to the sources. At the source level (such as ADF),

831   pollution results at the site are in agreement with exposure of people living at this site. However,

832   at the other sites, comparison is more difficult since the sites are under the influence of a mix

833   of transported sources. That shows the key importance of exposure studies to estimate air

834   quality and health impacts. That shows also the need of long-term studies to really understand

835   role of imported sources in urban air quality.

836   The main striking feature is that PM2.5 values are well above the annual and daily WHO

837   guidelines of 25 and 10 $\mu g.m^{-3}$, respectively, whatever the site and the season. Also, measured

838   concentrations from this study are situated in the middle to the high part of the range of

839   worldwide urban aerosol concentrations given at a daily scale. In addition, we have stressed the

840   importance of ultra-fine and fine particles in the studied aerosol and of species such as

841   particulate organic matter and water soluble organic carbon, which are well known to be

842   particularly harmful. This is again a warning signal for pollution levels in African capitals if

843   nothing is done to reduce emissions in the future.

844   Our study constitutes an original database to characterize urban air pollution from

845   specific African combustion sources. The next step will be to cross such an exhaustive aerosol

846 chemical characterization to biological data in order to evaluate the impact of aerosol size and
847 chemical composition on aerosol inflammatory properties.

848

849 **Acknowledgements**. The research leading to these results has received funding from the
850 European Union 7th Framework Programme (FP7/2007-2013) under Grant Agreement no.
851 603502 (EU project DACCIWA: Dynamics-aerosol-chemistry-cloud interactions in West
852 Africa). The authors greatly thank all the colleagues and operators who contribute to sampling
853 during the different campaigns.

854

855 **Author Contributions**
856 J.A. and C.L. conceived and designed the study. J.A., C.L. and E.T.D. contributed to the
857 literature search, data analysis/interpretation and manuscript writing. J.A., C.L., A.B. and
858 E.T.D. contributed to manuscript revision. J.A., C.L., J.F.L, H.C, V.Y., A.A, C.G, C.Z, E.C and
859 S.K. carried out the particulate samples collection and chemical experiments, analyzed the
860 experimental data.

861

862 **Additional Information**
863 Figure S1 and Appendix A-D accompany this manuscript can be found in
864 SupplementaryInformation.

865

866 **Competing financial interests**
867 The authors declare no competing financial interests

868

869

870

871 # References

872 Adon, M., Galy-Lacaux, C., Yoboué, V., Delon, C., Lacaux, J. P., Castera, P., Gardrat, E.,
873   Pienaar, J., Al Ourabi, H., Laouali, D., Diop, B., Sigha-Nkamdjou, L., Akpo, A., Tathy, J.
874   P., Lavenu, F. and Mougin, E.: Long term measurements of sulfur dioxide, nitrogen
875   dioxide, ammonia, nitric acid and ozone in Africa using passive samplers, Atmos. Chem.
876   Phys., 10(15), 7467-7487, doi:10.5194/acp-10-7467-2010, 2010.

877 Alastuey, A., Querol, X., Castillo, S., Escudero, M., Avila, A., Cuevas, E., Torres, C., Romero,
878   P., Exposito, F. and Garcia, O.: Characterisation of TSP and PM2.5 at Izaña and Sta. Cruz
879   de Tenerife (Canary Islands, Spain) during a Saharan Dust Episode (July 2002),

Atmospheric Environment, 39(26), 4715-4728, doi: 10.1016/j.atmosenv.2005.04.018, 2005.

Arditsoglou, A. and Samara, C.: Levels of total suspended particulate matter and major trace elements in Kosovo: a source identification and apportionment study, Chemosphere, 59(5), 669-678, doi: 10.1016/j.chemosphere.2004.10.056, 2005.

Arndt, R. L., Carmichael, G. R., Streets, D. G. and Bhatti, N.: Sulfur dioxide emissions and sectorial contributions to sulfur deposition in Asia, Atmospheric Environment, 31(10), 1553-1572, doi: 10.1016/S1352-2310(96)00236-1, 1997.

Avogbe, P. H., Ayi-Fanou, L., Cachon, B., Chabi, N., Debende, A., Dewaele, D., Aissi, F., Cazier, F. and Sanni, A.: Hematological changes among Beninese motor-bike taxi drivers exposed to benzene by urban air pollution, African Journal of Environmental Science and Technology, 5(7), 464-472, 2011.

Balarabe, M., Abdullah, K. and Nawawi, M.: Seasonal Variations of Aerosol Optical Properties and Identification of Different Aerosol Types Based on AERONET Data over Sub-Sahara West-Africa, ACS, 06(01), 13-28, doi:10.4236/acs.2016.61002, 2016.

Belis, C. A., Karagulian, F., Larsen, B. R. and Hopke, P. K.: Critical review and meta-analysis of ambient particulate matter source apportionment using receptor models in Europe, Atmospheric Environment, 69, 94-108, doi: 10.1016/j.atmosenv.2012.11.009, 2013.

Bisht, D.S., Dumka, U.C., Kaskaoutis, D.G., Pipal, A.S., Srivastava, A. K., Soni, V.K., Attri, S.D., Sateesh, M., Tiwari, S.: Carbonaceous aerosols and pollutants over Delhi urban environment: Temporal evolution, source apportionment and radiative forcing, Science of the Total Environment, 521-522: 431-445, 2015.

Bouhila, Z., Mouzai, M., Azli, T., Nedjar, A., Mazouzi, C., Zergoug, Z., Boukhadra, D., Chegrouche, S. and Lounici, H.: Investigation of aerosol trace element concentrations nearby Algiers for environmental monitoring using instrumental neutron activation analysis, Atmospheric Research, 166, 49-59, doi: 10.1016/j.atmosres.2015.06.013, 2015.

Cachier, H., Brémond, M.-P. and Buat-Ménard, P.: Carbonaceous aerosols from different tropical biomass burning sources, Nature, 340(6232), 371-373, doi:10.1038/340371a0, 1989.

Cachon, B. F., Firmin, S., Verdin, A., Ayi-Fanou, L., Billet, S., Cazier, F., Martin, P. J., Aissi, F., Courcot, D., Sanni, A. and Shirali, P.: Proinflammatory effects and oxidative stress within human bronchial epithelial cells exposed to atmospheric particulate matter ($PM_{2.5}$ and $PM_{>2.5}$) collected from Cotonou, Benin, Environmental Pollution, 185, 340-351, doi: 10.1016/j.envpol.2013.10.026, 2014.

Cao, J.J., Lee, S.C., Zhang, X.Y., Chow, J.C., An, Z.S., Ho, K.F., Watson, J.G., Fung, K., Wang, Y.Q. and Shen, Z.X.: Characterization of airborne carbonate over a site near Asian dust source regions during spring 2002 and its climatic and environmental significance, J. Geophys. Res., 110(D3), D03203, doi: 10.1029/2004JD005244, 2005.

Cassee, F. R., Héroux, M.-E., Gerlofs-Nijland, M. E. and Kelly, F. J.: Particulate matter beyond mass: recent health evidence on the role of fractions, chemical constituents and sources of emission, Inhalation Toxicology, 25(14), 802–812, doi:10.3109/08958378.2013.850127, 2013.

Celo, V., Dabek-Zlotorzynska, E., Mathieu, D., Okonskaia, I.: Validation of simple microwave-assisted acid digestion method using microvessels for analysis of trace elements in atmospheric PM2.5 in monitoring and fingerprinting studies, The Open Chemical & Biomedical Methods Journal 3., 141-150, 2010.

Cesari, D., Donateo, A., Conte, M., Merico, E., Giangreco, A., Giangreco, F. and Contini, D.: An inter-comparison of PM2.5 at urban and urban background sites: Chemical characterization and source apportionment, Atmospheric Research, 174-175, 106-119, doi: 10.1016/j.atmosres.2016.02.004, 2016.

Cheng, Z., Jiang, J., Chen, C., Gao, J., Wang, S., Watson, J. G., Wang, H., Deng, J., Wang, B., Zhou, M., Chow, J. C., Pitchford, M. L. and Hao, J.: Estimation of Aerosol Mass Scattering Efficiencies under High Mass Loading: Case Study for the Megacity of Shanghai, China, Environ. Sci. Technol., 49(2), 831-838, doi: 10.1021/es504567q, 2015.

Chiapello, I., Bergametti, G., Chatenet, B., Bousquet, P., Dulac, F. and Soares, E. S.: Origins of African dust transported over the northeastern tropical Atlantic, J. Geophys. Res., 102(D12), 13701-13709, doi: 10.1029/97JD00259, 1997.

Chow, J. C., Watson, J. G., Lu, Z., Lowenthal, D. H., Frazier, C. A., Solomon, P. A., Thuillier, R. H. and Magliano, K.: Descriptive analysis of PM2.5 and PM10 at regionally representative locations during SJVAQS/AUSPEX, Atmospheric Environment, 30(12), 2079-2112, doi:10.1016/1352-2310(95)00402-5, 1996.

Colbeck, I, Nasir, Z. A., Ahmad, S. and Ali, Z.: Exposure to PM10, PM2.5, PM1 and Carbon Monoxide on Roads in Lahore, Pakistan, Aerosol Air Qual. Res., 11(6), 689-695, doi:10.4209/aaqr.2010.10.0087, 2011.

Colette, A., Menut, L., Haeffelin, M. and Morille, Y.: Impact of the transport of aerosols from the free troposphere towards the boundary layer on the air quality in the Paris area, Atmospheric Environment, 42(2), 390-402, doi: 10.1016/j.atmosenv.2007.09.044, 2007.

Dieme, D., Cabral-Ndior, M., Garçon, G., Verdin, A., Billet, S., Cazier, F., Courcot, D., Diouf, A. and Shirali, P.: Relationship between physicochemical characterization and toxicity of fine particulate matter (PM2.5) collected in Dakar city (Senegal), Environmental Research, 113, 1-13, doi:10.1016/j.envres.2011.11.009, 2012.

Ding, A., Huang, X. and Fu, C.: Air Pollution and Weather Interaction in East Asia, Oxford Research Encyclopedias-Environmental Sience, doi: 10.1093/acrefore/9780199389414.013. 536, 2017.

Djossou, J., Léon, J.-F., Akpo, A. B., Liousse, C., Yoboué, V., Bedou, M., Bodjrenou, M., Chiron, C., Galy-Lacaux, C., Gardrat, E., Abbey, M., Keita, S., Bahino, J., Touré N'Datchoh, E., Ossohou, M. and Awanou, C. N.: Mass concentration, optical depth and

carbon composition of particulate matter in the major southern West African cities of Cotonou (Benin) and Abidjan (Côte d'Ivoire), Atmos. Chem. Phys., 18(9), 6275-6291, doi:10.5194/acp-18-6275-2018, 2018.

Doumbia, E.H.T., Liousse, C., Galy-Lacaux, C., Ndiaye, S.A., Diop, B., Ouafo, M., et al. Real time black carbon measurements in West and Central Africa urban sites. Atmospheric Environment. 2012;54(0):529-37.

Draxler, R. R., and G. D. Rolph: Evaluation of the Transfer Coefficient Matrix (TCM) approach to model the atmospheric radionuclide air concentrations from Fukushima, J. Geophys. Res., 117, D05107, doi:10.1029/2011JD017205, 2012.

Du, Z., He, K., Cheng, Y., Duan, F., Ma, Y., Liu, J., Zhang, X., Zheng, M. and Weber, R.: A yearlong study of water-soluble organic carbon in Beijing I: Sources and its primary vs. secondary nature, Atmospheric Environment, 92, 514-521, doi:10.1016/j.atmosenv.2014.04. 060, 2014.

Favez, O.: Caractérisation physico-chimique de la pollution particulaire dans des mégapoles contrastées, Thèse de l'Université PARIS.DIDEROT (Paris 7), France, 2008.

Favez, O., Sciare, J., Cachier, H., Alfaro, S. C. and Abdelwahab, M. M.: Significant formation of water-insoluble secondary organic aerosols in semi-arid urban environment, Geophys. Res. Lett., 35(15), L15801, doi:10.1029/2008GL034446, 2008.

Feng, J., Guo, Z., Chan, C. K. and Fang, M.: Properties of organic matter in PM2.5 at Changdao Island, China - A rural site in the transport path of the Asian continental outflow, Atmospheric Environment, 41(9), 1924-1935, doi: 10.1016/j.atmosenv.2006.10.064, 2007.

Feng, J., Hu, M., Chan, C. K., Lau, P. S., Fang, M., He, L. and Tang, X.: A comparative study of the organic matter in PM2.5 from three Chinese megacities in three different climatic zones, Atmospheric Environment, 40(21), 3983-3994, doi: 10.1016/j.atmosenv.2006.02.017, 2006.

Freitas, M.C., Pacheco, A.M.G., Baptista, M.S., Dionísio, I., Vasconcelos, M.T.S.D. and Cabral, J.P.: Response of exposed detached lichens to atmospheric elemental deposition, Proc. ECOpole., 1(1/2), 15-21, 2007.

Gaga, E. O., Arı, A., Akyol, N., Üzmez, Ö. Ö., Kara, M., Chow, J. C., Watson, J. G., Özel, E., Döğeroğlu, T. and Odabasi, M.: Determination of real-world emission factors of trace metals, EC, OC, BTEX, and semivolatile organic compounds (PAHs, PCBs and PCNs) in a rural tunnel in Bilecik, Turkey, Science of The Total Environment, 643, 1285-1296, doi: 10.1016/j.scitotenv.2018.06.227, 2018.

Gao, Y., Nelson, E. D., Field, M. P., Ding, Q., Li, H., Sherrell, R. M., Gigliotti, C. L., Van Ry, D. A., Glenn, T. R. and Eisenreich, S. J.: Characterization of atmospheric trace elements on PM2.5 particulate matter over the New York–New Jersey harbor estuary, Atmospheric Environment, 36(6), 1077–1086, doi:10.1016/S1352-2310(01)00381-8, 2002.

994 Genga, A., Ielpo, P., Siciliano, T. and Siciliano, M.: Carbonaceous particles and aerosol mass
995   closure in PM2.5 collected in a port city, Atmospheric Research, 183, 245-254, doi:
996   10.1016/j.atmosres.2016.08.022, 2017.

997 Goldberg, E.D., 1963. H.M. Hill (Ed.), Composition of sea Water, Comparative Oceanography,
998   Vol.2 of the seaWiley. New York. 1963

999 Gounougbe, F.: Pollution atmosphérique par les gaz d'échappement et état de santé des
1000   conducteurs de taxi-moto (Zemidjan) de Cotonou (Bénin), Thèse de doctorat en Médecine
1001   (832), 1999.

1002 Guinot, B., Cachier, H. and Oikonomou, K.: Geochemical perspectives from a new aerosol
1003   chemical mass closure, Atmos. Chem. Phys., 7(6), 1657-1670, doi: 10.5194/acp-7-1657-
1004   2007, 2007.

1005 Guttikunda, S. K. and Calori, G.: A GIS based emissions inventory at 1 km × 1 km spatial
1006   resolution for air pollution analysis in Delhi, India, Atmospheric Environment, 67, 101-
1007   111, doi:10.1016/j.atmosenv.2012.10.040, 2013.

1008 Hara, K., Osada, K., Kido, M., Hayashi, M., Matsunaga, K., Iwasaka, Y., Yamanouchi, T.,
1009   Hashida, G. and Fukatsu, T.: Chemistry of sea-salt particles and inorganic halogen species
1010   in Antarctic regions: Compositional differences between coastal and inland stations, J.
1011   Geophys. Res., 109, D20208, doi:10.1029/2004JD004713, 2004.

1012 He, K., Yang, F., Ma, Y., Zhang, Q., Yao, X., Chan, C. K., Cadle, S., Chan, T. and Mulawa, P.:
1013   The characteristics of PM2.5 in Beijing, China, Atmospheric Environment, 35(29), 4959-
1014   4970, doi: 10.1016/S1352-2310(01)00301-6, 2001.

1015 Hildemann, L. M., Markowski, G. R. and Cass, G. R.: Chemical composition of emissions from
1016   urban sources of fine organic aerosol, Environ. Sci. Technol., 25(4), 744-759, doi:
1017   10.1021/es00016a021, 1991.

1018 Huang, H., Ho, K. F., Lee, S. C., Tsang, P. K., Ho, S. S. H., Zou, C. W., Zou, S. C., Cao, J. J.
1019   and Xu, H. M.: Characteristics of carbonaceous aerosol in PM2.5: Pearl Delta River
1020   Region, China, Atmospheric Research, 104-105, 227-236, doi:
1021   10.1016/j.atmosres.2011.10.016, 2012.

1022 Jaffrezo, J.-L., Aymoz, G., Delaval, C., and Cozic, J.: Seasonal variations of the Water Soluble
1023   Organic Carbon mass fraction of aerosol in two valleys of the French Alps, Atmos. Chem.
1024   Phys., 5, 2809-2821, 2005.

1025 Keita, S., Liousse, C., Yoboué, V., Dominutti, P., Guinot, B., Assamoi, E.-M., Borbon, A.,
1026   Haslett, S. L., Bouvier, L., Colomb, A., Coe, H., Akpo, A., Adon, J., Bahino, J., Doumbia,
1027   M., Djossou, J., Galy-Lacaux, C., Gardrat, E., Gnamien, S., Léon, J. F., Ossohou, M.,
1028   N'Datchoh, E. T. and Roblou, L.: Particle and VOC emission factor
1029   measurements for anthropogenic sources in West Africa, Atmos. Chem. Phys., 18(10),
1030   7691-7708, doi:10.5194/acp-18-7691-2018, 2018.

Khan, Md. F., Shirasuna, Y., Hirano, K. and Masunaga, S.: Characterization of PM2.5, PM2.5-10 and PM>10 in ambient air, Yokohama, Japan, Atmospheric Research, 96(1), 159-172, doi:10.1016/j.atmosres.2009.12.009, 2010.

Kim, H., Liu, X., Kobayashi, T., Kohyama, T., Wen, F.-Q., Romberger, D. J., Conner, H., Gilmour, P. S., Donaldson, K., MacNee, W. and Rennard, S. I.: Ultrafine Carbon Black Particles Inhibit Human Lung Fibroblast-Mediated Collagen Gel Contraction, Am J Respir. Cell. Mol. Biol., 28(1), 111-121, doi:10.1165/rcmb.4796, 2003.

Knippertz, P., Tesche, M., Heinold, B., Kandler, K., Toledano, C. and Esselborn, M.: Dust mobilization and aerosol transport from West Africa to Cape Verde - a meteorological overview of SAMUM-2, Tellus B: Chemical and Physical Meteorology, 63(4), 430-447, doi:10.1111/j.1600-0889.2011. 00544.x, 2011.

Kouassi, K. S., Billet, S., Garçon, G., Verdin, A., Diouf, A., Cazier, F., Djaman, J., Courcot, D. and Shirali, P.: Oxidative damage induced in A549 cells by physically and chemically characterized air particulate matter (PM$_{2.5}$) collected in Abidjan, Côte d'Ivoire, J. Appl. Toxicol., doi:10.1002/jat.1496, 2009.

Lamaison, L. : Caractérisation des particules atmosphériques et identification de leurs sources dans une atmosphère urbaine sous influence industrielle, Thèse Doctorat, Univ des Sciences et Technologies, Lille, 2006.

Léon, J.F., Akpo, A., Bedou, M., Djossou, J., Bodjrenou, M., Yoboué, V., et Liousse, C.: Profondeur optique des aérosols sur le sud de l'Afrique de l'Ouest, soumis à ACPD, 2019.

Li, T.-C., Yuan, C.-S., Hung, C.-H., Lin, H.-Y., Huang, H.-C. and Lee, C.-L.: Chemical Characteristics of Marine Fine Aerosols over Sea and at Offshore Islands during Three Cruise Sampling Campaigns in the Taiwan Strait-Sea Salts and Anthropogenic Particles, Atmos. Chem. Phys. Discuss., 1-27, doi:10.5194/acp-2016-384, 2016.

Li, Y., Schwandner, F. M., Sewell, H. J., Zivkovich, A., Tigges, M., Raja, S., Holcomb, S., Molenar, J. V., Sherman, L., Archuleta, C., Lee, T. and Collett, J. L.: Observations of ammonia, nitric acid and fine particles in a rural gas production region, Atmospheric Environment, 83, 80-89, doi:10.1016/j.atmosenv.2013.10.007, 2014.

Liang, L., Engling, G., Du, Z., Cheng, Y., Duan, F., Liu, X. and He, K.: Seasonal variations and source estimation of saccharides in atmospheric particulate matter in Beijing, China, Chemosphere, 150, 365-377, 2016.

Liousse, C., Assamoi, E., Criqui, P., Granier, C., Rosset, R.: Explosive growth in African combustion emissions from 2005 to 2030, Environ. Res. Lett., 9, 035003, 2014.

Lonati, G., Ozgen, S. and Giugliano, M.: Primary and secondary carbonaceous species in PM$_{2.5}$ samples in Milan (Italy), Atmospheric Environment, 41(22), 4599-4610, doi:10.1016/j.atmosenv.2007.03.046, 2007.

Lowenthal, D., Zielinska, B., Samburova, V., Collins, D., Taylor, N. and Kumar, N.: Evaluation of assumptions for estimating chemical light extinction at U.S. national parks, Journal of

the Air & Waste Management Association, 65(3), 249-260, doi:10.1080/10962247.2014.986307, 2015.

Mason, B., Moore, B.C.: Principles of Geochemistry, fourth ed. John Wiley and Sons, New York, pp. 46-47, 1982.

Minguillón, M. C., Cirach, M., Hoek, G., Brunekreef, B., Tsai, M., de Hoogh, K., Jedynska, A., Kooter, I. M., Nieuwenhuijsen, M. and Querol, X.: Spatial variability of trace elements and sources for improved exposure assessment in Barcelona, Atmospheric Environment, 89, 268-281, doi: 10.1016/j.atmosenv.2014.02.047, 2014.

Mkoma, S. L.: Physico-Chemical characterisation of atmospheric aerosols in Tanzania, with emphasis on the carbonaceous aerosol components and on chemical mass closure, PhD, Ghent University, Ghent, Belguim, 2008.

Mmari, A. G., Potgieter-Vermaak, S. S., Bencs, L., McCrindle, R. I. and Van Grieken, R.: Elemental and ionic components of atmospheric aerosols and associated gaseous pollutants in and near Dar es Salaam, Tanzania, Atmospheric Environment, 77, 51-61, doi: 10.1016/j.atmosenv.2013.04.061, 2013.

MMEH (Ministère des Mines de l'Energie et d'Hydraulique): Tableau de bord de l'Energie 2002 au Bénin, Direction Générale de l'Energie, 2002.

Ngo, N. S., Asseko, S. V. J., Ebanega, M. O., Allo'o Allo'o, S. M. and Hystad, P.: The relationship among PM2.5, traffic emissions, and socioeconomic status: Evidence from Gabon using low-cost, portable air quality monitors, Transportation Research Part D: Transport and Environment, 68, 2-9, doi: 10.1016/j.trd.2018.01.029, 2019.

Ozer, P.: Estimation de la pollution particulaire naturelle de l'air en 2003 à Niamey (Niger) à partir de données de visibilité horizontale, 2005.

Pachauri, T., Singla, V., Satsangi, A., Lakhani, A. and Kumari, K. M.: Characterization of carbonaceous aerosols with special reference to episodic events at Agra, India, Atmospheric Research, 128, 98-110, doi: 10.1016/j.atmosres.2013.03.010, 2013.

Park, J. H., Mudunkotuwa, I. A., Mines, L. W. D., Anthony, T. R., Grassian, V. H. and Peters, T. M.: A Granular Bed for Use in a Nanoparticle Respiratory Deposition Sampler, Aerosol Science and Technology, 49(3), 179-187, doi:10.1080/02786826.2015.1013521, 2015.

Person, A. and Tymen, G.: Mesurage des particules en suspension dans l'air en relation avec la santé. Pollution atmosphèrique, 271-285, 2005.

Pipal, A. S., Jan, R., Satsangi, P. G., Tiwari, S. and Taneja, A.: Study of Surface Morphology, Elemental Composition and Origin of Atmospheric Aerosols (PM2.5 and PM10) over Agra, India, Aerosol Air Qual. Res., 14(6), 1685-1700, doi:10.4209/aaqr.2014.01.0017, 2014.

Pipal, A. S., Singh, S. and Satsangi, G. P.: Study on bulk to single particle analysis of atmospheric aerosols at urban region, Urban Climate, 27, 243-258, doi: 10.1016/j.uclim.2018.12.008, 2019.

1107   Prospero, J.M., Ginoux, P., Torres, O., Nicholson, S.E., Gill, T.E.: Environmental
1108   characterization of global sources of atmospheric soil dust identified with the NIMBUS 7
1109   Total Ozone Mapping Spectrometer (TOMS) absorbing aerosol product, Rev. Geophys.,
1110   40, 2-1-31, 2002.

1111   Qin, Y., Chan, C. K. and Chan, L. Y.: Characteristics of chemical compositions of atmospheric
1112   aerosols in Hong Kong: spatial and seasonal distributions, Science of The Total
1113   Environment, 206(1), 25-37, doi: 10.1016/S0048-9697(97)00214-3, 1997.

1114   Ramgolam K, Favez O, Cachier H, Gaudichet A, Marano F, Martinon L, Baeza-Squiban
1115   A: Size-partitioning of an urban aerosol to identify particle determinants involved in the
1116   proinflammatory response induced in airway epithelial cells. Part Fibre
1117   Toxicol 2009, 6: 10. 10.1186/1743-8977-6-10.

1118   Rengarajan, R., Sudheer, A. K. and Sarin, M. M.: Aerosol acidity and secondary organic aerosol
1119   formation during wintertime over urban environment in western India, Atmospheric
1120   Environment, 45(11), 1940-1945, doi: 10.1016/j.atmosenv.2011.01.026, 2011.

1121   Samara, C., Kouimtzis, T., Tsitouridou, R., Kanias, G. and Simeonov, V.: Chemical mass
1122   balance source apportionment of PM10 in an industrialized urban area of Northern Greece,
1123   Atmospheric Environment, 37(1), 41-54, doi:10.1016/S1352-2310(02)00772-0, 2003.

1124   Satsangi, A., Pachauri, T., Singla, V., Lakhani, A. and Kumari, K. M.: Organic and elemental
1125   carbon aerosols at a suburban site, Atmospheric Research, 113, 13-21, doi:
1126   10.1016/j.atmosres.2012.04.012, 2012.

1127   Saxena, P., and Hildemann, L.M.: Water-soluble organics in atmospheric particles: a critical
1128   review of the literature and application of thermodynamics to identify candidate
1129   compounds, J. Atmos. Chem., 24(1), 57-109, 1996.

1130   Sciare, J., Oikonomou, K., Cachier, H., Mihalopoulos, N., Andreae, M. O., Maenhaut, W. and
1131   Sarda-Estève, R.: Aerosol mass closure and reconstruction of the light scattering
1132   coefficient over the Eastern Mediterranean Sea during the MINOS campaign, Atmos.
1133   Chem. Phys., 5(8), 2253-2265, doi:10.5194/acp-5-2253-2005, 2005.

1134   Seinfeld, J. H.   and Pandis, S. N.: Atmospheric Chemistry and Physics: from Air
1135   Pollution to Climate Change, John Wiley and Sons, Inc. New York, 1998.

1136   Shahsavani, A., Naddafi, K., Jaafarzadeh Haghighifard, N., Mesdaghinia, A., Yunesian, M.,
1137   Nabizadeh, R., Arhami, M., Yarahmadi, M., Sowlat, M. H., Ghani, M., Jonidi Jafari, A.,
1138   Alimohamadi, M., Motevalian, S. A. and Soleimani, Z.: Characterization of ionic
1139   composition of TSP and PM10 during the Middle Eastern Dust (MED) storms in Ahvaz,
1140   Iran, Environ Monit Assess, 184(11), 6683-6692, doi:10.1007/s10661-011-2451-6, 2012.

1141   Stone, R. S., Herber, A., Vitale, V., Mazzola, M., Lupi, A., Schnell, R. C., Dutton, E. G., Liu,
1142   P. S. K., Li, S.-M., Dethloff, K., Lampert, A., Ritter, C., Stock, M., Neuber, R. and
1143   Maturilli, M.: A three-dimensional characterization of Arctic aerosols from airborne Sun
1144   photometer observations: PAM-ARCMIP, April 2009, J. Geophys. Res., 115(D13),
1145   D13203, doi: 10.1029/2009JD013605, 2010.

1146 Sullivan, A. P., Weber, R. J., Clements, A. L., Turner, J. R., Bae, M. S. and Schauer, J. J.: A
1147   method for on-line measurement of water-soluble organic carbon in ambient aerosol
1148   particles: Results from an urban site: on-line measurement of WSOC in aerosols, Geophys.
1149   Res. Lett., 31(13), doi: 10.1029/2004GL019681, 2004.

1150 Sun, Y., Zhuang, G., Wang, Y., Han, L., Guo, J., Dan, M., Zhang, W., Wang, Z. and Hao, Z.:
1151   The airborne particulate pollution in Beijing - concentration, composition, distribution and
1152   sources, Atmospheric Environment, 38(35), 5991-6004, doi:
1153   10.1016/j.atmosenv.2004.07.009, 2004.

1154 Tang, X., Zhang, X., Ci, Z., Guo, J. and Wang, J.: Speciation of the major inorganic salts in
1155   atmospheric aerosols of Beijing, China: Measurements and comparison with model,
1156   Atmospheric Environment, 133, 123-134, doi: 10.1016/j.atmosenv.2016.03.013, 2016.

1157 Tapsoba, D. : Caractérisation événementielle des régimes pluviométriques ouestafricains et de
1158   leur récent changement, Thèse de Doctorat, Univ.Paris-XI (Orsay). 100p, 1997.

1159 Taylor, S. R.: Abundance of chemical elements in the continental crust: a new table,
1160   Geochimica et Cosmochimica Acta, 28(8), 1273-1285, doi: 10.1016/0016-7037(64)90129-
1161   2, 1964.

1162 Terzi, E., Argyropoulos, G., Bougatioti, A., Mihalopoulos, N., Nikolaou, K. and Samara, C.:
1163   Chemical composition and mass closure of ambient PM10 at urban sites, Atmospheric
1164   Environment, 44(18), 2231-2239, doi: 10.1016/j.atmosenv.2010.02.019, 2010.

1165 Tunno, B., Longley, I., Somervell, E., Edwards, S., Olivares, G., Gray, S., Cambal, L., Chubb,
1166   L., Roper, C., Coulson, G. and Clougherty, J. E.: Separating spatial patterns in pollution
1167   attributable to woodsmoke and other sources, during daytime and nighttime hours, in
1168   Christchurch, New Zealand, Environmental Research, 171, 228-238, doi:
1169   10.1016/j.envres.2019.01.033, 2019.

1170 Turpin, B. J., Cary, R. A. and Huntzicker, J. J.: An In Situ, Time-Resolved Analyzer for Aerosol
1171   Organic and Elemental Carbon, Aerosol Science and Technology, 12(1), 161-171,
1172   doi:10.1080/02786829008959336, 1990.

1173 United Nations, Department of Economic and Social Affairs, Population Division (2019).
1174   World Population Prospects 2019: Volume II: Demographic Profiles. Made available under
1175   a Creative Commons license. http://creativecommons.org/licenses/by/3.0/igo/ 2019

1176 Val, S., Liousse, C., Doumbia, E. H. T., Galy-Lacaux, C., Cachier, H., Marchand, N., Badel,
1177   A., Gardrat, E., Sylvestre, A. and Baeza-Squiban, A.: Physico-chemical characterization of
1178   African urban aerosols (Bamako in Mali and Dakar in Senegal) and their toxic effects in
1179   human bronchial epithelial cells: description of a worrying situation, Part Fibre Toxicol,
1180   10(1), 10, doi:10.1186/1743-8977-10-10, 2013.

1181 Viana, M., López, J. M., Querol, X., Alastuey, A., García-Gacio, D., Blanco-Heras, G., López-
1182   Mahía, P., Piñeiro-Iglesias, M., Sanz, M. J., Sanz, F., Chi, X. and Maenhaut, W.: Tracers
1183   and impact of open burning of rice straw residues on PM in Eastern Spain, Atmospheric
1184   Environment, 42(8), 1941-1957, doi: 10.1016/j.atmosenv.2007.11.012, 2008.

Viana, M., Maenhaut, W., ten Brink, H. M., Chi, X., Weijers, E., Querol, X., Alastuey, A., Mikuška, P. and Večeřa, Z.: Comparative analysis of organic and elemental carbon concentrations in carbonaceous aerosols in three European cities, Atmospheric Environment, 41(28), 5972-5983, doi: 10.1016/j.atmosenv.2007.03.035, 2007.

Viidanoja, J., Sillanpää, M., Laakia, J., Kerminen, V.-M., Hillamo, R., Aarnio, P. and Koskentalo, T.: Organic and black carbon in PM2.5 and PM10: 1 year of data from an urban site in Helsinki, Finland, Atmospheric Environment, 36(19), 3183-3193, doi: 10.1016/S1352-2310(02)00205-4, 2002.

Wang, X., Bi, X., Sheng, G. and Fu, J.: Chemical Composition and Sources of PM10 and PM2.5 Aerosols in Guangzhou, China, Environ Monit Assess, 119(1-3), 425-439, doi: 10.1007/s10661-005-9034-3, 2006.

Washington, R., Todd, M., Middleton, N. J. and Goudie, A. S.: Dust-Storm Source Areas Determined by the Total Ozone Monitoring Spectrometer and Surface Observations, Annals of the Association of American Geographers, 93(2), 297-313, doi:10.1111/1467-8306.9302003, 2003.

Watson, J. G. and Chow, J. C.: Estimating middle-, neighborhood-, and urban-scale contributions to elemental carbon in Mexico City with a rapid response aethalometer, J. Air Waste Manag. Assoc., 51(11), 1522-1528, 2001.

Watson, J. G., Chow, J. C. and Houck, J. E.: PM2.5 chemical source profiles for vehicle exhaust, vegetative burning, geological material, and coal burning in Northwestern Colorado during 1995, Chemosphere, 43(8), 1141-1151, doi:10.1016/S0045-6535(00)00171-5, 2001.

WHO (World Health Organization), 7 million premature deaths annually linked to air pollution. Media Centre news release. Geneva: World Health Organization. (http: //www.who.int/ mediacentre/news/releases/2014/airpollution/en/, 2014.

Wilson, M. R., Lightbody, J. H., Donaldson, K., Sales, J. and Stone, V.: Interactions between ultrafine particles and transition metals in vivo and in vitro, Toxicol. Appl. Pharmacol., 184(3), 172-179, 2002.

Xiang, P., Zhou, X., Duan, J., Tan, J., He, K., Yuan, C., Ma, Y. and Zhang, Y.: Chemical characteristics of water-soluble organic compounds (WSOC) in PM2.5 in Beijing, China: 2011-2012, Atmospheric Research, 183, 104-112, doi: 10.1016/j.atmosres.2016.08.020, 2017.

Xie, Y., Wang, Y., Bilal, M. and Dong, W.: Mapping daily PM2.5 at 500 m resolution over Beijing with improved hazy day performance, Science of The Total Environment, 659, 410-418, doi: 10.1016/j.scitotenv.2018.12.365, 2019.

Xu, H., Léon, J.-F., Liousse, C., Guinot, B., Yoboué, V., Akpo, A. B., Adon, J., Ho, K. F., Ho, S. S. H., Li, L., Gardrat, E., Shen, Z. and Cao, J.: Personal exposure to PM2.5 emitted from typical anthropogenic sources in Southern West Africa (SWA): Chemical characteristics and associated health risks, Atmos. Chem. Phys. Discuss., 1-68, doi:10.5194/acp-2018-1060, 2019.

1224 Xu, J., Zhang, Y., Zheng, S. and He, Y.: Aerosol effects on ozone concentrations in Beijing: a
1225   model sensitivity study, J Environ Sci (China), 24(4), 645-656, 2012.

1226 Yu, P., Froyd, K. D., Portmann, R. W., Toon, O. B., Freitas, S. R., Bardeen, C. G., Katich, J.
1227   M., Schwarz, J. P., Williamson, C., Kupc, A., Brock, C., Liu, S., Gao, R.-S., Schill, G.,
1228   Fan, T., Rosenlof, K. H., and Murphy, D. M.: An improved treatment of aerosol convective
1229   transport and removal in a chemistry-climate model, Geophys. Res. Lett., submitted, 2018.

1230 Zghaid, M., Noack, Y., Bounakla, M., and Benyaich, F.: Pollution atmosphérique particulaire
1231   dans la ville de Kenitra (Maroc), Pollution atmosphérique [En ligne], N° 203, mis à jour le
1232   12/10/2015,   URL :   http://lodel.irevues.inist.fr/pollution-
1233   atmospherique/index.php?id=1184, https://doi.org/10.4267/pollution-atmospherique.1184

1234 Zhang, X. Y., Gong, S. L., Shen, Z. X., Mei, F. M., Xi, X. X., Liu, L.C., Zhou, Z. J., Wang, D.,
1235   Wang, Y. Q., and Cheng, Y.: Characterization of soil dust aerosol in China and its transport
1236   and distribution during 2001 ACE-Asia: 1. Network observations, J. Geophys. Res.
1237   Atmos., 108(D9), 4261, doi:10.1029/2002JD002632, 2003.

1238

1239

1240

1241

1242

1243

1244

1245

1246

1247

1248

1249

1250

1251

1252

1253 **Figure caption**

1254 Figure 1: Map of the city of Abidjan reporting the geographical location of DACCIWA urban
1255   sampling sites.

1256   Figure 2: Map of the city of Cotonou reporting the geographical location of DACCIWA urban
1257   sampling site.

1258   Figure 3: Pictures of the different sampling sites: (a) Traffic in Cotonou (Benin, CT station),
1259   (b) Waste burning in Abidjan (Côte d'Ivoire, AWB station), (c), Domestic fire, showing
1260   smoking activity in Yopougon, Abidjan (Côte d'Ivoire, ADF station), (d) '' woro-woro
1261   and Gbaka '' traffic in Abidjan (Côte d'Ivoire, AT station).

1262   Figure 4: Wind, pressure and temperature diagram at Abidjan and Cotonou during the different
1263   campaigns.

1264   Figure 5: Back trajectories arriving at Abidjan (a) and Cotonou (b) for each season (WS2015,
1265   WS2016, DS2016 and DS2017).

1266   Figure 6: Aerosol Mass concentrations at the different study sites for each campaign and for the
1267   different sizes (C in black, Fine in light Grey, Ultra-fine in grey). Bulk aerosol mass is
1268   indicated in boxes.

1269   Figure 7: Comparison of PM2.5 mass concentrations in $\mu g.m^{-3}$ at the four sites with those
1270   obtained by Djossou et al. (2018) and Xu et al. (2019) for the same sites and periods.
1271   Data for the following weeks were then selected in Djossou et al. (2018): 20-27/07/2015
1272   for WS15, 4-11/01/2016 for DS16, 4-11/07/2016 for WS16 and 9-16/01/2017 for DS17.

1273   Figure 8: EC relative concentrations in each size classes (C in black, Fine in light grey, Ultra-
1274   fine in grey) at the different study sites for each campaign. Bulk EC concentration for
1275   each site is indicated in boxes.

1276   Figure 9: OC relative concentrations in each size classes (C in black, Fine in light grey, Ultra-
1277   fine in grey) at the different study sites for each campaign. Bulk OC concentration for
1278   each site is indicated in boxes.

1279   Figure 10: OC/ EC ratio for the different campaigns and sites for each aerosol size (C in black,
1280   Fine in light grey, Ultra-fine in grey). Each box shows the median and the first and the
1281   third quartiles.

1282   Figure 11: Water-soluble ionic species speciation for each site, each campaign and each aerosol
1283   size.

1284   Figure 12: Dust concentrations at the different study sites for each campaign and for the
1285   different sizes (C in black, Fine in light grey, Ultra-fine in grey).

1286 Figure 13: Size-speciated aerosol chemical composition for each site, for each campaign and

1287 each aerosol size.

1288 Figure 14: MODIS Aerosol optical depth regional distribution over West Africa. Data are for

1289 2017, focusing on our campaign date at Abidjan (a-c 01/11-12-left part) and Cotonou

1290 (b-d 01/6-7, right part).

1291

1292

1293

1294
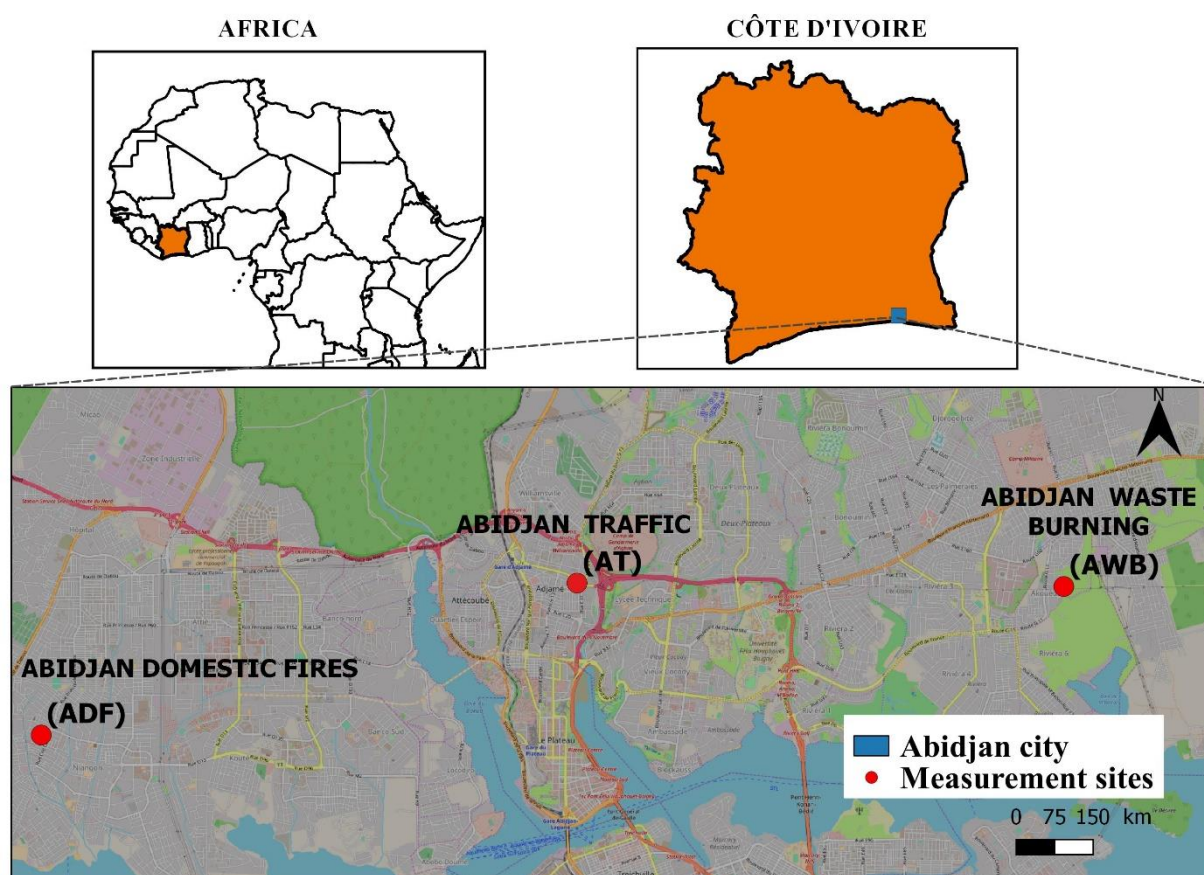
1295

1296

1297

1298

1299

1300

1301   Figure1
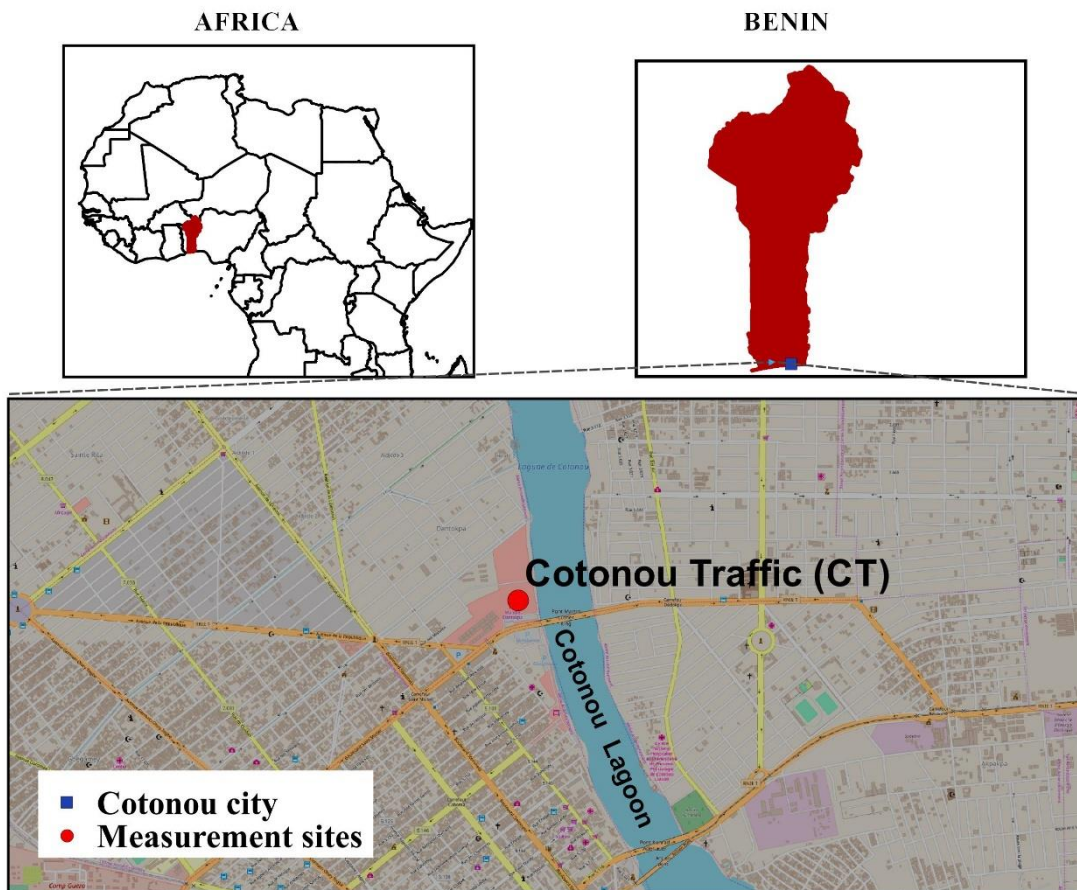
1302

1303

1304

1305

1306

1307

1308   **Figure 2**

1309

1310

1311

1312

1313

1314
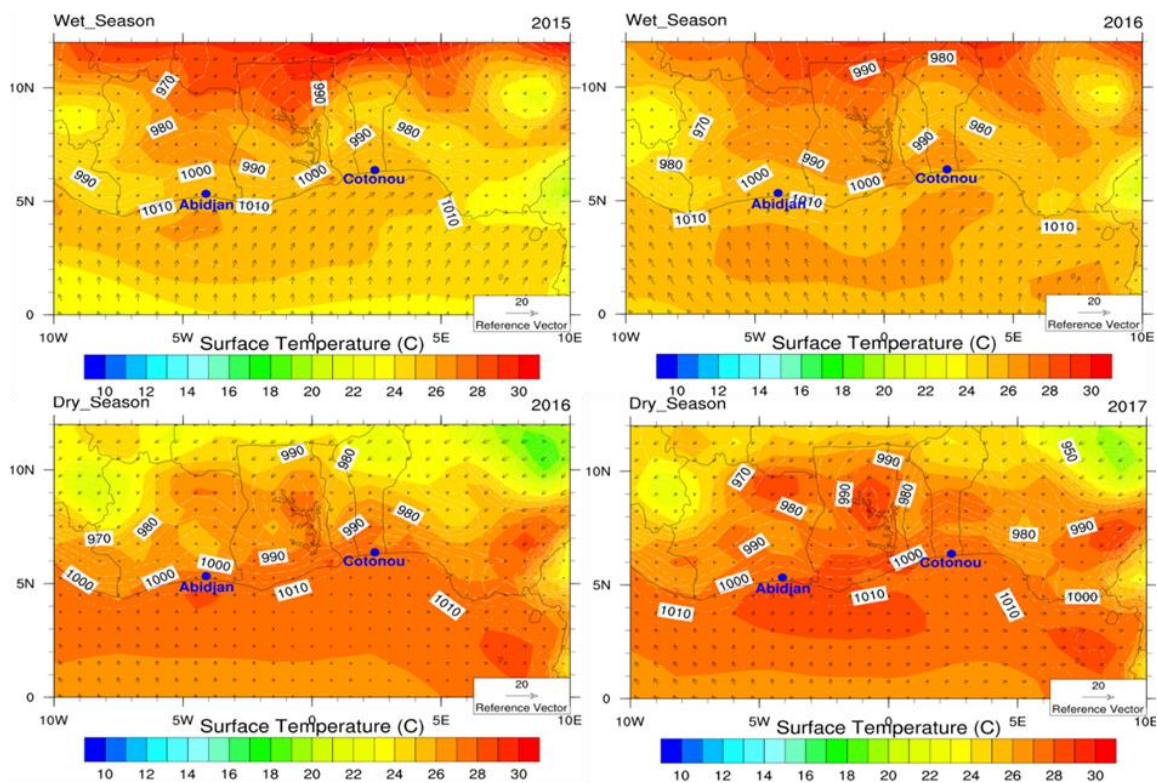
Figure 3

1326

1327

1328   **Figure 4**

1329

1330

1331

1332

1333

1334

1335

1336

1337

1338

1339

1340

1341

1342

1343

1344

Wet season 2015

Wet season 2016

Dry season 2016

Dry season 2017

1345

1346 **Figure 5-a**

Wet season 2015

Wet season 2016

Dry season 2016

Dry season 2017
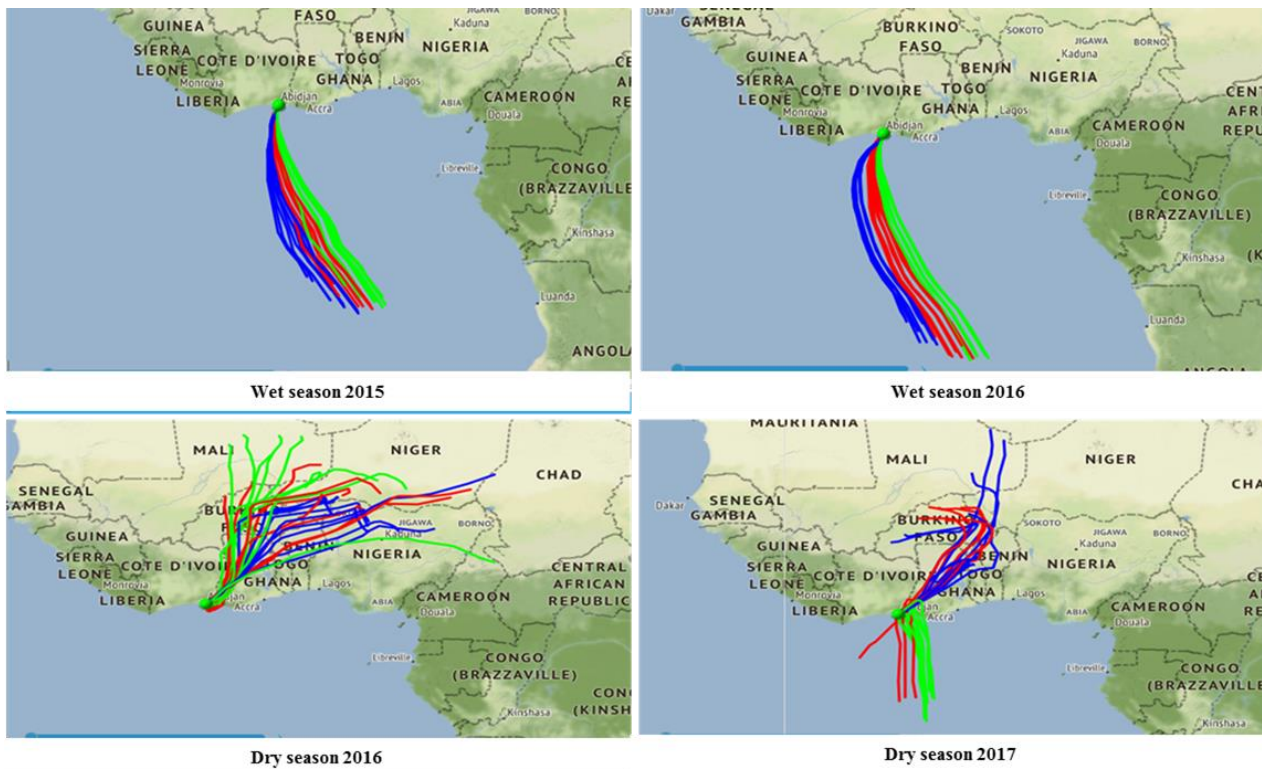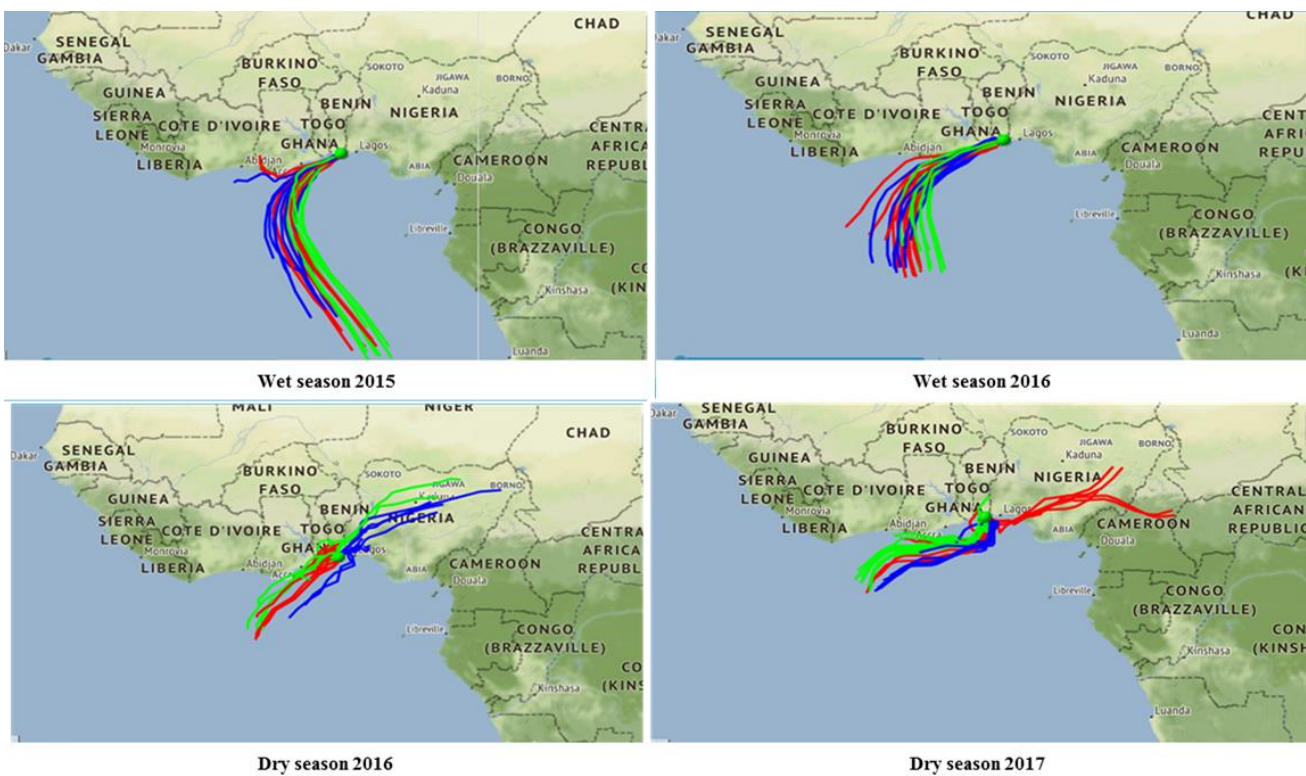
1347

1348 **Figure 5-b**

1349

1350

1351

1352
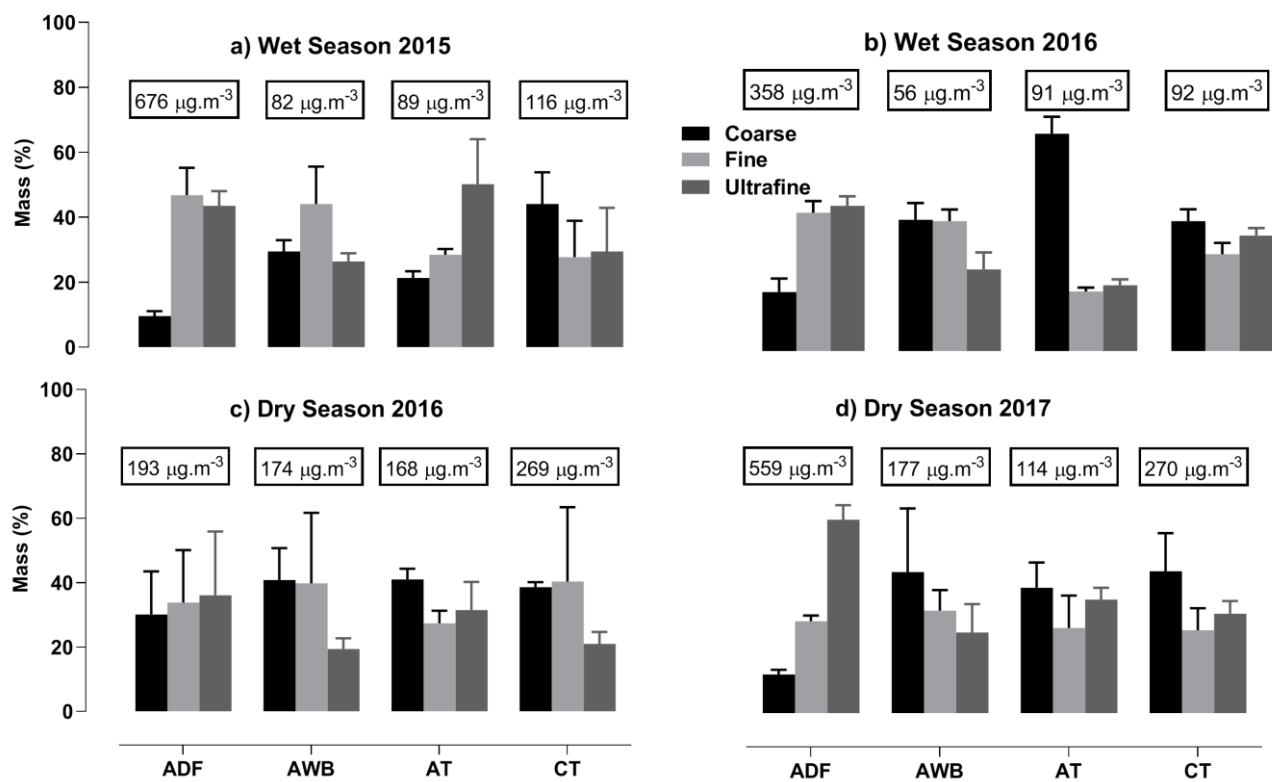
1353

1354 **Figure 6**

1355

1356
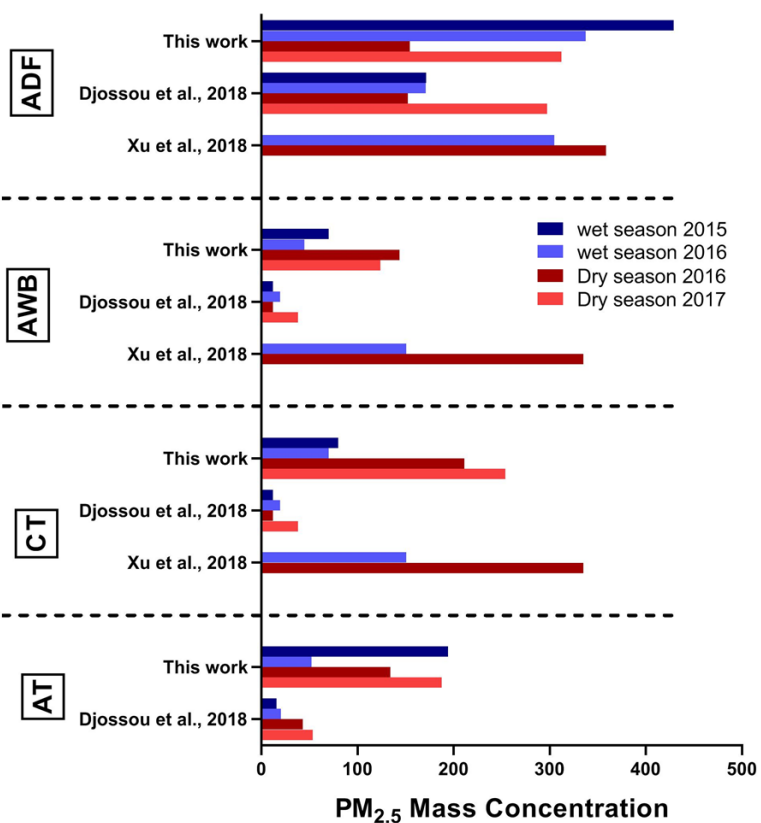
1357

1358   **Figure 7**

1359

1360

1361

1362
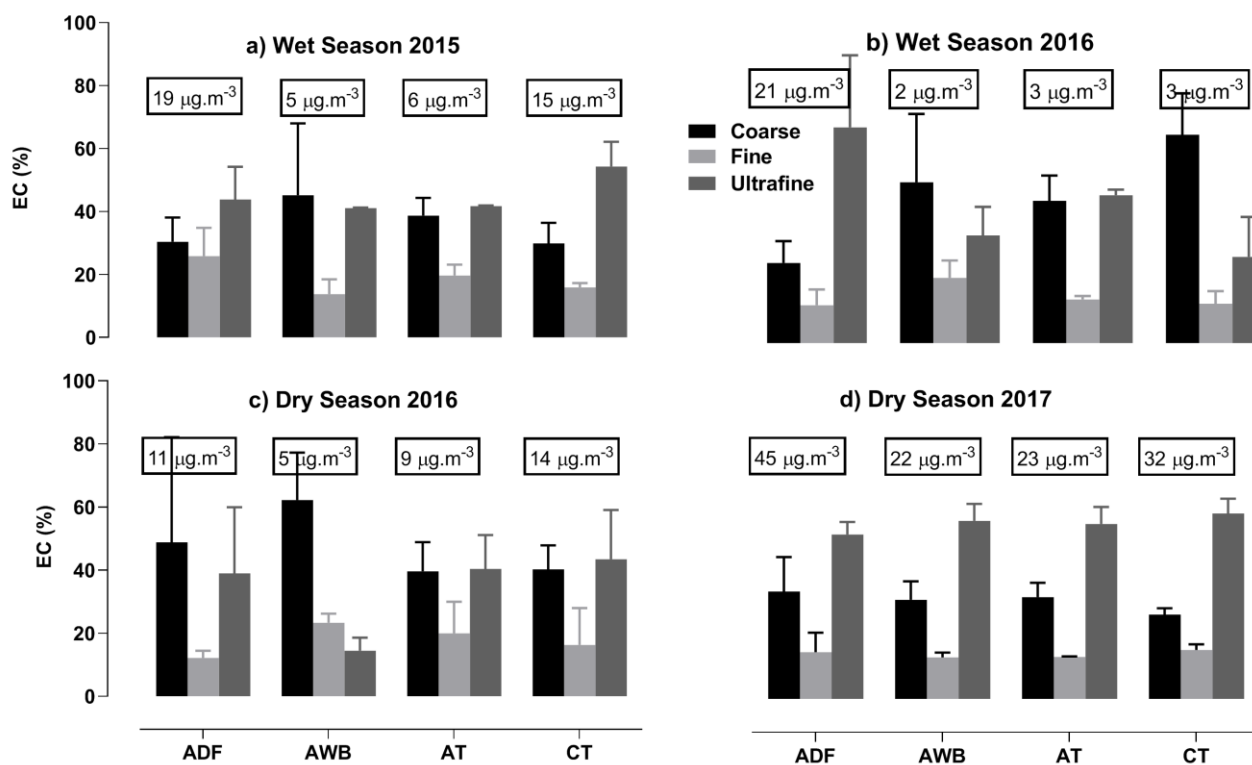
1363

1364 **Figure 8**

1365

1366

1367

1368

1369
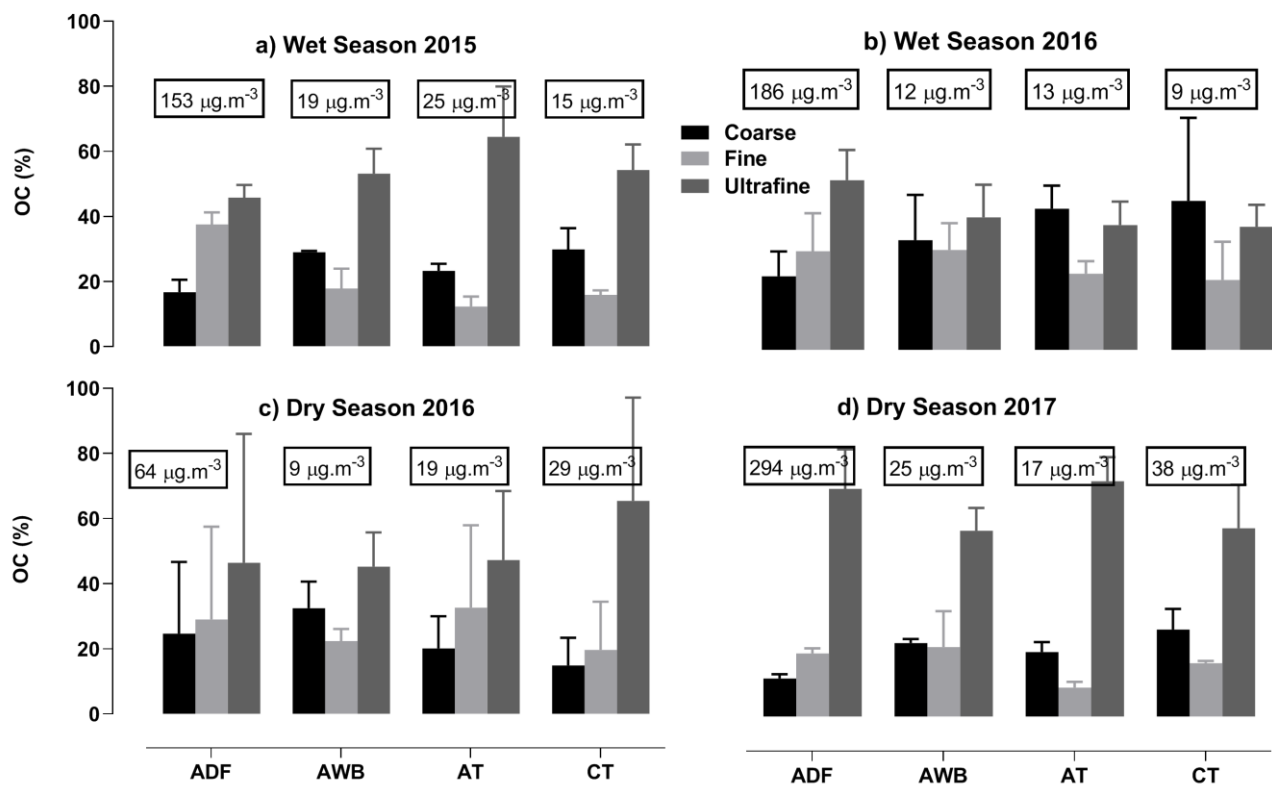
1371 **Figure 9**

1372

1373

1374

1375

1376
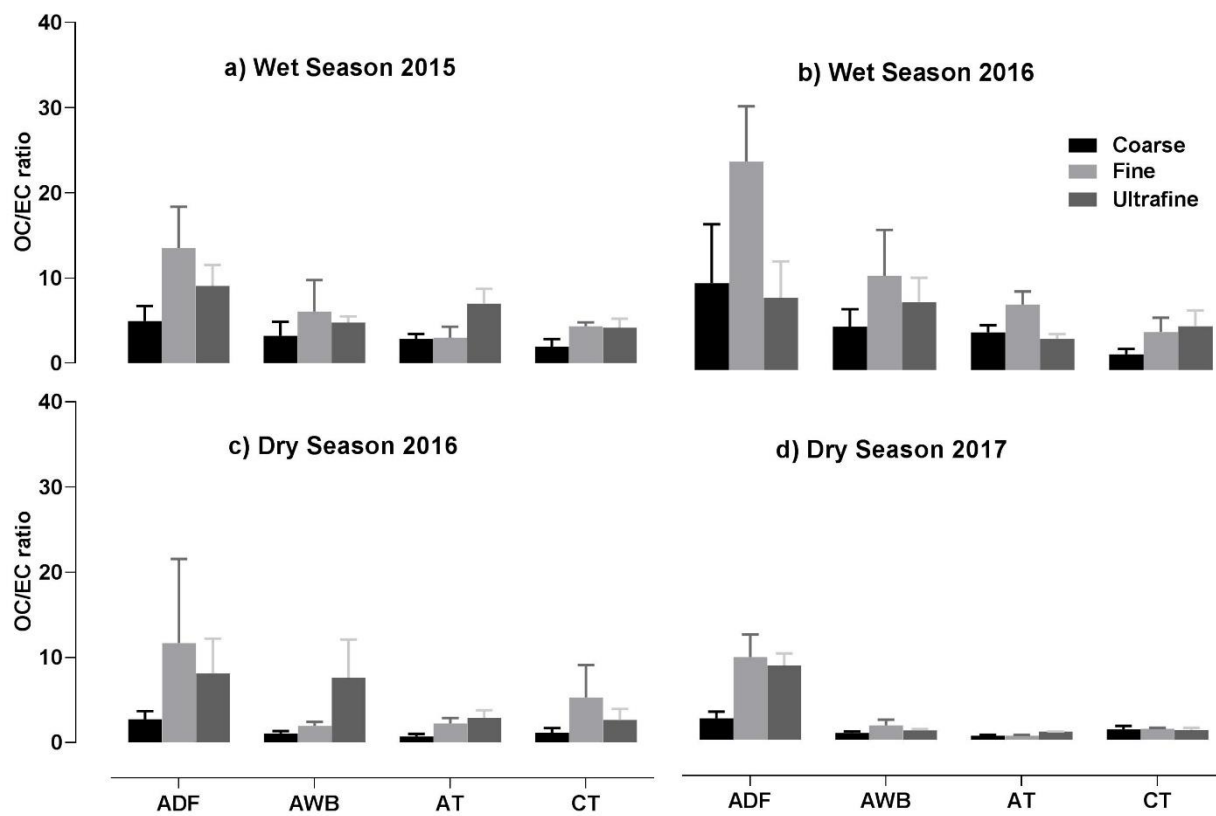
1377

Figure 10

1379

1380
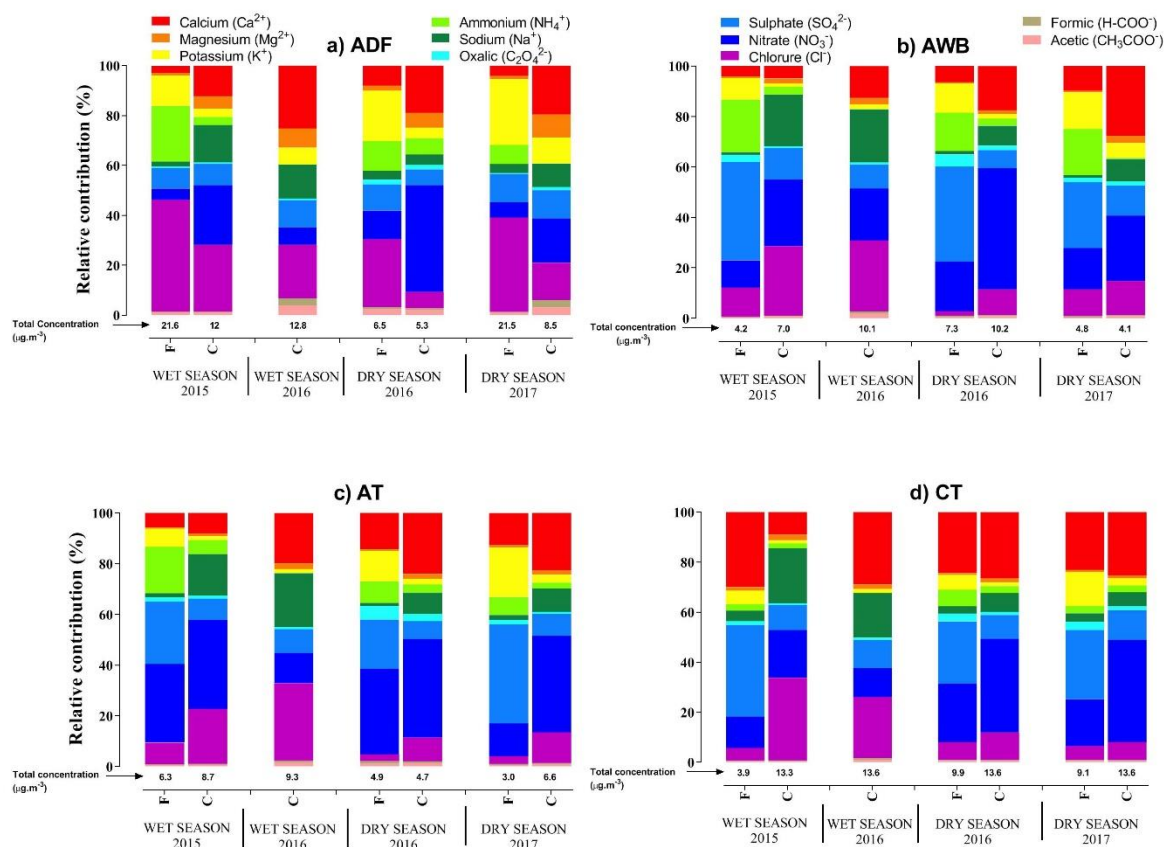
1381

1382 **Figure 11**

1383

1384
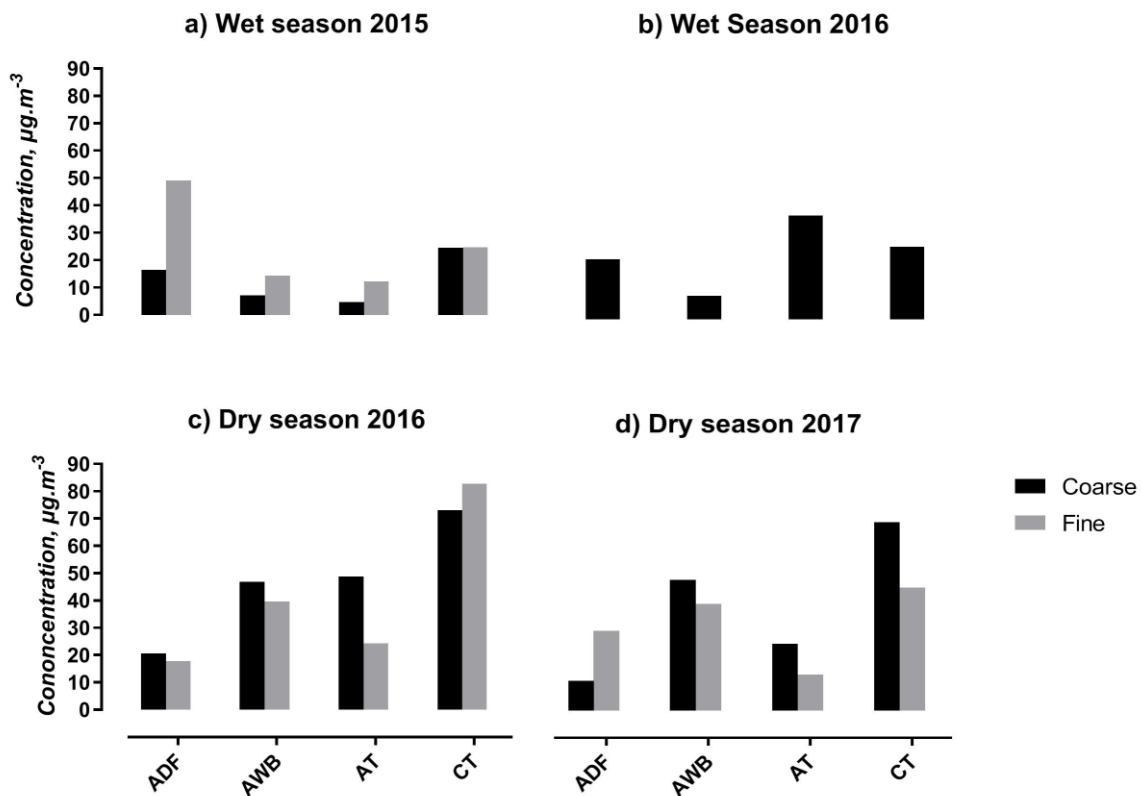
1385

1386   **Figure 12**

1387
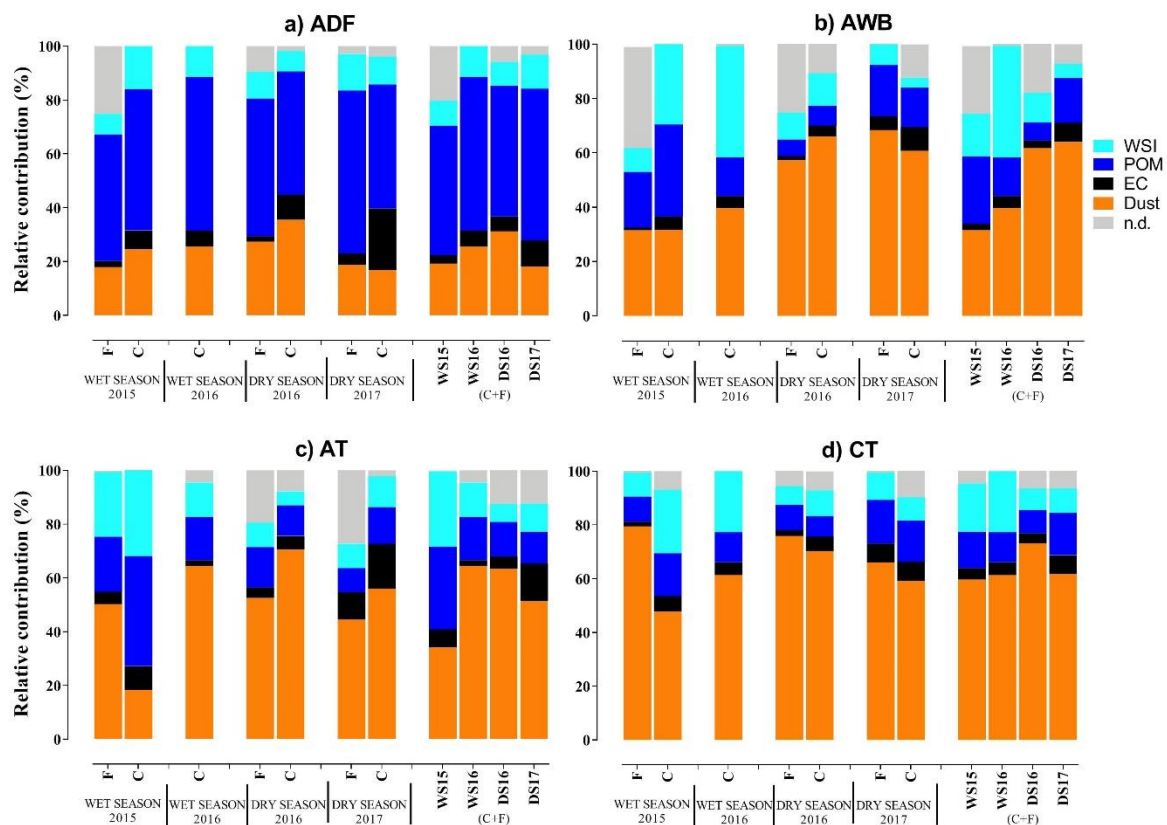
1388

1389 **Figure 13**

1390

1391

1392

1393
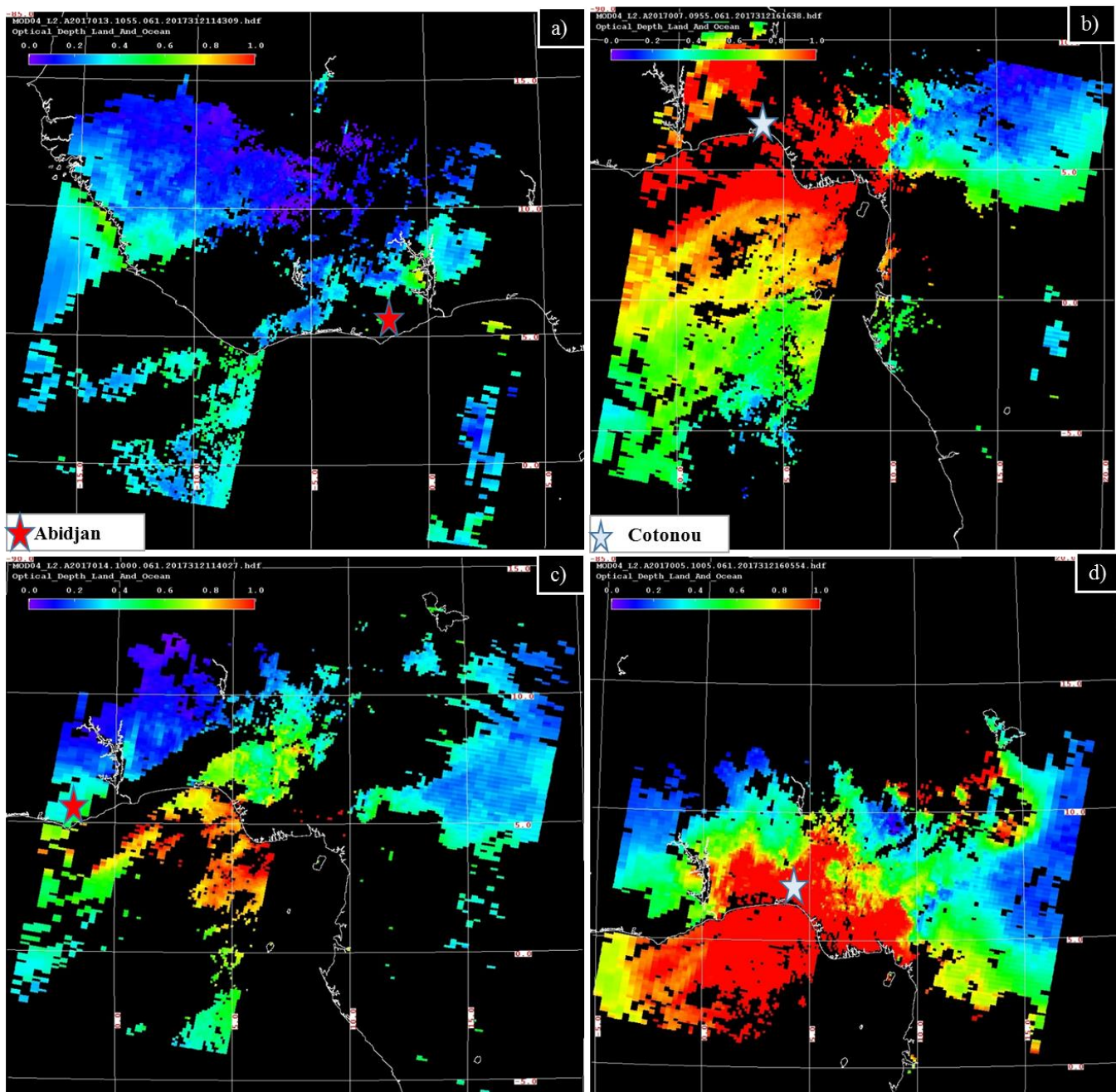
1394

1395 **Figure 14**

1396

1397

1398

1399

1400

1401

1402

1403

1404

1405   List of table

1406

1407   Table 1: Comparison of dust concentrations obtained from different methodologies

1408   Table 2: WSOC concentrations (μg.m^{-3}) and WSOC/OC ratios (%) for each site, each campaign and

1409   each aerosol size

1410   Table 3: Trace element concentrations for bulk aerosol for each site and for DS2017 and WS2016.

1411   Table 4: Comparison of PM2.5 concentrations with literature data. Only literature data given at a daily

1412   scale have been selected.

1413   Table 5: PM2.5-EC and PM2.5-OC comparison with Djossou et al. (2018) and Xu et al. (2019) values.

1414   Units are μgC.m^{-3}

1415   Table 6: EC and OC comparison with literature values. Only literature data given at a daily scale have

1416   been selected.

1417   Table 7: Comparison of WSOC concentrations with literature data. Only literature data given at a daily

1418   scale have been selected.

1419

1420

1421

1422

1423

1424

1425

1426

1427

1428

1429

1430

1431

1432

1433

1434

1435

1436

1437

1438

1439

1440

1441

1442   Table 1: Comparison of dust concentrations obtained from different methodologies in µg.m^{-3}

Dry 2017		Sciare et al. (2005)	Guinot et al. (2007)	Terzi et al. (2010)
ADF	C	18.5	11.2	86.9
	F	9.3	29.7	22.2
	bulk	27.7	40.9	109.1
AWB	C	12.3	48.5	126.4
	F	5.2	39.7	106.4
	bulk	17.6	88.2	232.8
AT	C	16.4	24.8	98.5
	F	4.3	13.4	34.2
	bulk	20.7	38.2	132.7
CT	C	37.9	70.0	98.4
	F	23.4	45.6	55.8
	bulk	61.3	115.6	154.2

1443

Wet 2016		Sciare et al., 2005	Guinot et al., 2007	Terzi et al.(2010)
ADF	C	35.34	21.5	27.9
AWB	C	13.46	8.6	21.1
AT	C	19.65	37.5	21.4
CT	C	42.98	26.2	52.5
	Bulk	42.98	26.2	52.5

1444

1445

1446

1447

1448

1449

1450

1451

1452 Table 2: WSOC concentrations (µg.m^{-3}) and WSOC/OC ratios (%) for each site, each campaign and

1453 each aerosol size

Site		Abidjan Waste Burning		Abidjan Domestic Fire	
Period	Size	WSOC	WSOC/OC	WSOC	WSOC/OC
Wet season 2015	Coarse	1.3	24,6	8.2	32.5
	Fine	0.7	19.9	12.8	22.7
	Ultra fine	4.1	43.6	51.3	72.5
	PM2.5	5.5	33.7	69.5	47.2
Dry season 2016	Coarse	0.4	12.3	4.4	18.8
	Fine	0.9	46.9	7.0	20.4
	Ultra fine	1.5	38.4	21.9	61.5
	PM2.5	2.7	32.7	31.0	32.0
Wet season 2016	Coarse	1.3	42.5	16.5	44.3
	Fine	0.8	26.3	17.1	33.0
	Ultra fine	2.0	41.2	79.7	84.5
	PM2.5	3.5	37.1	106.0	52.0
Dry season 2017	Coarse	1.9	32.9	12.1	36.0
	Fine	1.4	38.4	19.9	35.0
	Ultra fine	1.6	11.5	38.6	19.0
	PM2.5	4.0	30.0	65.8	29.0

1454

1455

1456 Table 2 (suite): WSOC concentrations (µg.m^{-3}) and WSOC/OC ratios (%) for each site, each campaign

1457 and each aerosol size

Site		Abidjan Traffic		Cotonou Traffic	
Period	Size	WSOC	WSOC/OC	WSOC	WSOC/OC
Wet season 2015	Coarse	2.4	39.6	1.1	23.3
	Fine	1.3	46.7	0.5	22.1
	Ultra fine	4.7	29.0	0.4	12.7
	PM2.5	6.9	34.0	2.2	18.0
Dry season 2016	Coarse	1.4	43.0	2.3	64.1
	Fine	1.9	59.0	0.6	10.5
	Ultra fine	4.9	62.0	6.3	42.9
	PM2.5	7.5	49.4	8.0	29.0
Wet season 2016	Coarse	1.1	23.1	1.2	34.7
	Fine	0.5	16.8	0.5	32.2
	Ultra fine	1.4	34.8	0.9	23.0
	PM2.5	2.4	26.0	1.9	28.0
Dry season 2017	Coarse	0.9	24.0	3.5	37.8
	Fine	0.3	24.3	2.4	39.6
	Ultra fine	1.8	14.8	1.9	10.4
	PM2.5	2.6	16.0	6.0	18.2

1458   Table 3: Trace element concentrations for bulk aerosol for each site and for DS2017 and WS2016.

	Bulk ng.m⁻³ (%)							
	DRY 2017				WET 2016			
	ADF	AWB	AT	CT	ADF	AWB	AT	CT
Al	10050.8 (1.8)	25186.1 (13.7)	14015.8 (12.26)	15480.4 (5.7)	1370.5 (0.4)	1990.1 (3.5)	2191.4 (2.4)	4010.5 (4.4)
K	8634.3 (1.5)	6093.7 (3.3)	3677.7 (3.22)	5068.9 (1.9)	1105.0 (0.3)	472.0 (0.8)	275.9 (0.3)	1076.0 (1.2)
Na	6847.8 (1.2)	23430.5 (12.8)	15372.1 (13.44)	11529.3 (4.3)	2070.6 (0.6)	3735.4 (6.6)	2861.5 (3.1)	5310.2 (5.8)
Ca	4321.2 (0.8)	2923.7 (1.6)	4117.6 (3.60)	6233.5 (2.3)	4124.7 (1.1)	447.5 (0.8)	374.7 (0.4)	4954.02 (5.4
Mg	1940.6 (0.3)	384.0 (0.2)	410.3 (0.36)	823.2 (0.3)	1524.7 (0.4)	294.9 (0.5)	283.5 (0.3)	619.2 (0.7)
Fe	1709.9 (0.3)	3807.9 (2.1)	1628.1 (1.42)	3406.8 (1.3)	1314.0 (0.4)	709.3 (1.3)	987.3 (1.1)	1549.4 (1.7)
P	1521.9 (0.3)	696.0 (0.4)	147.8 (0.13)	207.4 (0.1)	605.4 (0.2)	8.6	13.2	81.4 (0.1)
Ti	488.9 (0.1)	2270.3 (1.2)	282.8 (0.25)	457.9 (0.17)	170.8 (0.05)	75.7 (0.13)	96.8 (0.11)	154.7 (0.17)
Zn	189.7 (0.03)	80.9 (0.04)	57.9 (0.05)	149.4 (0.06)	60.3 (0.02)	1.9	41.1 (0.04)	36.2 (0.04)
Zr	172.1 (0.03)	390.3 (0.21)	217.9 (0.19)	145.3 (0.05)	-	22.4 (0.04)	36.7 (0.04)	31.2 (0.03)
Pb	87.1 (0.02)	11.0 (0.01)	4.8	11.5	8.3	2.1	2.3	9.3 (0.01)
Sn	79.7 (0.01)	38.4 (0.02)	21.6 (0.02)	37.4 (0.01)	0.77	0.09	0.0006	9.ç (0.01)
Mn	74.2 (0.01)	35.2 (0.02)	33.7 (0.03)	160.6 (0.06)	48.9 (0.01)	12.01 (0.02)	9.1 (0.01)	41.41 (0.05)
Rb	52.4 (0.01)	8.7	5.9 (0.01)	8.5	4.47	0.71	0.85	1.9
Sb	59.9 (0.01)	201.2 (0.11)	123.6 (0.11)	149.04 (0.06)	24.4 (0.01)	0	0.0006	2.9
Ba	37.3 (0.01)	53.3 (0.03)	47.4 (0.04)	65.8 (0.02)	18.5	8.02 (0.01)	9.9 (0.01)	32.0 (0.03)
Ni	36.5 (0.01)	34.5 (0.02)	27.9 (0.02)	50.2 (0.02)	18.00)	33.1 (0.06)	9.7 (0.01)	14.9 (0.02)
Cr	29.4 (0.01)	53.8 (0.03)	35.8 (0.03)	28.6 (0.01)	41.9 (0.01)	47.7 (0.08)	24.3 (0.03)	29.7 (0.03)
Sr	28.1 (0.01)	15.5 (0.01)	21.2 (0.02)	34.02 (0.01)	17.02	0	0.19	8.1 (0.01)
Cu	24.0	12.3 (0.01)	3.6	9.6	3.99	0.26	0.87	2.8)
Sr	12.6	-	-	-	17.1	-	0.22	8.9 (0.01)
Li	7.3	15.5 (0.01)	7.8 (0.01)	7.39	0.36	0.32	0.23	0.75
Cd	6.1	1.6	1.0	0.83	1.18	0.05	0.02	0.17
V	5.5	12.4 (0.01)	5.1	10.62	2.14	1.84	2.0	3.35
Mo	5.5	8.0	4.9	3.19	4.56	6.84 (0.01)	2.04	3.2
Cs	5.4	0.9	1.2	0.94	0.11	0.12	0.01	0.17
Hf	4.5	10.8 (0.01)	6.8 (0.01)	4.63	0	0.67	1.03	0.97
As	4.2	4.5	3.1	1.22	0	0 (0)	0.05	0.60
Li	4.0	9.8	5.9 (0.01)	5.82	0.27	0.37	0.16	0.93
Co	3.8	1.1	2.1	35.67 (0.01)	0.86	0.49	0.13	0.33
Ce	3.7	6.8	6.0 (0.01)	9.85	1.06	0.50	0.42	2.03
La	1.8	3.5	2.9	4.78	0.54	0.24	0.25	0.92
Nb	1.5	2.6)	1.4	2.48	0.98	0.46	0.5	0.63
Nd	1.5	2.5	2.4	4.15	0.05	0 (0)	-	0.40
Sc	0.69	1.4	1.1)	1.31		0,00		0.02
Be	0.13	0.19	0.2	0.28	0.003	-	-	0.03
Ga	0.61	1.15	0.8	0.98	0.2	0.11	0.12	0.37
Ge	0.42	1.02	0.8	0.68	0.01	0.07	0.02	0.11
Se	0.91	-	-	0.02	0.59	-	0.20	0.18
Rh	0.02	0.02	0.00002	0.002	-	0.002		0.0002
Te	0.06	0.08	0.08	0.05	0.02	0.02	0.02	0,00
Pr	0.40	0.74	0.7	1.13	0.06	0.01	0.004	0.15
Sm	0.27	0.46	0.45	0.76	0.01	0,00	-	0.07
Eu	0.05	0.08	0.08	0.15	0.01	0.003	-	0.0
Gd	0.31	0.57	0.54	0.86	0.05	0.02	0.001	0.15
Tb	0.04	0.07	0.07	0.10	0.005	-	-	0.02
Dy	0.24	0.42	0.40	0.57	0.001	-	-	0.05
Ho	0.05	0.09	0.09	0.12	0.01	0.008	0.01	0.03
Er	0.16	0.31	0.28	0.35	0.02	0.03	0.02	0.09

Tm	0.02	0.05	0.05	0.05	0.002	0.003	0.001	0.01
Yb	0.18	0.38	0.32	0.34	0.01	0.02	0.03	0.09
Lu	0.03	0.06	0.08	0.06	0.003	0.005	0.005	0.02
Ta	0.07	0.14	0.09	0.16	0.06	0.02	0.02	0.03
W	0.80	1.63	0.69	0.54	0.26	0.41	0.4	0.3
Tl	0.22	0.01	0.03	0.06		0.009		
Bi	0.32	0.26	0.02	0.08	0.06	-	-	0.08
Th	0.41	0.88	0.79	1.29	0.15	0.09	0.09	0.24
U	0.22	0.43	0.49	0.51	0.03	0.03	0.02	0.09
Total	36459.9	65817.6	40312.2	44159.2	12562.9	7874.7	7227.2	18001.1
Mass(μg/m³)	558.8	183.6	114.4	270.0	374.7	56.3	91.6	91.9

1459

1460

1461

1462

1463

1464

1465

1466

1467

1468

1469

1470

1471

1472

1473

1474

1475

1476

1477

1478

1479

1480

1481

1482

1483

1484

1485

Table 4: Comparison of PM2.5 concentrations with literature data. Only literature data given at a daily scale have been selected.

Location	PM2.5 (μg.m^{-3})	Reference
Abidjan, Côte d'Ivoire	142	This work
Cotonou, Benin	154	This work
Beijing, China	81.4	Xie et al., 2019
Christchurch, New Zealand	9.2	Tunno et al., 2019
Pune, India	98 ± 28	Pipal et al., 2019
Delhi, India	123	Guttikunda and Calori, 2013
Lahore, Pakistan	91	Colbeck et al., 2011
Ahvaz, Iran	69	Shahsavani et al., 2012
Hong Chong, Hong Kong	54.7 ± 25.6	Cheng et al., 2015
Lecce, Italia	16	Cesari et al., 2016
Libreville, Gabon	35.8	Ngo et al., 2019
Port Gentille, Gabon	60.9	Ngo et al., 2019
Kenitra, Morocco	51.3	Zghaid et al., 2009
Bilecik, Turkey	247	Gaga et al., 2018
Algiers, Algeria	34.8	Bouhila et al., 2015
Shobra, Egypt	216	Lowenthal et al.,2015

1506

1507 Table 5: PM2.5-EC and PM2.5-OC comparison with Djossou et al. (2018) and Xu et al. (2019) values.
1508 Units are $\mu gC.m^{-3}$.

Location	Period	PM2.5 OC	PM2.5 EC	References
Traffic Abidjan. Cote d'Ivoire	July 2015	22.6 ± 3.4	4.3 ± 0.2	This Work
	January 2016	15.2 ± 5.3	7.0 ± 2.6	
	July 2016	9.3 ± 1.3	2.2 ± 0.1	
	January 2017	16.1 ± 1.7	18.9 ± 1.4	
	July 2015	3.3 ± 0.2	2.3 ± 0.2	Djossou et al. 2018
	January 2016	7.7 ± 0.0	3.9 ± 0.0	
	July 2016	7.6 ± 0.2	4.9 ± 0.0	
	January 2017	19.1 ± 6.2	13.9 ± 5.5	
Traffic Cotonou. Benin	July 2015	13.1 ± 1.2	3.5 ± 0.7	This Work
	January 2016	27.8 ± 11.3	10.9 ± 2.6	
	July 2016	6.7 ± 1.9	2.0 ± 0.5	
	January 2017	33.1 ± 4.6	27.3 ± 0.9	
	July 2015	4.2 ± 0.7	1.5 ± 0.1	Djossou et al. 2018
	January 2016	3.0 ± 0.3	1.5 ± 0.2	
	July 2016	6.7 ± 0.2	1.6 ± 0.1	
	January 2017	14.5 ± 0.8	4.4 ± 0.7	
	January 2016	49.5 ± 12.5	13.6 ± 3.6	Xu et al. 2019
	July 2016	37.0 ± 3.5	9.3 ± 0.8	
Domestic fire Abidjan. Cote d'Ivoire	July 2015	147.2 ± 14.5	16.1 ± 1.6	This Work
	January 2016	56.5 ± 51.5	7.4 ± 3.1	
	July 2016	172.3 ± 39.0	17.9 ± 4.8	
	January 2017	283.9 ± 34.9	37.9 ± 4.3	
	July 2015	80.5 ± 1.1	32.2 ± 1.6	Djossou et al. 2018
	January 2016	76.3 ± 13.7	11.4 ± 0.2	
	July 2016	68.4 ± 16.5	17.4 ± 2.1	
	January 2017	66.4 ± 7.5	21.1 ± 6.6	
	January 2016	72.4 ± 24.6	19.5 ± 7.3	Xu et al. 2019
	July 2016	189.3 ± 197.8	11.5 ± 10.8	
Waste Burning Abidjan. Cote d'Ivoire	July 2015	14.8 ± 1.1	4.4 ± 0.1	This Work
	January 2016	7.7 ± 1.3	3.0 ± 0.3	
	July 2016	10.0 ± 2.4	1.5 ± 0.3	
	January 2017	21.9 ± 4.2	19.2 ± 2.4	
	July 2015	3.7 ± 2.2	4.3 ± 0.3	Djossou et al. 2018
	January 2016	13.9 ± 9.0	3.6 ± 1.8	
	July 2016	9.8 ± 4.4	2.8 ± 0.9	
	January 2017	22.4 ± 7.8	8.7 ± 3.0	
	January 2016	85 ± 57.4	15 ± 4.7	Xu et al. 2019
	July 2016	65.2± 65.2	12.3 ± 11.4	

1509

1510

1511

1512   Table 6: EC and OC comparison with literature values. Only literature data given at a daily scale have
1513   been selected.

1514

Location	OC (µg.m^{-3})	BC (µg.m^{-3})	Reference
Abidjan (Côte d'Ivoire)	16	8.1	This study
Cotonou (Benin)	20.2	11	This study
Bilecik (Turkey)	49.6-62.8	38.8-58.1	Gaga et al., 2018
Pune (India)	30	5	Pipal et al., 2019
Shanghai (China)	4.9-13.1	1.9-5	Ding et al., 2017
Lahore (Pakistan)	85.7-152	13.8-21	Stone et al., 2010
Agra (India)	25.4-70	3.3-9.5	Satsangi et al., 2012, Pipal et al., 2014
Delhi (India)	34.1-50	5.3-10.6	Bisht et al., 2015a, Pipal et al., 2014
Ahmedabad (India)	18.3	3	Rengarajan et al., 2011
Yokohama (Japan)	4	2	Khan et al., 2010
Beijing (China)	2.9-28.2	1.2-16.3	Guinot et al., 2007

1515

1516

1517

1518

1519

1520

1521

1522

1523

1524

1525

1526

1527

1528

1529

1530

1531

1532

1533

1534

1535

1536 Table 7: Comparison of WSOC concentrations with literature data. Only literature data given at a daily
1537 scale have been selected.

1538

Location	WSOC ($\mu g.m^{-3}$)	Reference
Abidjan, Côte d'Ivoire	2-8	This work
Cotonou, Benin	2-8	This work
Beijing, China	9-27	Yu et al., 2018
Beijing, China	4-6	Xiang et al., 2017
Beijing, China	8-12	Tang et al., 2016
Beijing, China	7	Du et al., 2014
Beijing, China	6-8	Feng et al., 2006
Shanghai, China	2-7	Feng et al., 2006, Huang et al., 2012
Guangzhou, Hong Kong	2	Huang et al., 2012
Guangzhou, Hong Kong	5-10	Feng et al., 2006
Gwangju, Korea	2-3.5	Park et al., 2015
Tokyo, Japan	3-23	Sempere and Kawamura, 1994
Cairo, Egypt	3	Favez et al., 2008
Amsterdam, Netherland	1-2	Feng et al., 2007
Barcelone, Spain	1-2	Viana et al., 2007 and 2008
Brindisi, Italy	1.5	Genga et al., 2017
Saint Jean de Maurienne, France	1-5	Sullivan et al., 2004, Jaffrezo et al., 2005a

1539